

Accelerated Article Preview

Genomic investigations of unexplained acute hepatitis in children

Received: 25 July 2022

Accepted: 23 March 2023

Accelerated Article Preview

Cite this article as: Morfopoulou, S. Genomic investigations of unexplained acute hepatitis in children. *Nature* <https://doi.org/10.1038/s41586-023-06003-w> (2023)

Sofia Morfopoulou, Sarah Buddle, Oscar Enrique Torres Montaguth, Laura Atkinson, José Afonso Guerra-Assunção, Mahdi Moradi Marjaneh, Riccardo Zenezini Chiozzi, Nathaniel Storey, Luis Campos, J. Ciaran Hutchinson, John R. Counsell, Gabriele Pollara, Sunando Roy, Cristina Venturini, Juan F. Antinao Diaz, Ala'a Siam, Luke J. Tappouni, Zeinab Asgarian, Joanne Ng, Killian S. Hanlon, Alexander Lennon, Andrew McArdle, Agata Czap, Joshua Rosenheim, Catarina Andrade, Glenn Anderson, Jack C. D. Lee, Rachel Williams, Charlotte A. Williams, Helena Tutill, Nadua Bayzid, Luz Marina Martin Bernal, Hannah Macpherson, Kylie-Ann Montgomery, Catherine Moore, Kate Templeton, Claire Neill, Matt Holden, Rory Gunson, Samantha J. Shepherd, Priyen Shah, Samantha Cooray, Marie Voice, Michael Steele, Colin Fink, Thomas E. Whittaker, Georgia Santilli, Paul Gissen, Benedikt B. Kaufer, Jana Reich, Julien Andreani, Peter Simmonds, Dimah K. Alrabiah, Sergi Castellano Hereza, Primrose Chikowore, Miranda Odam, Tommy Rampling, Catherine Houlihan, Katja Hoschler, Tiina Talts, Cristina Celma, Suam Gonzalez, Eileen Gallagher, Ruth Simmons, Conall Watson, Sema Mandal, Maria Zambon, Meera Chand, James Hatcher, Surjo De, Kenneth Baillie, Malcolm Gracie Semple, DIAMONDS Consortium, PERFORM Consortium, ISARIC Consortium, Joanne Martin, Ines Ushiro-Lumb, Mahdad Noursadeghi, Maesha Deheragoda, Nedin Hadzic, Tassos Grammatikopoulos, Rachel Brown, Chayarani Kelgeri, Konstantinos Thalassinou, Simon N. Waddington, Thomas S. Jacques, Emma Thomson, Michael Levin, Julianne R. Brown & Judith Breuer

This is a PDF file of a peer-reviewed paper that has been accepted for publication. Although unedited, the content has been subjected to preliminary formatting. Nature is providing this early version of the typeset paper as a service to our authors and readers. The text and figures will undergo copyediting and a proof review before the paper is published in its final form. Please note that during the production process errors may be discovered which could affect the content, and all legal disclaimers apply.

1 Genomic investigations of unexplained acute hepatitis in children

2 Sofia Morfopoulou^{1,2 *}, Sarah Buddle^{1 *}, Oscar Enrique Torres Montaguth¹, Laura Atkinson
3 ³, José Afonso Guerra-Assunção¹, Mahdi Moradi Marjaneh^{2,4}, Riccardo Zenezini Chiozzi⁵,
4 Nathaniel Storey³, Luis Campos⁶, J Ciaran Hutchinson⁶, John R Counsell⁷, Gabriele
5 Pollara⁸, Sunando Roy¹, Cristina Venturini¹, Juan F Antinao Diaz⁷, Ala'a Siam^{7,9}, Luke J
6 Tappouni⁷, Zeinab Asgarian⁷, Joanne Ng⁹, Killian S Hanlon⁷, Alexander Lennon³, Andrew
7 McArdle², Agata Czap⁸, Joshua Rosenheim⁸, Catarina Andrade⁶, Glenn Anderson⁶, Jack C D
8 Lee³, Rachel Williams¹⁰, Charlotte A Williams¹⁰, Helena Tutill¹⁰, Nadua Bayzid¹⁰, Luz
9 Marina Martin Bernal¹⁰, Hannah Macpherson¹¹, Kylie-Ann Montgomery^{10,11}, Catherine
10 Moore¹², Kate Templeton¹³, Claire Neill¹⁴, Matt Holden^{15,16}, Rory Gunson¹⁷, Samantha J
11 Shepherd¹⁷, Priyen Shah², Samantha Cooray², Marie Voice¹⁸, Michael Steele¹⁸, Colin Fink
12 ¹⁸, Thomas E Whittaker¹⁹, Giorgia Santilli¹⁹, Paul Gissen¹⁰, Benedikt B Kaufer²⁰, Jana
13 Reich²⁰, Julien Andreani^{21,22}, Peter Simmonds²¹, Dimah K. Alrabiah^{10,23}, Sergi Castellano
14 Hereza^{10,24}, Primrose Chikowore²⁵, Miranda Odam²⁵, Tommy Rampling^{8,26,27}, Catherine
15 Houlihan^{8,26,28}, Katja Hoschler²⁶, Tiina Talts²⁶, Cristina Celma²⁶, Suam Gonzalez²⁶, Eileen
16 Gallagher²⁶, Ruth Simmons²⁶, Conall Watson²⁶, Sema Mandal²⁶, Maria Zambon²⁶, Meera
17 Chand²⁶, James Hatcher³, Surjo De³, Kenneth Baillie²⁵, Malcolm Gracie Semple^{29,30},
18 DIAMONDS, PERFORM and ISARIC consortia, Joanne Martin³¹, Ines Ushiro-Lumb³²,
19 Mahdad Noursadeghi⁸, Maesha Deheragoda³³, Nedim Hadzic³³, Tassos Grammatikopoulos
20 ³³, Rachel Brown³⁴, Chayarani Kelgeri³⁵, Konstantinos Thalassinos^{5,36,37}, Simon N
21 Waddington^{9,38}, Thomas S Jacques^{6,39}, Emma Thomson⁴⁰, Michael Levin², Julianne R
22 Brown³, Judith Breuer^{1,3}

23

- 24 1. Infection, Immunity and Inflammation Department, Great Ormond Street Institute of
25 Child Health, University College London, London, UK
- 26 2. Section for Paediatrics, Department of Infectious Diseases, Faculty of Medicine,
27 Imperial College London, London, UK
- 28 3. Department of Microbiology, Virology and Infection Control, Great Ormond Street
29 Hospital for Children NHS Foundation Trust, London, UK
- 30 4. Section of Virology, Department of Infectious Diseases, Faculty of Medicine,
31 Imperial College London, London, UK
- 32 5. University College London Mass Spectrometry Science Technology Platform,
33 Division of Biosciences, University College London, London, UK
- 34 6. Histopathology Department, Great Ormond Street Hospital for Children NHS
35 Foundation Trust, London, UK
- 36 7. Research Department of Targeted Intervention, Division of Surgery and
37 Interventional Science, University College London, London, UK
- 38 8. Division of Infection and Immunity, University College London, London, UK
- 39 9. Gene Transfer Technology Group, EGA-Institute for Women's Health, University
40 College London, London, UK
- 41 10. Genetics and Genomic Medicine Department, Great Ormond Street Institute of Child
42 Health, University College London, London, UK

- 43 11. Department of Neurodegenerative Disease, Queen Square Institute of Neurology,
44 University College London, London, UK
- 45 12. Wales Specialist Virology Centre, Public Health Wales Microbiology Cardiff,
46 University Hospital of Wales, Cardiff, UK
- 47 13. Department of Medical Microbiology, Edinburgh Royal Infirmary, Edinburgh, UK,
48 14. Public Health Agency Northern Ireland, Belfast, UK
- 49 15. School of Medicine, University of St. Andrews, St. Andrews, UK
- 50 16. Public Health Scotland, Edinburgh, UK
- 51 17. West of Scotland Specialist Virology Centre, Glasgow, UK
- 52 18. Micropathology Ltd., University of Warwick Science Park, Coventry, UK
- 53 19. Molecular and Cellular Immunology, Great Ormond Street Institute of Child Health,
54 University College London, London, UK
- 55 20. Institute of Virology, Freie Universität Berlin, Berlin, Germany
- 56 21. Nuffield Department of Medicine, University of Oxford, Oxford, UK
- 57 22. Centre Hospitalier Universitaire (CHU) Grenoble \square Alpes, Grenoble, France,
- 58 23. National Centre for Biotechnology, King Abdulaziz City for Science and Technology,
59 Riyadh, Saudi Arabia
- 60 24. University College London Genomics, University College London, London, UK
- 61 25. Roslin Institute, University of Edinburgh, Edinburgh, UK
- 62 26. UK Health Security Agency, London, UK
- 63 27. Hospital for Tropical Diseases, University College London Hospitals NHS
64 Foundation Trust, London, UK
- 65 28. Department of Clinical Virology, University College London Hospitals, London, UK
- 66 29. Pandemic Institute, University of Liverpool, Liverpool, UK
- 67 30. Respiratory Medicine, Alder Hey Children's Hospital NHS Foundation Trust,
68 Liverpool, UK
- 69 31. Centre for Genomics and Child Health, The Blizzard Institute, Queen Mary University
70 London, London, UK
- 71 32. NHS Blood and Transplant, Bristol, UK
- 72 33. King's College Hospital, London, UK
- 73 34. Department of Cellular Pathology - University Hospitals Birmingham NHS
74 Foundation Trust, Birmingham, UK
- 75 35. Liver Unit, Birmingham Women's and Children's NHS Foundation Trust,
76 Birmingham, UK
- 77 36. Institute of Structural and Molecular Biology, Division of Biosciences, University
78 College London, London, UK
- 79 37. Institute of Structural and Molecular Biology, Birkbeck College, University of
80 London, London, UK
- 81 38. Medical Research Council Antiviral Gene Therapy Research Unit, Faculty of Health
82 Sciences, University of the Witwatersrand, Johannesburg, South Africa
- 83 39. Developmental Biology and Cancer Department, Great Ormond Street Institute of
84 Child Health, University College London, London, UK
- 85 40. Medical Research Council-University of Glasgow Centre for Virus Research,
86 Glasgow, UK

87 *These authors contributed equally to this work

88

89 Abstract

90 Since its first identification in Scotland, over 1000 cases of unexplained pediatric hepatitis in
91 children have been reported worldwide, including 278 cases in the UK¹. Here we report
92 investigation of 38 cases, 66 age-matched immunocompetent controls and 21
93 immunocompromised comparator subjects, using a combination of genomic, transcriptomic,
94 proteomic and immunohistochemical methods. We detected high levels of adeno-associated
95 virus 2 (AAV2) DNA in liver, blood, plasma or stool from 27/28 cases. We found low levels
96 of Adenovirus (HAdV) and Human Herpesvirus 6B (HHV-6B), in 23/31 and 16/23
97 respectively of the cases tested. In contrast, AAV2 was infrequently detected at low titre in
98 blood or liver from control children with HAdV, even when profoundly immunosuppressed.
99 AAV2, HAdV and HHV-6 phylogeny excluded emergence of novel strains in cases.
100 Histological analyses of explanted livers showed enrichment for T-cells and B-lineage cells.
101 Proteomic comparison of liver tissue from cases and healthy controls, identified increased
102 expression of HLA class 2, immunoglobulin variable regions and complement proteins.
103 HAdV and AAV2 proteins were not detected in the livers. Instead, we identified AAV2 DNA
104 complexes reflecting both HAdV and HHV-6B-mediated replication. We hypothesize that
105 high levels of abnormal AAV2 replication products aided by HAdV and in severe cases
106 HHV-6B, may have triggered immune-mediated hepatic disease in genetically and
107 immunologically predisposed children.

108 Introduction

109 The report, in March 2022, of five cases of severe hepatitis of unknown aetiology, led to the
110 UK Health Security Agency (UKHSA) identifying 278 cases in total as of 30 September
111 2022¹. Cases, defined as acute non-A-E hepatitis with serum transaminases >500IU in
112 children under ten years of age, were found to have been occurring since January 2022². In
113 the UK, 196 cases required hospitalization, 69 were admitted to intensive care, and 13
114 required liver transplantation¹. Case numbers have declined since April 2022³.

115 UKHSA investigations identified HAdV to be commonly associated with the unexplained
116 paediatric hepatitis, with 64.7% (156/241) testing positive in one or more samples from
117 whole blood (the most sensitive sample-type⁴) or mucosal swabs. 35/77 HAdVs from blood
118 were typed as F41. Seven of eight patients in England who required liver transplantation
119 tested HAdV positive in blood, with F41 found in 5/5 genotyped². SARS-CoV-2 infection
120 was detected in 8.9% (15/169) of UK and 12.8% (16/125) of English cases².

121 Given the uncertainty around the aetiology of this outbreak, and the potential that HAdV-F41
122 if implicated (**Figure 1A**), could be a new or recombinant variant, we undertook untargeted
123 metagenomic and metatranscriptomic sequencing, of liver biopsies from five liver transplant
124 cases and whole blood from five non-transplanted cases (**Table 1, Figure 1B**). The results
125 were further verified by confirmatory PCRs of liver, blood, stool and nasopharyngeal samples
126 from a total of 38 cases for which there was sufficient residual material. We compared our
127 results with those from 13 healthy children and 52 previously healthy children presenting to
128 hospital with other febrile illness, including adenovirus, hepatitis unrelated to the current

129 outbreak or a critical illness requiring admission to the Intensive Care Unit. We also tested
130 blood and liver biopsies from 17 profoundly immunosuppressed children with hepatitis who
131 were not part of the current outbreak, in whom reactivation of latent infections might be
132 expected.

133 **Results**

134 **Cases**

135 We received samples from 38 children meeting the case definition (**Table 1**). All cases were
136 aged less than ten years old and 22/23 previously tested were positive by adenovirus PCR
137 (**Supplementary Table 1, Table 2, Extended Data Table 1**). A summary of the samples
138 received from these cases and investigations carried out on them are shown in **Figure 1B&C**.

139 **Clinical details**

140 Pre-existing conditions, autoimmune, toxic and other infectious causes of hepatitis were
141 excluded in 12 transplanted (cases 1-5, 28, 29, 31-34, 36) and 4 non-transplanted (cases 30,
142 35, 37, 38) children, investigated at two liver transplant units, (**Supplementary Table 1**). The
143 12 transplanted cases reported gastrointestinal symptoms (nausea, vomiting, diarrhea)
144 preceding transplant by a median of 20 days (range 8-42 days). All 12 transplanted children
145 survived, while the four children who did not receive liver transplants recovered without
146 sequelae or evidence of chronic liver-related conditions. Five of the remaining 22 cases
147 referred by Health Security Agencies, for whom this information was available, recovered
148 without sequelae (**Table 1, Supplementary Table 1**).

149 **Metagenomic Sequencing**

150 We performed metagenomic and metatranscriptomic sequencing on samples of frozen
151 explanted liver tissue from five cases who received liver transplants (median age 3 years) and
152 six blood samples from five non-transplanted hepatitis cases (median age 5 years) (**Table 1,**
153 **Figure 1B**). The liver samples had uniform and consistently high sequencing depth both for
154 DNA-seq and RNA-seq, while the blood samples had variable sequencing depth particularly
155 for RNA-seq (**Supplementary Table 2**). We detected⁵ abundant AAV2 reads in DNA-seq
156 from 5/5 explanted livers and 4/5 blood samples from non-transplant cases (7-42 and 1.2-42
157 reads/million respectively) (**Table 2**). Lower levels of HHV-6B were present in DNA-seq of
158 all explanted liver samples (0.09-4 reads/million) but not in the six blood samples (**Table 2**).
159 HAdV was detected (five reads) in one blood sample (**Table 2**).

160 **Evidence of AAV2 replication**

161 Metatranscriptomics revealed AAV2, but not HHV-6B or HAdV, RNA reads, in liver and
162 blood samples (0.7-10 and 0-7.8 reads per million respectively). Mapping liver RNA-seq data
163 to the RefSeq AAV2 genome (NC_001401.2) identified high expression of the cap ORF,
164 particularly at the 3' end of the capsid, suggesting viral replication⁶ (**Extended Data Figure**
165 **1A**) while RT-PCR of two livers confirmed the presence of AAV2 mRNA from the cap ORF

166 (Extended Data Figure 1C). In the blood samples, which had not been treated to preserve
167 RNA, we detected low levels of AAV2 RNA reads mapping throughout the genome.
168 (Extended Data Figure 1B).

169 Nanopore sequencing of explanted livers

170 Ligation-based untargeted nanopore sequencing was applied to DNA from 4/5 frozen liver
171 samples. All four samples were initially sequenced at a lower depth (Average
172 N50: 8.37 kb). 6-16 AAV2 reads were obtained from each sample (5.57-22.24 million total
173 reads, **Supplementary Table 3**). Mapping revealed concatenation of the 4kb genome,
174 compatible with active AAV2 replication⁷. We observed alternating and head-to-tail
175 concatemers which could be consistent with both HAdV and human herpesvirus-mediated
176 rolling hairpin and rolling circle replication respectively⁸. Two of these samples were
177 sequenced more deeply, resulting in 52 and 178 AAV2 reads in 82.9 and 122 million total
178 (N50 4.40-8.52kb) (Supplementary Table 3). 42-48% of reads in the deeper sequences
179 comprised randomly linked, truncated and rearranged genomes with few that were intact and
180 full length (**Extended Data Figure 2**). The remaining reads were <3000 bp long and may
181 represent sections of either monomeric genomes or of more complex structures.

182 Integration analysis

183 There was some evidence of AAV2 integration by deeper nanopore sequencing of explanted
184 livers (**Supplementary Table 3**), however none of the integration sites were confirmed by
185 Illumina metagenomic or targeted AAV2 sequencing. The results are likely to represent
186 artefacts of this library preparation method, with chimeric reads described to occur in 1.7-3%
187 of reads^{9,10}. Given the number of human reads (72-120 million) we might expect to see this
188 artefact occurring most commonly between AAV2 and human than between AAV2 reads.

189 Confirmatory real-time PCR

190 Where sufficient residual material was available, PCR tests were performed for AAV2
191 (28/38), HAdV (31/38), and HHV-6B (23/38). The results confirmed high levels (CTs: 17-
192 21) of AAV2 DNA in all five frozen explanted livers that had undergone metagenomics
193 (**Table 2, Figure 2D**) with lower levels of HHV-6B and HAdV DNA (CTs: 27-32 and 37-42
194 respectively). AAV2 DNA was also detected (CTs: 19-25) in blood from 4/5 cases that had
195 undergone metagenomics while HAdV, at levels too low to genotype and HHV-6B were
196 detected in 2/4 and 3/4 respectively (one had insufficient material) (**Table 2**). One of the
197 blood metagenomics cases (case 9, JBB1) with insufficient material to test for HAdV and
198 HHV-6B, tested positive for both viruses in the referring laboratory. The AAV2-negative
199 blood sample (case 10, JBB15) was also negative for HAdV but positive for HHV-6B (**Table**
200 **2**). A further 10/10 blood samples tested from cases were positive for HAdV by PCR.
201 Sufficient material was available for AAV2 PCR in six of these (all positive; CTs: 20-23) and
202 HHV-6B PCR in two (one positive CT: 37) (**Extended Data Table 1**).

203 AAV2 PCR was positive in nine formalin fixed paraffin embedded (FFPE) liver samples,
204 including seven from transplanted (CTs: 23-25) and two from non-transplant cases (CTs:34-
205 36, **Extended Data Table 1**). HHV-6B PCR was positive in 6/7 FFPE samples (not case 32)
206 from transplanted (CTs: 30-37) and 0/2 (cases 30 & 35) from non-transplanted cases, with
207 HAdV positive (CTs: 40-44) in 4/9. Three each transplanted (32, 34, 36) and non-
208 transplanted (35, 37, 38) cases had serum available for testing. All were AAV2 positive (CTs:
209 27-32) and HHV-6B negative with one transplanted and one non-transplanted case testing
210 HAdV positive (**Extended Data Table 1**).

211 Taken together, 27/28 cases tested were AAV2 PCR positive, 23/31 HAdV positive and
212 16/23 HHV-6B positive. When results from referring laboratories were included, 33/38 were
213 positive for HAdV and 19/26 for HHV-6B (**Table 2, Extended Data Table 1**).

214 **Controls and comparators**

215 To better contextualize the findings in cases with unexplained hepatitis, we selected control
216 groups of children who were not part of the outbreak.

217 **Blood from immunocompetent children**

218 Whole blood from 65 immunocompetent children matched by age to cases (median age 3.8
219 years) (**Figure 1B, Extended Data Table 2A, Supplementary Table 4**) who were healthy,
220 or had adenovirus infection, hepatitis, or critical illness, including requiring critical care, were
221 selected from the PERFORM (Personalised Risk assessment in febrile illness to optimise
222 Real-life Management, www.perform2020.org) and DIAMONDS (Diagnosis and
223 Management of Febrile Illness using RNA Personalised Molecular Signature Diagnosis
224 study, www.diamonds2020.eu) studies. Both studies recruited children presenting to hospital
225 with an acute onset febrile illness between 2017 and 2020 (PERFORM) and July 2020 to
226 October 2021, during the COVID-19 pandemic (DIAMOND) (**Supplementary Table 4**). Of
227 the PERFORM/DIAMONDS control whole blood samples, 6/65 (9.2%) were AAV2 PCR
228 positive (**Supplementary Table 5**), as compared with 10/11 (91%) of whole blood samples
229 from cases (**Figure 2A**, $p = 8.466e-08$, Fisher's exact test). AAV2 DNA levels were
230 significantly higher in whole blood from cases as compared to controls (**Figure 2E**, $p =$
231 $2.747e-11$, Mann-Whitney Test).

232 One subject with an HAdV-F4 positive blood sample, originally thought to have unexplained
233 paediatric hepatitis, was later found to have a prior condition that explained the hepatitis and
234 was therefore reclassified as a control, (referred to as "reclassified control" or CONB40,
235 (**Supplementary Table 5**). This blood sample was negative for AAV2 by PCR
236 (**Supplementary Table 5**).

237 **Liver from immunocompromised children**

238 Frozen liver biopsy material from four immunocompromised children, (median age 10 years)
239 (CONL1-4) who had been investigated for other forms of hepatitis were also tested (**Figure**
240 **1B, Extended Data Table 2B**). In three, liver enzymes were raised (**Supplementary Table**

241 S6); no results were available for CONL4. AAV2 was detected in CONL3 (CT:39) and
242 HHV-6B (CT:34), in CONL2, while HAdV was negative (**Figure 2D, Suppl. Table 5**).

243 **Blood from immunocompromised comparators**

244 We also tested immunocompromised children who are more likely to reactivate latent
245 viruses. Whole blood from 17 immunocompromised children (median age 1 year) with raised
246 liver transaminases (AST/ALT>500IU) and viraemia (HAdV or CMV), all sampled in 2022
247 (**Figure 1B**) were tested for AAV2, HHV-6B and HAdV (**Supplementary Table 5,**
248 **Extended Table 2B**). The majority had received human stem cell or solid organ transplants,
249 and none were linked to the recent hepatitis outbreak (**Extended Data Table 2B**). 5/15 (33%)
250 were positive for HHV-6B while 6/17 (35%) were positive for AAV2, significantly fewer
251 than in cases ($p = 0.005957$, Fisher's exact) and at significantly lower CT levels ($p = 6.517e-$
252 05 , Mann-Whitney) (**Figure 2, Supplementary Table 5**). One HAdV and AAV2-positive
253 immunocompromised comparator (CONB23) was also positive for HHV-6B
254 (**Supplementary Table 5**).

255 Four of the six AAV2 positive children from the DIAMONDS/PERFORM cohort (**Figure**
256 **2A, Supplementary Table 5**) and all six of the AAV2 positive immunocompromised
257 children (**Figure 2A, Supplementary Table 5**) were also HAdV positive.

258 **Whole viral genome sequencing**

259 One full HAdV-F41 genome sequence from the stool of one case (OP174926, case 22)
260 (**Supplementary Table 7**) clustered phylogenetically with the HAdV-F41 sequence obtained
261 from the reclassified-control (CONB40) and with other HAdV-F41 sequences collected
262 between 2015-2022, including 23 contemporaneous stool samples from children without the
263 unexplained paediatric hepatitis (**Figure 3A, Figure 1C**). Sequencing and K-mer analysis¹¹
264 of HAdV from 13 cases with partial sequences, identified genotype HAdV-F41 in twelve
265 (**Supplementary Tables 7, 8**). The partial sequences showed most similarity to control
266 sequence OP047699 (**Supplementary Table 8**) mapping across the entire viral genome, thus
267 further excluding a recombinant virus.

268 Single nucleotides polymorphisms (SNPs) were largely shared between the single HAdV
269 positive case from stool (OP174926) and control whole genome sequences (**Extended Data**
270 **Figure 3A**). Given reported mutation rates for HAdV-F41 and other adenoviruses^{12,13}, any
271 differences are likely to have arisen before the outbreak. No new or unique amino acid
272 substitutions were noted in HAdV sequences from cases with only two substitutions overall
273 (**Extended Data Figure 2D**) and none in proteins critical for AAV2 replication.

274 AAV2 sequences from 15 cases, including five from the explanted livers and ten from whole
275 blood from non-transplanted cases, clustered phylogenetically with control AAV2 sequences
276 obtained from four immunocompromised HAdV positive children with elevated ALT in the
277 comparator group (**Extended Data Table 2B**) and two healthy children with recent HAdV-
278 F41 diarrhoea (**Figure 3B, Supplementary Table 9**). The degree of diversity and lack of a

279 unique common ancestor between case AAV2 genomes suggest these are not specific to the
280 hepatitis outbreak, but instead reflect the general population's current viral diversity. While
281 comparison of the AAV2 sequences showed no difference between cases and controls,
282 contemporary AAV2s showed changes in the capsid compared to historic AAV2 (**Extended**
283 **Data Figure 3C**). None of these changes were shared with the hepatotropic AAV7 and
284 AAV8 viruses (**Extended Data Figure 3B**). The majority of the contemporary AAV2
285 genomes in cases and controls (20/21) contained a stop codon in the X gene, which is
286 involved in viral replication¹⁴, while historic AAV2 genomes contained this less frequently
287 (11/35). The significance, if any, of this is currently unknown.

288 While mean read depths for four HHV-6B genomes recovered from explanted livers were
289 low (x5-x10) (**Supplementary Table S12**), phylogeny (**Figure 3C**) confirmed that all were
290 different.

291 **Transduction of AAV2 capsid mutants**

292 Using a recombinant AAV2 (rAAV2) vector with a VP1 sequence (**Extended Data Figure**
293 **4A**) containing the consensus amino acid sequence from AAV2 cases (**Extended Data**
294 **Figure 3B**) (AAV2Hepcase), we generated functional rAAV particles that transduced Huh-7
295 cells with comparable efficacy to both canonical AAV2 and the synthetic liver-tropic LK03
296 AAV vector¹⁵. Unlike canonical AAV2, AAV2Hepcase capsid, which contains mutations
297 (R585S and R588T) that potentially affect the heparin sulfate proteoglycan (HSPG) binding
298 domain, was unaffected by heparin competition, a feature that is associated with increased
299 hepatotropism (**Extended Data Figure 4B&C**)^{16,17}.

300

301 **Histology and Immunohistochemistry**

302

303 Histological examination of the 12 liver explants and two liver biopsies showed non-specific
304 features of acute hepatitis with ballooning hepatocytes, disrupted liver architecture with
305 varying degrees of perivenular, bridging or pan acinar necrosis. There was no evidence of
306 fibrosis suggestive of an underlying chronic liver disease. The appearances were similar to
307 historic cases of seronegative hepatitis of unknown cause in children. There were no typical
308 histological features of autoimmune hepatitis (AIH), notably no evidence of portal-based
309 plasma cell rich infiltrates. A cellular infiltrate was present in all cases which on staining
310 appeared to be predominantly of CD8 positive T-cells but also included CD20 positive B-
311 cells. More widespread staining with the CD79a pan-B cell lineage which also identifies
312 plasma cells was also observed (**Extended Data Figure 5**). Macrophage lineage cells showed
313 some C4d complement staining, while staining for immunoglobulins was non-specific with
314 disruption of the normal canalicular staining seen in controls due to the architectural collapse.
315 MHC Class I and II staining although increased in cases, was non-specific and associated
316 with sinusoid-containing blood cells and necrotic tissue (**Extended Data Figure 6A**). No
317 viral inclusions were observed and there were no features suggestive of direct viral cytopathic
318 effect.

319 Immunohistochemistry was negative for adenovirus. Staining of the five explanted livers with
320 AAV2 antibodies demonstrated evidence of non-specific ingested debris but not the nuclear
321 staining seen in the positive AAV2 infected cell lines and murine infected tissue (**Extended**
322 **Data Figure 6B**). All five liver explants showed positive staining of macrophage derived
323 cells with antibody to HHV-6B, with no staining of negative control serial sections
324 (**Extended Data Figure 6B**). No specific HHV-6B staining was observed in 13 control liver
325 biopsies from patients (including three children <18 years) with other viral hepatitis, toxic
326 liver necrosis, autoimmune and other hepatitis, and normal liver. The control set was also
327 negative for HAdV and AAV2 by IHC.

328 Liver sections were morphologically suboptimal for electron microscopy, but no viral
329 particles were identified in hepatocytes, blood vessel endothelial cells and Kupffer cells.

330 **Transcriptomic analysis**

331

332 We quantified functional cytokine activity by expression of independently derived cytokine-
333 inducible transcriptional signatures of cell mediated immunity (**Supplementary Table 11**) in
334 bulk genome-wide transcriptional profiles from four of the frozen explanted livers. Results
335 were compared to published data from normal adult livers (n=10) and adult hepatitis B-
336 associated acute liver failure (n=17) (GSE96851)¹⁸. Data from the unexplained hepatitis cases
337 revealed increased expression of diverse cytokines and pathways compared to normal liver.
338 These pathways included prototypic cytokines associated with T cell responses including
339 IFN γ , IL2, CD40LG, IL4, IL5, IL7, IL13 and IL15 (**Figure 4A, Supplementary Table 12**)
340 as well as some evidence of innate immune type 1 interferon (IFN) responses. Many of these
341 responses showed substantially greater activity in unexplained hepatitis compared to
342 fulminant hepatitis B virus disease. The most striking enrichment was for TNF expression,
343 and included other canonical pro-inflammatory cytokines including IL1 and IL-6 (**Extended**
344 **Data Figure 7**). These data are consistent with an inflammatory process involving multiple
345 pathways.

346 **Proteomics**

347 Proteomic analysis of the five frozen explanted livers did not detect AAV2 or HAdV
348 proteins. Expression of the HHV-6B U4, a protein of unknown function, was found in 4/5
349 cases, U43, part of the helicase primase complex in 2/5 and U84, a homologue of
350 cytomegalovirus UL117, implicated in HHV-6B nuclear replication, in 2/5 (**Extended Data**
351 **Figure 8**).

352 The human proteome from the five frozen liver explants was compared with publicly
353 available data from 7 control “normal” livers, taken from two different studies^{19,20}. Both
354 protein and peptide analyses (**Figure 4B & C, Supplementary Table 13&14**) found
355 increased expression in unexplained hepatitis cases of HLA class II proteins and peptides
356 (e.g. HLADRB1 and 4), multiple peptides from variable regions of the heavy and light chains
357 of immunoglobulin, complement proteins (such as C1q) and intracellular and extracellular
358 released proteins from neutrophils and macrophages (MMP8 and MPO).

359 There was no evidence of HAdV, AAV2 or HHV-6B in any of the control livers.

360

361 **Discussion**

362 Despite reports implicating HAdV-F41 as causing the recent outbreak of unexplained
363 paediatric hepatitis, we found very low levels of HAdV DNA, no proteins, inclusions or viral
364 particles, including in explanted liver tissue from affected cases and no evidence of a change
365 in the virus. In contrast, metagenomic and PCR analysis of liver tissue and blood identified
366 high levels of DNA from adeno-associated virus 2 (AAV2), a member of the
367 *Dependoparvovirus* genus, which has not previously associated with clinical disease, in 27/28
368 cases. Replication of AAV2 requires coinfection with a helper virus, such as HAdV,
369 herpesviruses, or papillomavirus²¹ and can also be triggered in the laboratory by cellular
370 damage²², raising the possibility that the AAV2 detected was a bystander of previous HAdV-
371 F41 infection and/or liver damage. Against this, we found little or no AAV2 in blood from
372 age-matched immunocompetent, children including those with adenovirus infection, hepatitis
373 or critical illness (**Figure 2D**). AAV2 has been reported to establish latency in liver²³,
374 however, even in critically ill immunosuppressed children with hepatitis in whom
375 reactivation might occur, we detected AAV2 infrequently and at significantly lower levels in
376 blood or liver biopsies (**Figure 2D, Figure 2G**).

377

378 RNA transcriptomic and rt-PCR data from explanted livers point to active AAV2 infection,
379 although we did not detect AAV2 proteins by immunohistochemistry (**Extended Data**
380 **Figure 6B**) or proteomics (**Extended Data Figure 8**) and no viral particles. The abundant
381 AAV2 genomes in the explanted liver are concatenated with many complex and abnormal
382 configurations. AAV genome concatenation may occur during AAV2 replication⁸, while
383 abnormal AAV2 DNA complexes and rearrangements have been observed in the liver
384 following AAV gene therapy^{7,44}. Hepatitis following AAV gene therapy is well described²⁴⁻
385 ²⁶ with deaths, albeit rarely²⁷. The pattern of complexes typify both HAdV and herpesvirus
386 (including HHV-6B)-mediated AAV2 DNA replication⁶. The presence of HHV-6B DNA in
387 11/12 explanted livers, but not in livers (0/2) of non-transplanted children, or control livers as
388 well as the expression, in 5/5 cases tested, of HHV-6B proteins, including U43, a homologue
389 of the HSV1 helicase primase UL52 which is known to aid AAV2 replication, highlight a
390 possible role for HHV-6B as well as HAdV, in the pathogenesis of AAV2 hepatitis,
391 particularly in severe cases. While AAV2 is also capable of chromosomal integration^{28 29 30}
392 we found little evidence of this by long read sequencing, computational analysis of
393 metagenomics data or examination of unmapped reads, although further confirmatory studies
394 may be required.

395

396 Although the pathogenesis of unexplained paediatric hepatitis and the role of AAV2, remain
397 to be determined, our results point strongly to an immune-mediated process. Transcriptomic
398 and proteomic data from the five explant livers identified significant immune dysregulation
399 involving genes and proteins that are strongly associated with activation of B and T cells,
400 neutrophils and macrophages as well as innate pathways. The findings are supported by
401 immunohistochemical staining showing infiltration into liver tissue of CD8+, B cell and B

402 cell lineage cells. Upregulation of canonical proinflammatory cytokines including IL15,
403 which has also been seen in a mouse model of AAV hepatitis⁴⁵, IL4 and TNF occurred at
404 levels greater even than are seen in fulminant liver failure following hepatitis B virus.
405 Increases in the same immunoglobulin variable region peptides and corresponding proteins
406 from both immunoglobulin heavy and light chains across all five livers points to specific
407 antibody involvement³¹. HLA DRB1*04:01 (12/13 tested) (**Supplementary Table 1**) among
408 children in our study supports the same genetic predisposition as mooted in a sister Scottish
409 study³².

410
411 An immune mediated process is consistent with studies of hepatitis following AAV gene
412 therapy, where raised AAV2 IgG and capsid specific CTLs are observed in the affected
413 patients, although whether these directly mediate the hepatitis remains unclear^{26,33}. While we
414 did not find that AAV2 sequences in cases differed from those in AAV2 occurring as
415 coinfections in HAdV-F41-positive stool collected from control children during the
416 contemporary HAdV -F41 gastroenteritis outbreak (**Figure 3B**), rAAV capsid expressing
417 consensus capsid sequence from the unexplained hepatitis cases (AAV2Hepcase), showed
418 reduced HSPG dependency, compared to canonical AAV2 (**Extended Data Figure 4**, whilst
419 retaining hepatocyte transduction ability. This points to likely greater *in vivo* hepatotropism
420 of currently circulating AAV2 than has hitherto been assumed from data on canonical AAV2
421 ¹⁷. Another member of the parvovirus family, Equine Parvovirus-Hepatitis (EqPV-H) has also
422 been associated with acute hepatitis in horses (Theiler's disease)³⁴.

423
424 There are a number of limitations to our study. While other known infectious, autoimmune,
425 toxic and metabolic aetiologies³ have been excluded including by other studies^{35,36}, numbers
426 of cases investigated here are small, the study is retrospective, the immunocompromised
427 controls were not perfectly age-matched, and only one immunocompetent and 17
428 immunocompromised controls were sampled during exactly the same period as the outbreak.
429 Age-matched DIAMONDS immunocompetent controls contemporaneous with the outbreak,
430 although few in number, were however found to be AAV2 negative in a separate study
431 carried out in Scotland³².

432
433 Finally, our data alone are not sufficient on their own to rule out a contribution from SARS-
434 CoV-2 Omicron, the appearance of which preceded the outbreak of unexplained hepatitis.
435 (**Supplementary Table 1**). We did not detect SARS-CoV-2 metagenomically even in three
436 subjects who tested positive on admission. Moreover, although seropositivity was higher in
437 our cases (15/20) compared to controls (3/10), this was not the case for another UK cohort³⁵
438 (38%) or in preliminary data from a UKHSA case-control study³, which showed similar
439 SARS-CoV-2 antibody prevalence between unexplained hepatitis cases and population
440 controls (<5y 60.5% versus 46.3% respectively, and 5-10y 66.7% versus 69.6%). In line with
441 UK national recommendations at the time, none of the children had received a COVID
442 vaccine.

443
444 While we find little evidence for SARS-CoV-2 directly causing the hepatitis outbreak, we
445 cannot exclude the impact of the COVID-19 pandemic on child mixing and infection

446 patterns. The contemporaneous development of unexplained paediatric hepatitis with a
447 national outbreak of HAdV-F41² and the finding of HAdV-F41 in many cases, suggests that
448 the two are linked. Enteric adenovirus infection is most common in those aged under five²
449 and infection is influenced by mixing and hygiene³⁷. Few cases of HAdV-F41 occurred
450 between 2020 and 2022 and no major outbreaks were recorded². The current HAdV outbreak
451 followed relaxation of restrictions due to the pandemic and represented one of many
452 infections, including other enteric pathogens that occurred in UK children following return to
453 normal mixing³⁸. Under normal circumstances, AAV2 antibodies levels are high at birth,
454 subsequently declining to reach their lowest point at 7-11 months, increasing thereafter
455 through childhood and adolescence³⁹. AAV2 is known to be spread with respiratory
456 adenoviruses, infections which declined during the COVID-19 pandemic, and has not been
457 detected by us in over 30 SARS-CoV-2 positive nasopharyngeal aspirates (data not shown).
458 We also found AAV2 DNA to be present in HAdV-F41-positive stool from both cases and
459 controls (**Supplementary Table 5**). With loss of child mixing during the COVID-19
460 pandemic, reduced spread of common respiratory and enteric viral infections and no evidence
461 of AAV2 in SARS-CoV-2 positive nasal pharyngeal swabs, it is likely that immunity to both
462 HAdV-F41 and AAV2 declined sharply in the age group affected by this unexplained
463 hepatitis outbreak. Pre-existing antibody is known to reduce levels of AAV DNA in the liver
464 of non-human primates following infusion of AAV gene therapy vectors⁴⁰. The possibility
465 that, in the absence of protective immunity, excessive replication of HAdV-F41 and AAV2
466 with accumulation of AAV2 DNA in the liver led to immune-mediated hepatic disease in
467 genetically predisposed individuals now needs further investigation. Evaluation of drugs that
468 inhibit TNF and other cytokines massively elevated in this condition may identify important
469 therapeutic options for future cases.
470

471 **Main Text References**

- 472 1. Joint ECDC-WHO Regional Office for Europe Hepatitis of Unknown Origin in Children
473 Surveillance Bulletin. <https://cdn.ecdc.europa.eu/novhep-surveillance/>.
- 474 2. Ukhsa. Investigation into acute hepatitis of unknown aetiology in children in England:
475 Technical briefing 3.
- 476 3. Investigation into acute hepatitis of unknown aetiology in children in England:
477 technical briefing 4. (2022).
- 478 4. Marsh, K. *et al.* Investigation into cases of hepatitis of unknown aetiology among
479 young children, Scotland, 1 January 2022 to 12 April 2022. *Euro Surveill* **27**, 1–7
480 (2022).
- 481 5. Morfopoulou, S. & Plagnol, V. Bayesian mixture analysis for metagenomic community
482 profiling. *Bioinformatics* **31**, 2930–2938 (2015).
- 483 6. Berns, K. I. Parvovirus replication. *Microbiol Rev* **54**, 316–329 (1990).
- 484 7. Sun, X. *et al.* Molecular Analysis of Vector Genome Structures After Liver
485 Transduction by Conventional and Self-Complementary Adeno-Associated Viral
486 Serotype Vectors in Murine and Nonhuman Primate Models.
487 <https://home.liebertpub.com/hum> **21**, 750–762 (2010).
- 488 8. Meier, A. F. *et al.* Herpes simplex virus co-infection facilitates rolling circle replication
489 of the adeno-associated virus genome. *PLoS Pathog* **17**, (2021).
- 490 9. Xu, Y. *et al.* Detection of viral pathogens with multiplex nanopore MinION sequencing:
491 Be careful with cross-Talk. *Front Microbiol* **9**, 2225 (2018).
- 492 10. Eccles, D., White, R., Pellefigues, C., Ronchese, F. & Lamiable, O. Investigation of
493 chimeric reads using the MinION. *F1000Research* **2017** 6:631 **6**, 631 (2017).
- 494 11. Guerra-Assunção, J. A., Goldstein, R. & Breuer, J. AYUKA: A toolkit for fast viral
495 genotyping using whole genome sequencing. *bioRxiv* 2022.09.07.506755 (2022)
496 doi:10.1101/2022.09.07.506755.
- 497 12. Risso-Ballester, J., Cuevas, J. M. & Sanjuán, R. Genome-Wide Estimation of the
498 Spontaneous Mutation Rate of Human Adenovirus 5 by High-Fidelity Deep
499 Sequencing. *PLoS Pathog* **12**, e1006013 (2016).
- 500 13. Liu, L. *et al.* Genetic diversity and molecular evolution of human adenovirus serotype
501 41 strains circulating in Beijing, China, during 2010–2019. *Infection, Genetics and*
502 *Evolution* **95**, 105056 (2021).
- 503 14. Cao, M., You, H. & Hermonat, P. L. The X Gene of Adeno-Associated Virus 2 (AAV2)
504 Is Involved in Viral DNA Replication. *PLoS One* **9**, e104596 (2014).
- 505 15. Lisowski, L. *et al.* Selection and evaluation of clinically relevant AAV variants in a
506 xenograft liver model. *Nature* **506**, 382–386 (2014).
- 507 16. Cabanes-Creus, M. *et al.* Novel human liver-tropic AAV variants define transferable
508 domains that markedly enhance the human tropism of AAV7 and AAV8. *Mol Ther*
509 *Methods Clin Dev* **24**, 88–101 (2022).
- 510 17. Cabanes-Creus, M. *et al.* Restoring the natural tropism of AAV2 vectors for human
511 liver. *Sci Transl Med* **12**, (2020).
- 512 18. Chen, Z. *et al.* Role of humoral immunity against hepatitis B virus core antigen in the
513 pathogenesis of acute liver failure. *Proc Natl Acad Sci U S A* **115**, E11369–E11378
514 (2018).
- 515 19. Wang, D. *et al.* A deep proteome and transcriptome abundance atlas of 29 healthy
516 human tissues. *Mol Syst Biol* **15**, e8503 (2019).
- 517 20. Niu, L. *et al.* Dynamic human liver proteome atlas reveals functional insights into
518 disease pathways. *Mol Syst Biol* **18**, e10947 (2022).

- 519 21. Timpe, J. M., Verrill, K. C. & Trempe, J. P. Effects of Adeno-Associated Virus on
520 Adenovirus Replication and Gene Expression during Coinfection. *J Virol* **80**, 7807
521 (2006).
- 522 22. Yakobson, B., Koch, T. & Winocour, E. Replication of adeno-associated virus in
523 synchronized cells without the addition of a helper virus. *J Virol* **61**, 972 (1987).
- 524 23. la Bella, T. *et al.* Adeno-associated virus in the liver: Natural history and
525 consequences in tumour development. *Gut* **69**, 737–747 (2020).
- 526 24. Chowdary, P. *et al.* Phase 1–2 Trial of AAVS3 Gene Therapy in Patients with
527 Hemophilia B. *New England Journal of Medicine* **387**, 237–247 (2022).
- 528 25. Chand, D. *et al.* Hepatotoxicity following administration of onasemnogene
529 abeparvovec (AVXS-101) for the treatment of spinal muscular atrophy. *J Hepatol* **74**,
530 560–566 (2021).
- 531 26. Mullard, A. Gene therapy community grapples with toxicity issues, as pipeline
532 matures. *Nat Rev Drug Discov* **20**, 804–805 (2021).
- 533 27. Morales, L., Gambhir, Y., Bennett, J. & Stedman, H. H. Broader Implications of
534 Progressive Liver Dysfunction and Lethal Sepsis in Two Boys following Systemic
535 High-Dose AAV. *Molecular Therapy* **28**, 1753 (2020).
- 536 28. Hüser, D. *et al.* Integration preferences of wildtype AAV-2 for consensus rep-binding
537 sites at numerous loci in the human genome. *PLoS Pathog* **6**, 1–14 (2010).
- 538 29. Nault, J. C. *et al.* Recurrent AAV2-related insertional mutagenesis in human
539 hepatocellular carcinomas. *Nature Genetics* 2015 47:10 **47**, 1187–1193 (2015).
- 540 30. Dalwadi, D. A. *et al.* AAV integration in human hepatocytes. *Molecular Therapy* **29**,
541 2898–2909 (2021).
- 542 31. Nathwani, A. C. Gene therapy for hemophilia. *Hematology: the American Society of*
543 *Hematology Education Program* **2019**, 1 (2019).
- 544 32. Ho, A. *et al.* Adeno-associated virus 2 infection in children with non-A-E hepatitis.
545 *medRxiv* 2022.07.19.22277425 (2022) doi:10.1101/2022.07.19.22277425.
- 546 33. Perrin, G. Q., Herzog, R. W. & Markusic, D. M. Update on clinical gene therapy for
547 hemophilia. *Blood* **133**, 407–414 (2019).
- 548 34. Divers, T. J., Tomlinson, J. E. & Tennant, B. C. The history of Theiler's disease and
549 the search for its aetiology. *The Veterinary Journal* **287**, 105878 (2022).
- 550 35. Kelgeri, C. *et al.* Clinical Spectrum of Children with Acute Hepatitis of Unknown
551 Cause. <https://doi.org/10.1056/NEJMoa2206704> (2022)
552 doi:10.1056/NEJMoa2206704.
- 553 36. Sanchez, L. H. G. *et al.* A Case Series of Children with Acute Hepatitis and Human
554 Adenovirus Infection. <https://doi.org/10.1056/NEJMoa2206294> (2022)
555 doi:10.1056/NEJMoa2206294.
- 556 37. Yang, W. X. *et al.* Prevalence of serum neutralizing antibodies to adenovirus type 5
557 (Ad5) and 41 (Ad41) in children is associated with age and sanitary conditions.
558 *Vaccine* **34**, 5579 (2016).
- 559 38. Ukhsa. National norovirus and rotavirus bulletin. Week 28 report: data to week 26 (3
560 July 2022).
- 561 39. Calcedo, R. *et al.* Adeno-Associated Virus Antibody Profiles in Newborns, Children,
562 and Adolescents. *Clin Vaccine Immunol* **18**, 1586 (2011).
- 563 40. Nathwani, A. C. *et al.* Sustained high-level expression of human factor IX (hFIX) after
564 liver-targeted delivery of recombinant adeno-associated virus encoding the hFIX gene
565 in rhesus macaques. *Blood* **100**, 1662–1669 (2002).
- 566

567 **Tables**

568

569 **Table 1: Characteristics of unexplained pediatric hepatitis cases and related specimens**

570

CASE ID	Sex	Liver Transplant	Sender	Specim. 1	ID 1	Specim. 2	ID 2	Specim. 3	ID 3
1	M	Yes	BCH	Liver	JBL1				
2	M	Yes	BCH/PHW	Liver	JBL4	NPA	JBN1		
3	F	Yes	BCH	Liver	JBL3				
4	M	Yes	BCH/UKHSA	Liver	JBL2	Blood	JBB25		
5	F	Yes	BCH	Liver	JBL5				
6	F	No	UKHSA	Blood	JBB9	Blood	JBB14	Blood	JBB16
7	F	No	UKHSA	Blood	JBB11	Blood	JBB10		
8	F	No	UKHSA	Serum	JBPL1	Blood	JBB13		
9	M	No	UKHSA	Blood	JBB1				
10	M	No	UKHSA	Blood	JBB15				
11	NA	No	GRI	Blood	JBB2				
12	M	No	UKHSA	Blood	JBB12				
13	NA	No	GRI	Blood	JBB7				
14	NA	No	GRI	Blood	JBB8				
15	NA	No	GRI	Blood	JBB4	Blood	JBB3		
16	NA	No	GRI	Blood	JBB5				
17	F	No	UKHSA	Throat.S	JBB18	Stool	JBB17		
18	F	No	UKHSA	Blood	JBB19				
19	F	No	UKHSA	Blood	JBB20	Blood	JBB23		
20	M	No	UKHSA	Blood	JBB21				
21	NA	No	PHW	NPA	JBB26				
22	NA	No	GRI	Stool	JBB27				
23	NA	No	GRI	Throat.s	JBB28	Stool	JBB30		
24	NA	No	GRI	Stool	JBB29				
25	NA	No	NHSL	Blood	JBB31				
26	NA	No	NHSL	Stool	JBB32				
27	F	No	UKHSA	Blood	JBB24				
28	M	Yes	KCH	Liver	JBL6				
29	F	Yes	KCH	Liver	JBL7	Liver	JBL8		
30	F	No	KCH	Liver	JBL9				
31	F	Yes	KCH	Liver	JBL10				
32	M	Yes	KCH	Liver	JBL11	Serum	JBB34		
33	F	Yes	KCH	Liver	JBL12				
34	M	Yes	KCH	Liver	JBL13	Serum	JBB36		
35	F	No	KCH	Liver	JBL14	Serum	JBB35		
36	M	Yes	KCH	Liver	JBL15	Serum	JBB37		
37	F	No	KCH	Serum	JBB38				
38	M	No	KCH	Serum	JBB39				

571

572 The median age for the cases is 3 years old (age range: 1y-9y). **Case 10** was 9 years old. All
 573 other cases were aged 7 or under.

574 **Cases 1-5** underwent liver transplant and had mNGS, PCR and viral WGS of their
575 specimens. **Cases 28, 29, 31-34, 36** also underwent liver transplant and had PCR for all three
576 viruses under investigation.
577 **Cases 6-27, 30, 35, 37, 38** did not receive a liver transplant. **Cases 30 & 35** had liver
578 biopsies. **Cases 6-10** had mNGS, PCR and viral WGS on their samples. **Cases 11-22** had
579 PCR for 1-2 of the viruses under investigation and viral WGS of PCR positives. **Cases 23-27**
580 only had HAdV WGS on their samples and there was no residual material for further testing.
581 **Cases 31,36,38,39** had PCR for all three viruses under investigation.
582 NPA: Nasopharygeal aspirate BCH: Birmingham Children's Hospital, PHW: Public Health
583 Wales, GRI: Glasgow Royal Infirmary, NHSL: NHS Lothian, KCH: King's College Hospital
584

ACCELERATED ARTICLE PREVIEW

585 **Table 2: PCR, metagenomics and viral WGS results from cases where metagenomic**
586 **sequencing was performed**
587

Case ID	Sample ID	PCR CT values			Metagenomics reads						Viral WGS Coverage (10X)		
		AAV2	HAdV	HHV-6B	DNA			RNA			AAV2	HAdV	HHV-6B
					AAV2	HAdV	HHV-6B	AAV2	HAdV	HHV-6B			
Liver													
1	JBL1	17	37	29	1343	0	8	574	0	0	97	-	3
2	JBL4	21	42	32	360	0	8	49	0	0	93	-	2
3	JBL3	20	37	30	1189	0	4	95	0	0	98	-	2
4	JBL2	20	37	27	1564	0	203	42	0	0	98	-	94
5	JBL5	21	37	28	266	0	12	F	F	F	-	-	-
Blood													
6*	JBB14/ JBB16/ JBB9	24	36	37	151	0	0	77	0	0	95	35.5	-
7	JBB10/ JBB11	21	36	37	103	0	0	F	F	F	49	F	-
8	JBPL1/ JBB13	25	P/N	-/N	277	0	0	165	0	0	94	F	-
9	JBB1	19	P/-	P/-	1936	5	0	0	0	0	94	F	-
10	JBB15	-/N	N/N	37	0	0	0	F	F	F	-	F	-

588 - : Not tested (at GOSH due to insufficient residual material)

589 N: negative PCR result

590 P: Positive PCR result in referring laboratory

591 Where two results are shown, the first refers to the referring laboratory and the second to
592 GOSH.

593 Where there was a discrepancy, the positive result is shown.

594 F: Failed

595 Where there is more than one sample for a single patient, CT values represent the mean
596 across the samples that were tested.

597 *Metagenomics reads: the result of combining the datasets from two blood samples from the
598 same case

599 *De novo* assembly of unclassified metagenomics reads was unremarkable

600

601 **Figure Legends**

602

603 **Figure 1: HAdV Epidemiology and experimental outline**

604 **a**, HAdV in all sample types; epidemiology since January 2022. Source: secondary
605 Generation Surveillance system data, ie laboratory reports to UKHSA of a positive
606 adenovirus result conducted by a laboratory in England, and includes any sample type. Dots
607 represent the day of presentation for the 28/38 cases for which we had data, in green the liver-
608 transplant cases and in red the non-transplant cases. **b**, Case and control specimens by source.
609 **c**, Tests carried out by specimen type. More detail on samples tested and the results can be
610 found in Tables 1 and 2. Not all tests were carried out on all samples due to lack of material.
611 N refers to the total number of cases/controls. Numbers of each sample type may not sum to
612 this total because samples of more than one type were sometimes taken from the same
613 patient. For details, see Table 1.

614

615 **Figure 2: Proportion of positive cases and viral loads (CT values) for cases and controls**

616 * indicates immunocompromised comparators. Proportion of PCR positive and negative
617 results for **a** AAV2, **b** HAdV and **c** HHV-6. CT values < 38 were defined as positive. CT >38
618 where the virus was detected within the maximum 45 cycles were defined as low-level
619 positive (LLP). **d**, AAV2 in blood from cases, PERFORM /DIAMOND immunocompetent
620 controls and immunocompromised comparators. Blue: HAdV infection, green: non-HAdV
621 hepatitis, red: healthy. **e**, HAdV levels in whole blood from cases and immunocompromised
622 comparators. **f**, HHV-6 in whole blood from cases and immunocompromised comparators. **g**,
623 HAdV, AAV2 and HHV-6 levels in frozen liver tissue from cases and immunocompromised
624 comparators. In the box plots, the bold middle line represents the median and the upper and
625 lower horizontal lines represent the upper (75th percentile) and lower (25th percentile)
626 quartiles respectively. Whiskers show maximum and minimum values. Each point represents
627 one case or control. N refers to the number of cases or controls. Where more than one sample
628 for a case was tested, the midpoint of the CT has been plotted. All repeat tests had values
629 <2CTs apart, ie within the limits of methodological error. The dotted line marked LLP
630 indicates the low-level positive threshold (CT=38). Points below the second dotted line
631 represent samples below the limit of PCR detection (CT=45). Wilcoxon non-parametric rank
632 sum tests were conducted for **e & g** and a Kruskal-Wallis test followed by pairwise Wilcoxon
633 tests with a Benjamini-Hochberg correction for multiple comparisons for **d & f**. All tests
634 were two-tailed. Numbers show the p-value compared to cases. NS: not significant. tr:
635 received liver transplant.

636

637 **Figure 3: Phylogenetic trees for HAdV, AAV2 and HHV-6B**

638 Maximum likelihood phylogenetic trees combining reference sequences from the RefSeq
639 database, publicly available complete genomes from GenBank, UK non-outbreak controls
640 (open squares) and unexplained hepatitis cases (black squares) for the different viruses
641 involved: **a** HAdV **b** AAV2 and **c** HHV-6. HAdV and HHV-6B trees are mid-point rooted,
642 while AAV2 is rooted the RefSeq sequence: NC_001401.2. Bootstrap values less than 90 are
643 not shown.

644

645
646
647
648
649
650
651
652
653
654
655
656
657
658
659
660
661

Figure 4: Transcriptomic and proteomic analysis of case liver samples

Transcriptomic analysis was conducted for the five frozen case liver samples from transplanted patients. **a**, Expression of cytokine-inducible transcriptional modules in normal liver, and AAV2 (n=4) or HBV (n=17) associated hepatitis requiring transplantation are shown as DZ scores for the expression of each module, reflecting the difference from the average score from normal liver (n=10) data sets, all from different patients. Each point represents the score from a single data set/sample. **b & c**, Volcano plots of differentially expressed proteins (**b**) and peptides (**c**). The volcano plots illustrate fold changes and corresponding p-values for the comparison between 5 liver explants from 5 patients and 7 control healthy livers from 7 controls. Each dot represents a protein/peptide. The p-values were calculated by applying two-tailed empirical Bayes moderated t-statistics on protein/peptide-wise linear models. Proteins (**b**) and peptides (**c**) differentially expressed (absolute $\log_2(\text{fold change}) > 6$ and $P < 1e-07$) are coloured as red (up-regulated) and blue (down-regulated). The p-values illustrated here are not adjusted for multiple comparisons. Full tables can be found in **Supplementary Tables 12-14**.

ACCELERATED ARTICLE PREVIEW

662 **METHODS**

663 **Ethics**

664 Metagenomic analysis and adenovirus sequencing were carried out by the routine diagnostic
665 service at Great Ormond Street Hospital. Additional PCRs, Immunohistochemistry and
666 proteomics on samples received for metagenomics are part of the Great Ormond Street
667 Hospital (GOSH) protocol for confirmation of new and unexpected pathogens. The use for
668 research of anonymised laboratory request data, diagnostic results and residual material from
669 any specimen received in the GOSH diagnostic laboratory, including all cases received from
670 Birmingham's Children Hospital UKHSA, Public Health Wales, Public health Scotland as
671 well as non-case samples from UKHSA, Public Health Scotland and Great Ormond Street
672 Hospital research was approved by UCL Partners Pathogen Biobank under ethical approval
673 granted by the NRES Committee London-Fulham (REC reference: 17/LO/1530).

674 Children undergoing liver transplant were consented for additional research under the
675 International Severe Acute Respiratory and Emerging Infections Con Ethics sortium
676 (ISARIC) WHO Clinical Characterisation Protocol UK (CCP-UK) [ISRCTN 66726260]
677 (RQ3001-0591, RQ301-0594, RQ301-0596, RQ301-0597, RQ301-0598). Ethical approval
678 for the ISARIC CCP-UK study was given by the South Central–Oxford C Research Ethics
679 Committee in England (13/SC/0149), the Scotland A Research Ethics Committee
680 (20/SS/0028), and the WHO Ethics Review Committee (RPC571 and RPC572).

681 The United Kingdom Health Security Agency (UKHSA) has legal permission, provided by
682 Regulation 3 of The Health Service (Control of Patient Information) Regulations 2002, to
683 process patient confidential information for national surveillance of communicable diseases
684 and as such, individual patient consent is not required.

685 Control subjects from the EU horizon 2020 research and innovation program
686 DIAMONDS/PERFORM (grant agreement No. 668303 and 848196) were recruited
687 according to the approved enrolment procedures of each study, and with the informed consent
688 of parents or guardians: DIAMONDS (London – Dulwich Research Ethics Committee:
689 20/HRA/1714); PERFORM (London – Central Research Ethics Committee: 16/LO/1684).

690
691 The sample IDs for the cases and controls are anonymised IDs that cannot reveal the identity
692 of the study subjects and are not known to anyone outside the research group, such as the
693 patients or the hospital staff.

694

695 **Samples**

696 Initial diagnostic testing by metagenomics and PCR was performed at Great Ormond Street
697 Hospital Microbiology and Virology clinical laboratories. Further whole genome sequencing
698 and characterization was performed at UCL.

699 Cases

700 Birmingham Children's Hospital provided us with explanted liver tissue from five biopsy
701 sites from five cases, five whole blood 500ul from four cases and serum plasma from one
702 case (**Table 1, Figure 1B**). These were used in metagenomics testing (**Table 2**), followed by
703 HAdV, HHV-6 and AAV2 testing by PCR and, depending on CT value, whole genome
704 sequencing (**Supplementary Table 7, 9, 10**). We subsequently received 25 additional
705 specimens from UKHSA, Public Health Wales and Public Health Scotland / Edinburgh Royal
706 Infirmary, including 16 additional blood samples, four respiratory specimens and five stool
707 samples, for HAdV WGS and depending on residual material for AAV2 PCR testing
708 followed by sequencing (**Table 1, Table 2, Figure 1B, Supplementary Table 7, 9, 10**). We
709 also received 10 formalin fixed, paraffin embedded (FFPE) liver biopsy samples and 6 serum
710 samples from 11 cases from King's College Hospital (**Table 1**). Of these cases, 7 had
711 received liver transplants.

712 Controls from DIAMONDS and PERFORM

713 PERFORM (Personalised Risk assessment in Febrile illness to Optimise Real-life
714 Management across the European Union) recruited children from 10 EU countries (2016-
715 2020. PERFORM was funded by the European Union's Horizon 2020 program under GA No
716 668303.

717 DIAMONDS (Diagnosis and Management of Febrile Illness using RNA Personalised
718 Molecular Signature Diagnosis) is funded by the European Union Horizon 2020 program
719 grant number 848196. Recruitment commenced in 2020 and is ongoing. Both studies
720 recruited children presenting with suspected infection or inflammation and assigned them to
721 diagnostic groups according to a standardised algorithm.

722 Controls from GOSH for PCR

723 Blood samples from 17 patients not linked to the non-A-E hepatitis outbreak were tested by
724 real-time PCR targeting AAV2 (**Extended Data Table 2B**). These comparators were patients
725 with ALT/AST >500 and HAdV or CMV viraemia. These were purified DNA from residual
726 diagnostic specimens received in the GOSH Microbiology and Virology laboratory in the
727 previous year. All residual specimens were stored at -80 °C prior to testing and pseudo-
728 anonymised at the point of processing and analysis. Viraemia was initially detected using
729 targeted real-time PCR during routine diagnostic testing with UKAS-accredited lab-
730 developed assays that conform to ISO:15189 standards.

731 In addition to the blood samples, four residual liver biopsies from four control patients
732 referred for investigation of infection were tested by AAV2 and HHV-6B PCR. The liver
733 biopsies were submitted to the GOSH microbiology laboratory for routine diagnosis by
734 bacterial broad-range 16S rRNA gene PCR or metagenomics testing in 2021 and 2022. 3/4 of
735 the control patients were known to have elevated liver enzymes. Two adult frozen liver

736 samples previously tested by metagenomics were negative for AAV2 and positive for HHV6
737 (**Supplementary Table 5**).

738

739 **Controls from UKHSA**

740 We received a blood sample from one patient with raised liver enzymes and HAdV infection.
741 We also received one control stool sample from Public Health Scotland/Edinburgh Royal
742 Infirmary and 22 control stool samples for sequencing.

743 **Controls from King's College Hospital**

744 A single formalin fixed paraffin embedded (FFPE) liver biopsy control of normal marginal
745 tissue from a hepatoblastoma from a child was negative for AAV2 and HAdV, but positive
746 for HHV-6B (CT = 37).

747

748 **Controls from QMUL**

749 We received FFPE liver control samples from 10 adults and 3 children (under 18) with other
750 viral hepatitis, toxic liver necrosis, autoimmune and other hepatitis, and normal liver, from
751 Queen Mary University of London. PCR gave valid results for samples from 2 children and 8
752 adults, all of which were negative by PCR for AAV2 and HHV6, apart from one adult sample
753 which was positive for HHV6 at high CT value (**Supplementary Table 5**).

754

755 **Metagenomic sequencing**

756 **Nucleic acid purification**

757 Frozen liver biopsies were infused overnight at -20°C with RNAlater-ICE. Up to 20 mg
758 biopsy was lysed with 1.4mm ceramic, 0.1mm silica and 4mm glass beads, prior to DNA and
759 RNA purification using the Qiagen AllPrep DNA/RNA Mini kit as per manufacturers'
760 instructions, with a 30 µl elution volume for RNA and 50 µl for DNA.

761 Up to 400 µl whole blood was lysed with 0.5mm and 0.1 mm glass beads prior to DNA and
762 RNA purification on a Qiagen EZ1 instrument with an EZ1 virus mini kit as per
763 manufacturer's instructions, with a 60 µl elution volume.

764 For quality assurance, every batch of samples was accompanied by a control sample
765 containing feline calicivirus RNA and cowpox DNA which was processed alongside clinical
766 specimens, from nucleic acid purification through to sequencing. All specimens and controls
767 were spiked with MS2 phage RNA internal control prior to nucleic acid purification.

768 **Library preparation and sequencing**

769 RNA from whole blood samples with RNA yield >2.5 ng/μl and from biopsies underwent
770 ribosomal RNA depletion and library preparation with KAPA RNA HyperPrep kit with
771 RiboErase, according to manufacturer's instructions. RNA from whole blood with RNA yield
772 <2.5 ng/μl did not undergo rRNA depletion prior to library preparation.

773 DNA from whole blood samples with DNA yield >1 ng/μl and from biopsies underwent
774 depletion of CpG-methylated DNA using the NEBNext® Microbiome DNA Enrichment Kit,
775 followed by library preparation with NEBNext Ultra II FS DNA Library Prep Kit for
776 Illumina, according to manufacturer's instructions. DNA from whole blood with DNA yield
777 <1 ng/μl did not undergo depletion of CpG-methylated DNA prior to library preparation.

778 Sequencing was performed with a NextSeq High output 150 cycle kit with a maximum of 12
779 libraries pooled per run, including controls.

780 **Metagenomics data analysis**

781 **Pre-processing pipeline**

782 An initial quality control step was performed by trimming adapters and low-quality ends
783 from the reads (Trim Galore!⁴¹ version 0.3.7). Human sequences were then removed using the
784 human reference GRCH38 p.9 (Bowtie2⁴², version 2.4.1) followed by removal of low quality
785 and low complexity sequences (PrinSeq⁴³, version 0.20.3). An additional step of human seq
786 removal followed (megaBLAST⁴⁴, version 2.9.0). For RNA-seq, ribosomal RNA sequences
787 were also removed using a similar 2 step-approach (Bowtie2 and megaBLAST). Finally,
788 nucleotide similarity and protein similarity searches were performed (megaBLAST and
789 DIAMOND⁴⁵ (version 0.9.30) respectively) against custom reference databases that consisted
790 of nucleotide and protein sequences of the RefSeq collections (downloaded March 2020) for
791 viruses, bacteria, fungi, parasites and human.

792

793 **Taxonomic classification**

794 DNA and RNA sequence data was analysed with metaMix⁵ (version 0.4) nucleotide and
795 protein analysis pipelines.

796 metaMix resolves metagenomics mixtures using Bayesian mixture models and parallel
797 MCMC search of the potential species space to infer the most likely species profile.

798 metaMix considers all reads simultaneously to infer relative abundances and probabilistically
799 assign the reads to the species most likely to be present. It uses an 'unknown' category to
800 capture the fact that some reads cannot be assigned to any species. The resulting
801 metagenomic profile includes posterior probabilities of species presence as well as Bayes
802 factor for presence versus absence of specific species. There are two modes, metaMix-

803 protein, which is optimal for RNA virus detection and metaMix-nucl, which is best for
804 speciation of DNA microbes. Both modes were used for RNA-seq while metaMix-nucl for
805 DNA-seq.

806 For sequence results to be valid, MS2 phage RNA had to be detected in every sample and
807 feline calicivirus RNA and cowpox DNA, with no additional unexpected organisms, detected
808 in the controls.

809 Confirmatory mapping of AAV2

810 The RNA-Seq reads were mapped to the AAV2 reference genome (NCBI reference sequence
811 NC_001401) using Bowtie2, with the `-very-sensitive` option. Samtools⁴⁶ version 1.9) and
812 Picard (version 2.26.9, <http://broadinstitute.github.io/picard/>) were used to sort, deduplicate
813 and index the alignments, and to create a depth file, which was plotted using a custom script
814 in R.

815 de novo assembly of unclassified reads

816 We performed a *de novo* assembly step with metaSPADES⁴⁷(v3.15.5), using all the reads
817 with no matches to the nucleotide database we used for our similarity search. A search using
818 megaBLAST with the standard nucleotide collection was carried out on all resulting contigs
819 over 1000bp in length. All of the contigs longer than 1000bp matched to human, except two
820 which mapped to Torque Teno virus (TTV).

821

822

823 **Nanopore Sequencing**

824

825 DNA from up to 20 mg of liver was purified using the Qiagen DNeasy Blood & Tissue kit as
826 per manufacturer's instructions. Samples with limited amount of DNA were fragmented to an
827 average size of 10kb using a Megaruptor 3 (Diagenode) to reach an optimal molar
828 concentration for library preparation. QC was performed using a Femto Pulse System (Agilent
829 Technologies) and a Qubit fluorometer (Invitrogen). Samples were prepared for Nanopore
830 sequencing using the Ligation Sequencing Kit SQK-LSK110. DNA was sequenced on a
831 PromethION using R9.4.1 flowcells (Oxford Nanopore Technologies). Samples were run for
832 72 hours including a washing and reload step after 24 and 48 hours.

833

834 All library preparation and sequencing were performed by UCL Long Read Sequencing
835 facility.

836

837 Passed reads from Minknow were mapped to the reference AAV2 genome (NC_001401)
838 using minimap²⁴⁸ using the default parameters. Reads were trimmed of adapters using
839 Porechop v0.2.4 (<https://github.com/rrwick/Porechop/>), with the sequences of the adapters
840 used added to adapters.py, and using an adapter threshold of 85. Reads that also mapped by
841 minimap to the human genome (Ensemble GRCh38_v107), which could be ligation artefacts,

842 were excluded from further analysis. The passed reads were also classified using Kraken2⁴⁹
843 with the PlusPF database (5/17/2021). The data relating to AAV2 reads in Supplementary
844 Table 3 refer to reads that were classified as AAV2 by both minimap2 and Kraken2 (version
845 2.0.8-beta), since the results from both methods were similar. Four reads across all four
846 lower-depth samples were classified as HHV-6B by the EPI2ME WIMP⁵⁰ pipeline. No reads
847 were classified as HAdV or HHV-6B by Kraken2 in the two higher-depth samples.
848 Alignment dot plots were created for the AAV2 reads using redotable (version 1.1)⁵¹, with a
849 window size of 20. These were manually classified into possible complex and monomeric
850 structures.

851

852 **Integration analysis of Illumina data**

853

854 We investigated potential integrations of AAV2 and HHV-6 viruses into the genome using
855 the Illumina metagenomics data for 5 liver transplant cases. We first processed the pair-end
856 reads (average sequence coverage per genome=5x), first quality checking using FastQC⁵²,
857 with barcode and adaptor sequence trimmed by TrimGalore (phred-score=20). Potential
858 viral integrations were investigated with Vseq-Toolkit⁵³ (Mode 3 with default settings except
859 for high stringency levels). Predicted genomic integrations were visualized with IGV⁵⁴,
860 requiring at least 3 reads supporting an integration site, spanning both human and viral
861 sequences. Predicted integrations were supported by only one read, thus not fulfilling the
862 algorithm criteria. Sequencing was performed at a lower depth than optimal for integration
863 analysis but no evidence was found for AAV2 or HHV-6B integration into cases' genomes.

864

865 **PCR**

866 Real-time PCR targeting a 62 nt region of the AAV2 inverted terminal repeat (ITR) sequence
867 was performed using primers and probes previously described⁵⁵. This assay is predicted to
868 amplify AAV2 and AAV6. The Qiagen QuantiNova probe PCR kit (PERFORM and
869 DIAMONDS controls) or Qiagen Quantifast probe PCR kit (all other samples) were used.
870 Each 25 µl reaction consisted of 0.1 µM forward primer, 0.34 µM reverse primer, 0.1 µM
871 probe with 5 µl template DNA.

872 Real-time PCR targeting a 74 bp region of the HHV6 DNA polymerase gene was performed
873 using primers and probes previously described⁵⁶ multiplexed with an internal positive control
874 targeting mouse (*mus*) DNA spiked into each sample during DNA purification, as previously
875 described⁵⁷. Briefly, each 25 µl reaction consisted of 0.5 µM each primer, 0.3 µM HHV-6
876 probe, 0.12 µM each *mus* primer, 0.08 µM *mus* probe and 12.5 µl Qiagen Quantifast Fast
877 mastermix with 10 µl template DNA.

878 Real-time PCR targeting a 132 bp region of the Adenovirus hexon gene was performed using
879 primers and probes previously described⁵⁸ multiplexed with an internal positive control
880 targeting mouse (*mus*) DNA spiked into each sample during DNA purification, as previously
881 described⁵⁷. Briefly, each 25 µl reaction consisted of 0.6 µM each HHV6 primer, 0.4 µM

882 HHV6 probe, 0.12 μ M each *mus* primer, 0.08 μ M *mus* probe and 12.5 μ l Qiagen Quantifast
883 Fast mastermix with 10 μ l template DNA.

884 PCR cycling for all targets, apart from the controls from the PERFORM and DIAMONDS
885 studies, was performed on an ABI 7500 Fast thermocycler and consisted of 95 $^{\circ}$ C for 5
886 minutes followed by 45 cycles of 95 $^{\circ}$ C for 30 seconds and 60 $^{\circ}$ C for 30 seconds. For the
887 PERFORM and DIAMONDS controls, PCR was performed on a StepOnePlus™ Real-Time
888 PCR System and consisted of 95 $^{\circ}$ C for 2 minutes followed by 45 cycles of 95 $^{\circ}$ C for 5
889 seconds and 60 $^{\circ}$ C for 10 seconds. Each PCR run included a no template control and a DNA
890 positive control for each target.

891 Neat DNA extracts of the FFPE material were inhibitory to PCR so PCR results shown were
892 performed following a 1 in 10 dilution,

893 **AAV2 RT-qPCR**

894 RNA samples were treated with Turbo-DNA free kit (Thermo) to remove residual genomic
895 DNA. cDNA was synthesised using QuantiTect Reverse Transcription kit. Briefly, 12 μ l of
896 RNA were mixed with 2 μ l of gDNA Wipeout buffer and incubated at 42 $^{\circ}$ C for 2 minutes
897 and transferred to ice. 6 μ l of reverse transcription mastermix and incubated at 42 $^{\circ}$ C for 20
898 min followed by 3 min at 95 $^{\circ}$ C.

899
900 Real-time PCR targeting a 120 nt region of the AAV2 *cap* ORF sequence was performed
901 using primers *AAV2_cap_Fw*- ATCCTTCGACCACCTTCAGT, *AAV2_cap_Rv* – GATT
902 CCAGCGTTTGCTGTT and probe *AAV2_cap_Pr* FAM-ACACAGTAT/ZEN/TCC ACGG
903 GACAGGT-IBFQ. This assay is predicted to amplify AAV2 and AAV6. The Qiagen
904 QuantiNova probe PCR kit was used. Each 25 μ l reaction consisted of 0.1 μ M forward
905 primer, 0.1 μ M reverse primer, 0.2 μ M probe with 2.5 μ l template cDNA.

906
907 PCR was performed on a StepOnePlus™ Real-Time PCR System and consisted of 95 $^{\circ}$ C for
908 2 minutes followed by 45 cycles of 95 $^{\circ}$ C for 5 seconds and 60 $^{\circ}$ C for 10 seconds. Each PCR
909 run included a no template control, a DNA positive control and a RNA control from each
910 sample to verify efficient removal of gDNA.

911 **Immunohistochemistry (IHC)**

912 All IHC was done on Formalin Fixed Paraffin Embedded tissue cut at 3 μ m thickness.

913 **Adenovirus**

914 Adenovirus immunohistochemistry was carried out using the Ventana Benchmark ULTRA,
915 Optiview Detection Kit, PIER with Protease 1 for 4min, Ab incubation 32min (Adenovirus
916 clone 2/6 & 20/11, Roche, 760-4870, pre-diluted). The positive control was a known
917 Adenovirus positive gastrointestinal surgical case.

918

919 **Preparation of AAV2 positive controls**

920

921 The plasmid used for transfection was pAAV2/2 (addgene, Plasmid #104963,
922 <https://www.addgene.org/104963/>) which expresses the Rep/Cap genes of AAV2. This was
923 delivered by tail-vein hydrodynamic injection⁵⁹ into albino C57Bl/6 mice (5 microgrammes
924 in 2 mls PBS). Negative controls received PBS alone. At 48 hours, mice were terminally
925 exsanguinated and perfused by PBS. Livers were collected into 10% Neutral Buffered
926 Formalin (CellPath UK). This was performed under Home Office License PAD4E6357.

927 AAV2 immunohistochemistry was carried out with four commercially available antibodies:

- 928 • Leica Bond-III, Bond Polymer Refine Detection Kit with DAB Enhancer, HIER with
929 Bond Epitope Retrieval Solution 1 (citrate based pH 6) for 30min, Ab incubation
930 30min (Anti-AAV VP1/VP2/VP3 clone B1, PROGEN, 690058S, 1:100).
- 931 • Leica Bond-III, Bond Polymer Refine Detection Kit with DAB Enhancer, HIER with
932 Bond Epitope Retrieval Solution 1 (citrate based pH 6) for 40min, Ab incubation
933 30min (Anti-AAV VP1/VP2/VP3 rabbit polyclonal, OriGene, BP5024, 1:100)
- 934 • • Leica Bond-III, Bond Polymer Refine Detection Kit with DAB Enhancer, HIER
935 with Bond Epitope Retrieval Solution 1 (citrate based pH 6) for 40min, Ab incubation
936 30min (Anti-AAV VP1 clone A1, OriGene, BM5013, 1:100).
- 937 • • Leica Bond-III, Bond Polymer Refine Detection Kit with DAB Enhancer, HIER
938 with Bond Epitope Retrieval Solution 1 (citrate based pH 6) for 40min, Ab incubation
939 30min (Anti-AAV VP1/VP2 clone A69, OriGene, BM5014, 1:100)

940 HHV6 immunohistochemistry staining was carried out with:

- 941 • Leica Bond-III, Bond Polymer Refine Detection Kit with DAB Enhancer, PIER with
942 Bond Enzyme 1 Kit 10min, Ab incubation 30min (Mouse monoclonal [C3108-103] to
943 HHV6, ABCAM, ab128404, 1:100).

944 Negative reagent control slides were stained using the same antigen retrieval conditions and
945 staining protocol incubation times using only Bond™ Primary Antibody Diluent #AR9352
946 for the antibody incubation.

947

948 **Electron Microscopy**

949 Samples of liver were fixed in 2.5% glutaraldehyde in 0.1M cacodylate buffer followed by
950 secondary fixation in 1.0% osmium tetroxide. Tissues were dehydrated in graded ethanol,
951 transferred to an intermediate reagent, propylene oxide and then infiltrated and embedded in
952 Agar 100 epoxy resin. Polymerisation was undertaken at 60 °C for 48 hours. 90nm ultrathin
953 sections were cut using a Diatome diamond knife on a Leica UC7 ultramicrotome. Sections
954 were transferred to copper grids and stained with alcoholic uranyl acetate and Reynold's lead
955 citrate. The samples were examined using a JEOL 1400 transmission electron microscope.
956 Images were captured on an AMT XR80 digital camera.

957

958 **Whole genome sequencing**

959 **Bait Design**

960 To produce the capture probes for hybridisation, biotinylated RNA oligonucleotides (baits)
961 used in the SureSelectXT protocols for HAdV and HHV6 WGS were designed in-house
962 using Agilent community design baits with part numbers 5191-6711 and 5191-6713
963 respectively. They were synthesised by Agilent Technologies, Santa Clara, California
964 (Agilent Technologies, 2021) (available through Agilent's Community Designs programme:
965 SSXT CD Pan Adenovirus and SSXT CD Pan HHV6 and used previously^{60,61}).

966 **Library preparation and sequencing**

967 For whole genome sequencing of HAdV and HHV-6B, DNA (bulked with male human
968 gDNA (Promega) if required) was sheared using a Covaris E220 focused ultra-sonication
969 system (PIP 75, duty factor 10, cycles per burst 1000). End-repair, non-templated addition of
970 3' poly A, adapter ligation, hybridisation, PCR (pre-capture cycles dependent on DNA input
971 and post capture cycles dependent on viral load), and all post-reaction clean-up steps were
972 performed according to either the SureSelectXT Low Input Target Enrichment for Illumina
973 Paired-End Multiplexed Sequencing protocol (version A0), the SureSelectXT Target
974 Enrichment for Illumina Paired-End Multiplexed Sequencing protocol (version C3) or
975 SureSelectXTHS Target Enrichment using the Magnis NGS Prep System protocol (version
976 A0) (Agilent Technologies). Quality control steps were performed on the 4200 TapeStation
977 (Agilent Technologies). Samples were sequenced using the Illumina MiSeq platform. Base
978 calling and sample demultiplexing were performed as standard for the MiSeq platform,
979 generating paired FASTQ files for each sample. A negative control was included on each
980 processing run. A targeted enrichment approach was used due to the predicted high
981 variability of the HHV-6 and HAdV genomes.

982 For AAV2 WGS, an AAV2 primer scheme was designed using primalscheme⁶² with 17
983 AAV2 sequences from NCBI and 1 AAV2 sequence provided by GOSH from metagenomic
984 sequencing of a liver biopsy DNA extract as the reference material. These primers amplify 15
985 overlapping 400 bp amplicons. Primers were supplied by Merck. Two multiplex PCR
986 reactions were prepared using Q5® Hot Start High-Fidelity 2X Master Mix, with a 65°C, 3
987 min annealing/extension temperature. Pool 1 and 2 multiplex PCRs were run for 35 cycles.
988 10uL of each PCR reaction were combined and 20uL nuclease-free water added. Libraries
989 were prepared either manually or on the Agilent Bravo NGS workstation option B, following
990 a reduced-scale version of the Illumina DNA protocol as used in the CoronaHiT protocol⁶³.
991 Equal volumes of the final libraries were pooled, bead purified and sequenced on the Illumina
992 MiSeq. A negative control was included on each processing run.

993 All library preparation and sequencing were performed by UCL Genomics.

994 **AAV2 Sequence Analysis**

995 The raw fastq reads were adapted, trimmed and low-quality reads removed. The reads were
996 mapped to NC_001401 reference sequence and then the amplicon primers regions were
997 trimmed using the location provided in a bed file. Consensus sequences were then called at a
998 minimum of 10X coverage. The entire processing of raw reads to consensus was carried out
999 using nf-core/viralrecon pipeline (<https://nf-co.re/viralrecon/2.4.1>)
1000 (doi:<https://doi.org/10.5281/zenodo.3901628>). Basic quality metrics for the samples
1001 sequenced are in **Supplementary Table 9**. All samples that gave 10x genome coverage over
1002 90% were then used for further phylogenetic analysis. Samples were aligned along with
1003 known reference strains from genbank using MAFFT⁶⁴ (version v7.271) and the trees were
1004 built with IQ-TREE⁶⁵ (multicore version 1.6.12) with 1000 rapid bootstraps and aLRT
1005 support. The samples were then labelled based on type and provider on the trees (Fig 3A).

1006 For each AAV2 sample, we aligned the consensus nucleotide sequence to the AAV2
1007 reference sequence. From these alignments, the exact coordinates of the sample capsid were
1008 determined. We then used the coordinates to extract the corresponding nucleotide sequence
1009 and translated it to find the amino acid sequence. We then compared each sample to the
1010 reference to identify amino acid changes. Amino acid sequences from AAV capsid sequences
1011 were retrieved from GenBank for AAV1 to AAV12. Amino acid sequences of capsid
1012 constructs designed to be more hepatotropic were retrieved from ^{16,66}. These sequence sets
1013 were then aligned to the AAV2 reference sequence using MAFFT⁶⁴. We then compared each
1014 construct to the AAV2 reference to identify amino acid changes present, while retaining the
1015 AAV2 coordinate set.

1016 **HAdV and HHV-6B sequence analysis**

1017 Raw data quality control is performed using trim-galore (v.0.6.7) on the raw FASTQ files.

1018 For HHV-6B, short reads were mapped with BWA mem⁶⁷ (0.7.17-r1188) using the RefSeq
1019 reference NC_000898.

1020 For adenovirus, genotyping is performed using AYUKA¹¹(version 22-111). This novel tool is
1021 used to confidently assign one or more adenovirus genotypes to a sample of interest,
1022 assessing inter-genotype recombination if more than one genotype detected. The results from
1023 this screening step guide which downstream analyses are performed, and which reference
1024 genome(s) are used. If mixed infection is suspected, reads are separated using bbsplit
1025 (<https://sourceforge.net/projects/bbmap/>), and each genotype is analysed independently as
1026 normal. If recombination is suspected, a more detailed analysis is performed using RDP and
1027 the sample is excluded from phylogenetic analysis. After genotyping, the cleaned read data is
1028 mapped using BWA to the relevant reference sequence(s), single nucleotide polymorphisms
1029 and small insertions and deletions are called using bcftool (version 1.15.1,
1030 <https://github.com/samtools/bcftools>) and a consensus sequence is generated also with
1031 bcftools, masking with Ns positions that do not have enough read support (15X by default).
1032 Consensus sequences generated with the pipeline are then concatenated to previously
1033 sequenced samples and a multiple sequence alignment is performed using the G-INS-I
1034 algorithm in the MAFFT software (MAFFT G-INS-I v7.481). The multiple sequence

1035 alignment is then used for phylogenetic analysis with IQ-TREE (IQ-TREE 2 2.2.0), using
1036 modelfinder and performing 1000 rapid bootstraps.

1037 **Proteomics Data generation**

1038 Liver explant tissue from cases was homogenized in lysis buffer, 100 mM Tris (pH 8.5), 5%
1039 Sodium dodecyl sulfate, 5 mM tris(2-carboxyethyl)phosphine, 20 mM chloroacetamide then
1040 heated at 95 degrees for 10 minutes and sonicated in ultrasonic bath for other 10. The lysed
1041 proteins were quantified with NanoDrop 2000 (Thermo Fisher Scientific). 100 µg were
1042 precipitated with Methanol/Chloroform protocol and then protein pellets were reconstituted
1043 in 100 mM tris (pH 8.5) and 4% sodium deoxycholate (SDC). The proteins were subjected to
1044 proteolysis with 1:50 trypsin overnight at 37°C with constant shaking. Digestion was stopped
1045 by adding 1% trifluoroacetic acid to a final concentration of 0.5%. Precipitated SDC was
1046 removed by centrifugation at 10,000g for 5 min, and the supernatant containing digested
1047 peptides was desalted on an SOLAµ HRP (Thermo Fisher Scientific). 50 µg of the desalted
1048 peptide were then fractionated on Vanquish HPLC (Thermo Fisher Scientific) using a
1049 Acquity BEH C18 column (2.1 x 50 mm with 1.7µm particles from Waters): buffer A was 10
1050 mM ammonium formate at pH 10, while buffer B was 80% Acetonitrile and the flow was set
1051 to 500µL/min. We used a gradient of 8 minutes to collect 24 fractions that were then
1052 concatenated to obtain 12. These 12 fractions were dried and dissolved in 2% formic acid
1053 before liquid chromatography–tandem mass spectrometry (MS/MS) analysis. An estimated
1054 total of 2000 ng from each fraction was analysed using an Ultimate3000 high-performance
1055 liquid chromatography system coupled online to an Eclipse mass spectrometer (Thermo
1056 Fisher Scientific). Buffer A consisted of water acidified with 0.1% formic acid, while buffer
1057 B was 80% acetonitrile and 20% water with 0.1% formic acid. The peptides were first
1058 trapped for 1 min at 30 µl/min with 100% buffer A on a trap (0.3 mm by 5 mm with PepMap
1059 C18, 5 µm, 100 Å; Thermo Fisher Scientific); after trapping, the peptides were separated by a
1060 50-cm analytical column (Acclaim PepMap, 3 µm; Thermo Fisher Scientific). The gradient
1061 was 9 to 35% B in 103 min at 300 nl/min. Buffer B was then raised to 55% in 2 min and
1062 increased to 99% for the cleaning step. Peptides were ionized using a spray voltage of 2.1 kV
1063 and a capillary heated at 280°C. The mass spectrometer was set to acquire full-scan MS
1064 spectra (350 to 1400 mass/charge ratio) for a maximum injection time set to Auto at a mass
1065 resolution of 120,000 and an automated gain control (AGC) target value of 100%. For a
1066 second the most intense precursor ions were selected for MS/MS. HCD fragmentation was
1067 performed in the HCD cell, with the readout in the Orbitrap mass analyser at a resolution of
1068 15,000 (isolation window of 3 Th) and an AGC target value of 200% with a maximum
1069 injection time set to Auto and a normalized collision energy of 30%. All raw files were
1070 analysed by MaxQuant⁶⁸ v2.1 software using the integrated Andromeda search engine and
1071 searched against the Human UniProt Reference Proteome (February release with 79,057
1072 protein sequences) together with UniProt reported AAVs proteins and specific fasta created
1073 using EMBOSS Sixpack translating patient's virus genome. MaxQuant was used with the
1074 standard parameters with only the addition of deamidation (N) as variable modification. Data
1075 analysis was then carried out with Perseus⁶⁹ v2.05: Proteins reported in the file
1076 "proteinGroups.txt" were filtered for reverse and potential contaminants. Figures were
1077 created using Origin pro version 2022b.

1078
1079
1080
1081
1082
1083
1084
1085
1086
1087
1088
1089
1090
1091
1092
1093
1094
1095
1096
1097
1098
1099
1100
1101
1102
1103
1104
1105
1106
1107
1108
1109
1110
1111
1112
1113
1114
1115
1116
1117
1118
1119
1120
1121

Transduction of AAV2 capsid mutants

A transgene sequence containing enhanced green fluorescent protein (EGFP) was packaged into rAAV2 particles to track their expression in transduced cells, compared with rAAV capsids derived from canonical AAV2, AAV9, and a synthetic liver-tropic AAV vector called LK03¹⁵.

rAAV vector particles were delivered to Huh-7 hepatocytes at a multiplicity of infection (MOI) of 100,000 vector genomes per cell before analysing EGFP expression by flow cytometry 72-hours later.

Recombinant AAV capsid sequence

The VP1 sequence was generated by generating a consensus sequence from a multiple sequence alignment of sequenced AAV2 genomes derived from patient samples, using Biopython⁷⁰ package AlignIO. The designed VP1 sequence was then synthesised as a 'gBlock' (Integrated DNA Technologies) and incorporated into an AAV2 RepCap plasmid (AAV2/2 a gift from Melina Fan, Addgene plasmid # 104963) between the SwaI and XmaI restriction sites, using InFusion cloning reagent (Clontech product 638948).

AAV vector production

rAAV particles were generated by transient transfection of HEK 293T cells as described previously⁷¹. Briefly, 1.8×10^7 cells were plated in 15cm dishes before transfecting the pAAV-CAG-EGFP transgene plasmid (a gift from Edward Boyden, Addgene plasmid # 37825), the relevant RepCap plasmid, and the pAdDeltaF6 helper plasmid (a gift from James M. Wilson, Addgene plasmid # 112867), at a ratio of 10.5 μ g, 10.5 μ g, and 30.5 μ g, respectively, using PEIPro transfection reagent (PolyPlus) at a ratio of 1 μ L per 1 μ g DNA. 72-hours post-transfection, cell pellets and supernatant were harvested and rAAV particles were purified using an Akta HPLC platform. rAAV particle genome copy numbers were calculated by qPCR targeting the vector transgene region. The rAAV2 vector used in this study was purchased as ready-to-use AAV2 particles from Addgene (Addgene viral prep # 37825-AAV2).

Analysis of rAAV transduction

Huh-7 hepatocytes (a gift from Dr Julien Baruteau, UCL) were plated in DMEM medium supplemented with 10% Foetal Bovine Serum and 1% Penicillin Streptomycin supplement. The cell line was validated by testing for Glypican-3 and was not tested for mycoplasma contamination. Cells were plated at a density of 1.5×10^3 cells per cm^2 and transduced with 1×10^5 viral genomes per cell. Transductions were performed in the presence or absence of 400 μ g/mL heparin which was supplemented directly to cell media. 72-hours after transduction,

1122 cells were analysed by microscopy using an EVOS Cell Imaging System (Thermo Fisher
1123 Scientific) before quantifying EGFP expression by flow cytometry using a Cytoflex Flow
1124 Cytometer (Beckman). EGFP positive cells were determined by gating the live cell population
1125 and quantifying the level of EGFP signal versus untransduced controls.

1126

1127 **Human Short Read Data Analysis**

1128

1129 **Transcriptomics: cytokine analysis**

1130 Cytokine inducible gene expression modules were derived from previously published bulk
1131 tissue genome-wide transcriptomes of the tuberculin skin test that have been shown to reflect
1132 canonical human in vivo cell mediated immune pathways⁷² using a validated bioinformatic
1133 approach⁷³. Cytokine regulators of genes enriched in the tuberculin skin⁷² test (ArrayExpress
1134 Accession Number E-MTAB-6816) were identified using Ingenuity Pathway Analysis
1135 (Qiagen, Venlo, The Netherlands). Average correlation of Log₂ transformed transcripts per
1136 million (TPM) data for every gene-pair in each of the target gene modules was compared to
1137 100 iterations of randomly selected gene modules of the same size, to select cytokine-inducible
1138 modules that showed significantly greater co-correlation (adjusted p value<0.05), representing
1139 co-regulated transcriptional networks for each 59 cytokines. We then used the average Log₂
1140 TPM expression of all the genes in each these co-regulated modules to quantify the biological
1141 activity of the associated upstream cytokine within bulk genome-wide transcriptional profiles
1142 from AAV2-associated hepatitis (n=4) obtained in the present study, compared to published
1143 Log₂ transformed and normalised microarray data from normal adult liver (n=10) and hepatitis
1144 B adult liver (n=17)(Gene Expression Omnibus Accession Number GSE96851)¹⁸. To enable
1145 comparison across the data sets, we transformed average gene expression values for each
1146 cytokine-inducible module to standardised (Z scores) using mean and standard deviation of
1147 randomly selected gene sets of the same size within each individual data set. Statistical
1148 significant differences in Z scores between groups were identified by t-tests with multiple
1149 testing correction (adjusted p value<0.05).

1150

1151

1152 **Proteomics differential expression**

1153 To compare the proteomics data from our cases' explanted livers with data from healthy
1154 livers, we downloaded the raw files from 2 studies^{19,20} from PRIDE. The raw files were
1155 searched together with our files using the same settings and databases.

1156

1157 We performed differential expression analyses at protein-level and peptide-level using a
1158 hybrid approach including statistical inference on the abundance (quantitative approach) as
1159 well as presence/absence (binary approach) of proteins/peptides. DEP R package version
1160 1.18.0 was used for the quantitative analysis⁷⁴. Proteins/peptides were filtered for those
1161 detected in all replicates of at least one group (case or control). The data were background
1162 corrected and variance normalized using variance stabilizing transformation. Missing
1163 intensity values were not distributed randomly and were biased to specific samples (either
1164 cases or controls). Therefore, for imputing the missing data, we applied random draws from a
1165 manually defined left-shifted Gaussian distribution using the DEP *impute* function with
1166 parameters *fun:"man"*, *shift:1.8*, and *scale:0.3*. The *test_diff* function based on linear models

1167 and empirical Bayes method was used for testing differential expressions between the case
1168 and control samples.

1169
1170
1171

1172 **HLA typing methods**

1173 Typing was undertaken in the liver centre units. Next Generation Sequencing (Sequencing by
1174 synthesis (Illumina) using AllType kits (VHBio/OneLambda) – high resolution HLA typing
1175 method.

1176 **Statistical analysis**

1177 Fisher's exact test and two-sided Wilcoxon (Mann-Whitney) non-parametric rank sum test
1178 were used for differences between case and control groups. Where multiple groups were
1179 compared, Kruskal-Wallis tests followed by Wilcoxon pairwise tests using a Benjamini-
1180 Hochberg correction were performed. All analysis were performed in R version 4.2.0.

1181

1182

1183 **Data availability**

1184 The consensus genomes from viral WGS data are deposited in Genbank. IDs can be found in
1185 **Supplementary Table 7** (HAdV), **Supplementary Table 9** (AAV2) and **Supplementary**
1186 **Table 10** (HHV6).

1187 The mass spectrometry proteomics data have been deposited to the ProteomeXchange
1188 Consortium via the PRIDE partner repository with the dataset identifier PXD035925.

1189 **Code availability**

1190 Code for metagenomics and PCR analysis can be found at:

1191 <https://github.com/sarah-buddle/unknown-hepatitis>

1192 The transcriptomics analysis code is in

1193 [https://github.com/innate2adaptive/Bulk-RNAseq-](https://github.com/innate2adaptive/Bulk-RNAseq-analysis/tree/main/Zscore_gene_expression_module_analysis)
1194 [analysis/tree/main/Zscore_gene_expression_module_analysis](https://github.com/innate2adaptive/Bulk-RNAseq-analysis/tree/main/Zscore_gene_expression_module_analysis)

1195 The proteomics differential expression analysis code is in:

1196 https://github.com/MahdiMoradiMarjaneh/proteomics_and_transcriptomics_of_hepatitis

1197 **Funding**

1198 The work was part funded by the National Institute for Health Research Blood and Transplant
1199 Research Unit in Genomics to Enhance Microbiology Screening (GEMS). S.M is funded by
1200 a W.T. Henry Wellcome fellowship (206478/Z/17/Z). S.B. and O.E.T.M. are funded by the
1201 NIHR Blood and Transplant Research Unit (GEMS). MM and ML are supported in part by the
1202 NIHR Biomedical Research Centre of Imperial College NHS Trust. JB receives NIHR Senior
1203 Investigator Funding.M.N and JB are supported by the Wellcome Trust (207511/Z/17/Z) and
1204 (203268/Z/16/Z). M.N, J.B and G.P are supported by the National Institute for Health
1205 Research University College London Hospitals Biomedical Research Centre. P.S is supported
1206 by NIHR (NIHR203338). T.J is grateful for funding from the Brain Tumour Charity,
1207 Children with Cancer UK, Great Ormond Street Hospital Children's Charity, Olivia Hodson
1208 Cancer Fund, Cancer Research UK and the National Institute of Health Research.
1209 DIAMONDS is funded by the European Union (Horizon 2020; grant 848196). PERFORM
1210 was funded by the European Union (Horizon 2020; grant 668303).

1211

1212 **Acknowledgements**

1213 UKHSA for funding of the metagenomics and adenovirus sequencing.

1214 Amit Nathwani for helpful discussions.

1215 We acknowledge the considerable contribution from the Great Ormond Street Hospital NHS
1216 Foundation Trust (GOSH) microbiology laboratory. All research at Great Ormond Street
1217 Hospital NHS Foundation Trust and UCL Great Ormond Street Institute of Child Health is
1218 made possible by the NIHR Great Ormond Street Hospital Biomedical Research Centre. The
1219 views expressed are those of the author(s) and not necessarily those of the NHS, the NIHR or
1220 the Department of Health.

1221 For the purpose of open access, the author has applied a CC BY public copyright licence to
1222 any Author Accepted Manuscript version arising from this submission.

1223

1224 **Author Contributions**

1225 JBre, SM and SB conceived the study, analysed the data and wrote the manuscript. JRB, LA,
1226 NS, AL, JCDL, JH, SD coordinated samples and carried out the metagenomics and
1227 confirmatory PCRs. OETM, JAGA, SR, CV, LMMB, RW, CAW, HT, NB, HM, KAM, SCH
1228 DKA carried out genome sequencing and analyses. MMM, MN, GP, AC, AM, CV and ML
1229 analysed transcriptomic data, KT, ML, MMM, RZC generated and analysed proteomic data.
1230 SNW, JRC, JFAD, AS, LJT, ZA, JN, KSH carried out AAV2 tropism experiments. GS, PG,
1231 TEW, SNW JRC helped with AAV2 PCR development. LC, RB, MD, JM, JCH, CA, GA,
1232 TSJ carried out histology, immunohistochemistry and electron microscopy. BBK & JR
1233 provided control HHV6 material. PSh, JA provided control samples. ML, PSi, SC, MV, CF,
1234 MS provided PERFORM & DIAMONDS control samples. KB, MGS, PC, MO coordinated

1235 ISARIC consents and data collection TG, NH, CK provided data and samples from Kings and
1236 Birmingham Liver Units. IUL, MC, MZ, SM, CW, RS, EG, SG, CC, TT, KH, CH, TR, CM,
1237 KT, CN, MH, RG, SJS provided data and samples from UKHSA and devolved nations.ET
1238 provided reagents and contributed helpful discussions.

1239 **Competing Interests Declaration**

1240 JB declares the following:

1241 MHRA member of COVID Vaccines committee

1242 Holder of Wellcome Trust, UKRI, NIHR funding

1243 PI on the GSK LUNAR study to investigate SARS-CoV-2 sequences in patients treated with
1244 Sotrovimab. Commissioned by the MHRA

1245

1246 **Additional Information**

1247 **Supplementary information** The online version contains supplementary information.

1248 **Correspondence** should be addressed to Judith Breuer at j.breuer@ucl.ac.uk

1249 **Methods References**

1250

- 1251 41. Babraham Bioinformatics - Trim Galore!
1252 https://www.bioinformatics.babraham.ac.uk/projects/trim_galore/.
- 1253 42. Langmead, B. & Salzberg, S. L. Fast gapped-read alignment with Bowtie 2. (2012)
1254 doi:10.1038/nmeth.1923.
- 1255 43. Schmieder, R., Edwards, R. & Bateman, A. Quality control and preprocessing of
1256 metagenomic datasets. *BIOINFORMATICS APPLICATIONS NOTE* **27**, 863–864
1257 (2011).
- 1258 44. Morgulis, A. *et al.* Database indexing for production MegaBLAST searches.
1259 *Bioinformatics* **24**, 1757–1764 (2008).
- 1260 45. Buchfink, B., Xie, C. & Huson, D. H. Fast and sensitive protein alignment using
1261 diamond. **12**, (2015).
- 1262 46. Li, H. *et al.* The Sequence Alignment/Map format and SAMtools. *Bioinformatics* **25**,
1263 2078–2079 (2009).
- 1264 47. Nurk, S., Meleshko, D., Korobeynikov, A. & Pevzner, P. A. metaSPAdes: a new
1265 versatile metagenomic assembler. (2017) doi:10.1101/gr.213959.116.
- 1266 48. Li, H. Minimap2: pairwise alignment for nucleotide sequences. *Bioinformatics* **34**,
1267 3094–3100 (2018).
- 1268 49. Wood, D. E., Lu, J. & Langmead, B. Improved metagenomic analysis with Kraken 2.
1269 *Genome Biol* **20**, 1–13 (2019).
- 1270 50. EPI2ME WIMP workflow: quantitative, real-time species identification from
1271 metagenomic samples. [https://nanoporetech.com/resource-centre/epi2me-wimp-](https://nanoporetech.com/resource-centre/epi2me-wimp-workflow-quantitative-real-time-species-identification-metagenomic)
1272 [workflow-quantitative-real-time-species-identification-metagenomic](https://nanoporetech.com/resource-centre/epi2me-wimp-workflow-quantitative-real-time-species-identification-metagenomic).
- 1273 51. Babraham Bioinformatics - reDOTable DotPlot tool.
1274 <https://www.bioinformatics.babraham.ac.uk/projects/redotable/>.
- 1275 52. Babraham Bioinformatics - FastQC A Quality Control tool for High Throughput
1276 Sequence Data. <https://www.bioinformatics.babraham.ac.uk/projects/fastqc/>.
- 1277 53. Afzal, S., Fronza, R. & Schmidt, M. VSeq-Toolkit: Comprehensive Computational
1278 Analysis of Viral Vectors in Gene Therapy. *Mol Ther Methods Clin Dev* **17**, 752–757
1279 (2020).
- 1280 54. Robinson, J. T. *et al.* Integrative genomics viewer. *Nature Biotechnology* 2011 29:1
1281 **29**, 24–26 (2011).
- 1282 55. Aurnhammer, C. *et al.* Universal Real-Time PCR for the Detection and Quantification
1283 of Adeno-Associated Virus Serotype 2-Derived Inverted Terminal Repeat Sequences.
1284 <https://home.liebertpub.com/hgtb> **23**, 18–28 (2011).
- 1285 56. Watzinger, F. *et al.* Real-time quantitative PCR assays for detection and monitoring of
1286 pathogenic human viruses in immunosuppressed pediatric patients. *J Clin Microbiol*
1287 **42**, 5189–5198 (2004).
- 1288 57. Tann, C. J. *et al.* Prevalence of bloodstream pathogens is higher in neonatal
1289 encephalopathy cases vs. controls using a novel panel of real-time PCR assays.
1290 *PLoS One* **9**, (2014).
- 1291 58. Brown, J. R., Shah, D. & Breuer, J. Viral gastrointestinal infections and norovirus
1292 genotypes in a paediatric UK hospital, 2014–2015. *Journal of Clinical Virology* **84**, 1–6
1293 (2016).
- 1294 59. Karda, R. *et al.* Production of lentiviral vectors using novel, enzymatically produced,
1295 linear DNA. *Gene Ther* **26**, 86–92 (2019).

- 1296 60. Myers, C. E. *et al.* Using Whole Genome Sequences to Investigate Adenovirus
1297 Outbreaks in a Hematopoietic Stem Cell Transplant Unit. *Front Microbiol* **12**, (2021).
1298 61. Gaccioli, F. *et al.* Fetal inheritance of chromosomally integrated HHV-6 predisposes to
1299 preeclampsia in the mother Europe PMC Funders Group. **5**, 901–908 (2020).
1300 62. Quick, J. *et al.* Multiplex PCR method for MinION and Illumina sequencing of Zika and
1301 other virus genomes directly from clinical samples. *Nat Protoc* **12**, 1261–1267 (2017).
1302 63. Baker, D. J. *et al.* CoronaHiT: high-throughput sequencing of SARS-CoV-2 genomes.
1303 doi:10.1186/s13073-021-00839-5.
1304 64. Nakamura, T., Yamada, K. D., Tomii, K. & Katoh, K. Parallelization of MAFFT for
1305 large-scale multiple sequence alignments. *Bioinformatics* **34**, 2490–2492 (2018).
1306 65. Minh, B. Q. *et al.* IQ-TREE 2: New Models and Efficient Methods for Phylogenetic
1307 Inference in the Genomic Era. *Mol Biol Evol* **37**, 1530–1534 (2020).
1308 66. Hsu, H. L. *et al.* Structural characterization of a novel human adeno-associated virus
1309 capsid with neurotropic properties. *Nat Commun* **11**, (2020).
1310 67. Li, H. & Durbin, R. Fast and accurate short read alignment with Burrows-Wheeler
1311 transform. **25**, 1754–1760 (2009).
1312 68. Cox, J. & Mann, M. MaxQuant enables high peptide identification rates, individualized
1313 p.p.b.-range mass accuracies and proteome-wide protein quantification. *Nature*
1314 *Biotechnology* 2008 26:12 **26**, 1367–1372 (2008).
1315 69. Tyanova, S. *et al.* The Perseus computational platform for comprehensive analysis of
1316 (prote)omics data. *Nature Methods* 2016 13:9 **13**, 731–740 (2016).
1317 70. Cock, P. J. A. *et al.* Biopython: freely available Python tools for computational
1318 molecular biology and bioinformatics. *Bioinformatics* **25**, 1422–1423 (2009).
1319 71. Ng, J. *et al.* Gene therapy restores dopamine transporter expression and ameliorates
1320 pathology in iPSC and mouse models of infantile parkinsonism. *Sci Transl Med* **13**,
1321 (2021).
1322 72. Pollara, G. *et al.* Exaggerated IL-17A activity in human in vivo recall responses
1323 discriminates active tuberculosis from latent infection and cured disease. *Sci Transl*
1324 *Med* **13**, (2021).
1325 73. Chandran, A. *et al.* Rapid synchronous type 1 IFN and virus-specific T cell responses
1326 characterize first wave non-severe SARS-CoV-2 infections. *Cell Rep Med* **3**, 100557
1327 (2022).
1328 74. Zhang, X. *et al.* Proteome-wide identification of ubiquitin interactions using UbIA-MS.
1329 *Nature Protocols* 2018 13:3 **13**, 530–550 (2018).
1330
1331
1332

1333 **Extended Data Figure Legends**

1334

1335 **Extended Data Figure 1: Evidence of AAV2 replication from meta-transcriptomics and**
1336 **RT-PCR**

1337 Mapping of AAV2 reads to the reference genome for **a** liver RNA-Seq from 4 cases, **b** blood
1338 RNA-Seq from 2 cases. The horizontal lines in the same colour as the coverage graph are the
1339 predicted transcripts for each case. The horizontal lines in purple and green are the AAV2
1340 genes. **c**, RT-PCR results for liver cases. N: Negative PCR result

1341

1342 **Extended Data Figure 2: Examples of AAV2 complexes**

1343 The y axis shows the coordinates of a full length AAV2 genome (rep gene in green and cap
1344 gene in yellow). X axis is the nanopore read with the length of the read indicated. Red dots
1345 indicate alignment to the forward strand and blue dots the reverse. **a**, indicative complexes
1346 based on literature⁸ **b and c**. Examples of complex structures with both head to tail and
1347 alternating repeats, from a total of n=25 and n=75 such reads for cases 3 and 5 respectively. **b**
1348 shows the longest 2 reads for each case. **d**. Examples of truncated monomeric structures,
1349 from a total of n=27 and n=103 such reads for cases 3 and 5 respectively (Supplementary
1350 Table 3). The longest such read for each case is shown.

1351

1352 **Extended Data Figure 3: HAdV and AAV2 sequence analysis**

1353 **a**, HAdV SNP plot: Visualisation of the multiple alignment of HAdV-F41 genomic
1354 sequences from the same clade as the single sequence from a case (highlighted in grey)
1355 (Figure 3A). Includes both contemporary controls and publicly available HAdV-F41
1356 genomes from GenBank. Consensus-level mutations differing from the reference sequence
1357 (bottom) are highlighted across the genome. Genomic position of the mutation is shown at
1358 the top of the plot. **b**, Variants between stool complete HAdV genome from case JBB27 and
1359 combined blood partial genomes from other cases. **c**, Frequency table of capsid residues in
1360 cases and historical controls. There is no difference between the capsid sequences of cases
1361 and contemporaneously circulating controls. However, there are changes compared with
1362 historical controls in all contemporary sequences. None of the recently acquired capsid
1363 changes are shared with known hepatotropic strains in AAV7, 8 and 9. **d**, Amino acid
1364 differences between AAV2 capsid sequences from cases, contemporaneously circulating
1365 controls and historical publicly available sequences compared with the AAV2 reference
1366 sequence NC_001401.2. Also shown are the capsid sequences from known AAV7,8 and 9
1367 hepatotropic capsids compared to the reference sequence NC_001401.2.

1368

1369 **Extended Data Figure 4: AAV2 capsid analysis**

1370 **a**, Amino acid sequence of novel AAV capsid variant. The consensus sequence of the VP1
1371 sequence used for investigation of capsid transduction characteristics (AAVHepcase) is shown
1372 with alignment to canonical AAV2 VP1 (AAV2gp05). The alignment shows AAV2 amino
1373 acids that are different to the AAVHepcase sequence, with dots indicating matched amino acids
1374 sequence. **b**, In vitro analysis of AAV capsid transduction characteristics. Huh-7 hepatocytes
1375 were treated at MOI 100,000 with rAAV vectors containing capsid sequences derived from
1376 canonical AAV2, a consensus sequence derived from patient sequencing samples (Hepcase),
1377 LK03, or AAV9 (n=3 each treatment). Transduction efficiency was determined by flow

1378 cytometry, based on the percentage of EGFP-positive cells, the EGFP fluorescence intensity in
1379 positive cells, and the 'relative activity' of EGFP expression (calculated by multiplying %GFP-
1380 positive cells by MFI/10070). Transductions were performed in the presence or absence of 400
1381 $\mu\text{g}/\text{mL}$ heparin to investigate the role of HSPG interaction. rAAV2 was significantly affected
1382 by heparin competition, whereas other capsids, including that derived from AAV Hepcase,
1383 were not. Heparin competition significantly affected rAAV2 transduction in terms of
1384 percentage of GFP-positive cells ($P=0.0016$), MFI ($P=0.000008$), and relative activity
1385 ($P=0.000008$), whereas other capsids, including that derived from AAV Hepcase, were not
1386 affected by heparin. All data were analysed by 2-sided t-test with Bonferroni post-hoc analysis.
1387 Error bars indicate standard deviation from the mean value. **c**, Images of Huh-7 cells treated
1388 with rAAV vectors *in vitro*. Images of transduced Huh-7 cells. Each cell population was treated
1389 with MOI 100,000 of the relevant viral vector, in the presence or absence of 400 $\mu\text{g}/\text{mL}$ heparin
1390 and analysed by EGFP fluorescence 72-hours post-transduction. Scale bars = 300 μm .

1391
1392

1393 **Extended Data Figure 5: Representative histology of case livers**

1394 **a & b**, H&E sections x100 and x 200 showing a pattern of acute hepatitis with parenchymal
1395 disarray, there is a normal, uninflamed, portal tract lower left image **a**. Spotty inflammation
1396 and apoptotic bodies are shown in **b** along with perivenular hepatocyte loss/necrosis.
1397 Immunohistochemistry shows fewer mature B lymphocytes (CD20 panel **c**) than T
1398 lymphocytes (CD3, panel **d**, pan T cell marker) most of which are cytotoxic CD8 lymphocytes
1399 (panel **e**). In conclusion the livers of these children have a distinctive pattern of damage which
1400 does not indicate a specific aetiology, it does not exclude but does not offer positive support
1401 for either autoimmune hepatitis or a direct cytopathic effect of virus on hepatocytes. Each
1402 image shows a representative result from histology carried out on a minimum of five cases.

1403

1404 **Extended Data Figure 6: Immunohistochemistry results for cases of unexplained hepatitis 1405 and control tissues**

1406 **a**, Inflammatory markers (IgG, C4d, HLA-ABC, HLA-DR) in acute hepatitis cases and control
1407 liver. IgG, HLA-ABC and HLA-DR show a canalicular pattern in the control liver. This pattern
1408 is disrupted in the acute hepatitis cases due to the architectural collapse. In addition, there is
1409 increased staining associated with inflammatory cell/macrophage infiltrates. C4d shows very
1410 weak staining in the acute hepatitis cases associated with macrophages but with without
1411 endothelial staining. All stains were undertaken on 5 affected cases and 13 control cases. **b**,
1412 Representative images of the immunohistochemistry (IHC). Acute hepatitis liver explant cases
1413 stained for HHV6, arrow shows staining of **A** representative cells, **B** adenovirus, AAV2 (**C**
1414 polyclonal antibody, **E** monoclonal antibody, clone A1). Paraffin embedded AAV2 transfected
1415 cell lines stained as positive controls for AAV2 (**D** polyclonal antibody, **F** monoclonal
1416 antibody, clone A1). All scale bars are 60 micrometres. HHV6, AAV2 (polyclonal) stains were
1417 undertaken on 15 affected cases and 13 controls. AAV2 (A1) stains were undertaken on 5
1418 affected cases and 13 control cases. Staining for adenovirus was undertaken on 5 affected cases.

1419

1420 **Extended Data Figure 7: Cytokine inducible transcriptional modules**

1421 Volcano plot of cytokine inducible transcriptional modules (n=52) comparing their Z score
1422 expression in AAV2-associated hepatitis (n=4) and HBV-associated hepatitis (n=17) requiring
1423 transplantation using two-tailed unpaired t tests with Holm Sidak multiple testing correction
1424 for adjusted p values (n refers to number of patients). Each point represents a specific module
1425 listed in full in Supplementary Table 13. Labels for selected modules are shown.

1426

1427 **Extended Data Figure 8: HLA and HHV-6B proteins in case livers**

1428 **a & b** Ranking of the quantified proteins using the log10 of iBAQ values for **a** JBL1, **b** JBL2,
1429 **c** JBL3, **d** JBL4, **e** JBL5. **f**, Scatter plot of quantified proteins in sample JBL4 versus JBL5.
1430 HLA proteins are highlighted in red. Red arrows denote HLA-DRB1 proteins. HHV6 proteins
1431 are highlighted in green and marked with green arrows.

1432

1433

1434 **Extended Data Table titles and footnotes**

1435

1436 **Extended Data Table 1: PCR and whole genome sequencing for samples from cases**
1437 **where metagenomic sequencing was not performed.**

1438 - : Not tested due to insufficient residual material

1439 N: negative PCR result

1440 P: Positive PCR result in referring laboratory

1441 Where two results are shown, the first refers to the referring laboratory and the second to
1442 GOSH. Where there was a discrepancy, the positive result is shown.

1443 F: Failed

1444 Where there is more than one sample for a single patient, CT values represent the mean
1445 across the samples that were tested.

1446 *Metagenomics reads: the result of combining the datasets from two blood samples from the
1447 same case

1448 *De novo* assembly of unclassified metagenomics reads was unremarkable

1449

1450

1451 **Extended Data Table 2: Controls and comparators**

1452 **a** Summary of DIAMONDS and PERFORM immunocompetent controls. **b**

1453 immunocompromised comparators. **c** age distribution of blood comparator and control

1454 patients from GOSH, DIAMONDS and PERFORM

1455

1456 CONSORTIA

1457 DIAMONDS Consortium

1458

1459 Michael Levin², Evangelos Bellos², Claire Broderick², Samuel Channon-Wells², Samantha
 1460 Cooray², Tisham De², Giselle D'Souza², Leire Estramiana Elorrieta², Diego Estrada-
 1461 Rivadeneyra², Rachel Galassini², Dominic Habgood-Coote², Shea Hamilton², Heather
 1462 Jackson², James Kavanagh², Mahdi Moradi Marjaneh², Stephanie Menikou², Samuel
 1463 Nichols², Ruud Nijman², Harsita Patel², Ivana Pennisi², Oliver Powell², Ruth Reid², Priyen
 1464 Shah², Ortensia Vito², Elizabeth Whittaker², Clare Wilson², Rebecca Womersley², Amina
 1465 Abdulla⁴¹, Sarah Darnell⁴¹, Sobia Mustafa⁴¹, Pantelis Georgiou⁴², Jesus-Rodriguez
 1466 Manzano⁴³, Nicolas Moser⁴², Michael Carter^{44,45}, Shane Tibby^{44,45}, Jonathan Cohen⁴⁴,
 1467 Francesca Davis⁴⁴, Julia Kenny⁴⁴, Paul Wellman⁴⁴, Marie White⁴⁴, Matthew Fish⁴⁶, Aislinn
 1468 Jennings⁴⁷, Shankar-Hari^{46,47}, Katy Fidler⁴⁸, Dan Agranoff⁴⁹, Vivien Richmond^{48,50}, Matthew
 1469 Seal⁴⁹, Saul Faust^{51,52}, Dan Owen^{51,52}, Ruth Ensom⁵¹, Sarah McKay⁵¹, Diana Mondo⁵³,
 1470 Mariya Shaji⁵³, Rachel Schranz⁵³, Prita Rughnani^{54,55,56}, Amutha Anpananthar^{54,55,56}, Susan
 1471 Liebeschuetz⁵⁵, Anna Riddell⁵⁴, Nosheen Khalid^{54,56}, Ivone Lancoma Malcolm⁵⁷, Teresa
 1472 Simagan⁵⁶, Mark Peters⁵⁸, Alasdair Bamford^{58,59}, Nazima Pathan^{60,61}, Esther Daubney⁶⁰,
 1473 Deborah White⁶⁰, Melissa Heightman⁶², Sarah Eisen⁶², Terry Segal⁶², Lucy Wellings⁶²,
 1474 Simon B. Drysdale⁶³, Nicole Branch⁶³, Lisa Hamzah⁶³, Heather Jarman⁶³, Maggie
 1475 Nyirenda^{64,65}, Lisa Capozzi⁶⁴, Emma Gardiner⁶⁴, Robert Moots⁶⁶, Magda Nasher⁶⁷, Anita
 1476 Hanson⁶⁷, Michelle Linforth⁶⁶, Sean O'Riordan⁶⁸, Donna Ellis⁶⁸, Akash Deep³³, Ivan Caro³³,
 1477 Fiona Shackley⁶⁹, Arianna Bellini⁶⁹, Stuart Gormley⁶⁹, Samira Neshat⁷⁰, Barnaby J.
 1478 Scholefield⁷¹, Ceri Robbins⁷¹, Helen Winmill⁷¹, Stéphane C. Paulus^{72,73,74,75}, Andrew J.
 1479 Pollard^{72,73,74,75}, Sarah Hopton⁷², Danielle Miller⁷², Zoe Oliver⁷², Sally Beer⁷², Bryony
 1480 Ward⁷², Shrijana Shrestha⁷⁶, Meeru Gurung⁷⁶, Puja Amatya⁷⁶, Bhishma Pokhrel⁷⁶, Sanjeev
 1481 Man Bijukchhe⁷⁶, Tim Lubinda⁷⁴, Sarah Kelly⁷⁴, Peter O'Reilly⁷⁴, Federico Martín-
 1482 Torres^{77,78}, Antonio Salas^{77,78,79,80}, Fernando Álvez González^{77,78,79,80}, Xabier Bello^{77,78,79,80},
 1483 Mirian Ben García^{77,78}, Sandra Carnota^{77,78}, Miriam Cebey-López^{77,78}, María José Curras-
 1484 Tuala^{77,78,79,80}, Carlos Durán Suárez^{77,78}, Luisa García Vicente^{77,78}, Alberto Gómez-
 1485 Carballa^{77,78,79,80}, Jose Gómez Rial^{77,78}, Pilar Leboráns Iglesias^{77,78}, Nazareth Martín-
 1486 Torres^{77,78}, José María Martínón Sánchez^{77,78}, Belén Mosquera Pérez^{77,78}, Jacobo Pardo-
 1487 Seco^{77,78,79,80}, Lidia Piñeiro Rodríguez^{77,78}, Sara Pischetta^{77,78,79,80}, Sara Rey Vázquez^{77,78},
 1488 Irene Rivero Calle^{77,78}, Carmen Rodríguez-Tenreiro^{77,78}, Lorenzo Redondo-Collazo^{77,78},
 1489 Miguel Sadiki Ora^{77,78}, Sonia Serén Fernández^{77,78}, Cristina Serén Trasorras^{77,78}, Marisol
 1490 Vilas Iglesias^{77,78}, Enitan D. Carrol^{81,82,83}, Elizabeth Cocklin⁸¹, Aakash Khanijau⁸¹, Rebecca
 1491 Lenihan⁸¹, Nadia Lewis-Burke⁸¹, Karen Newal⁸⁴, Sam Romaine⁸¹, Maria Tsolia⁸⁵, Irini
 1492 Eleftheriou⁸⁵, Nikos Spyridis⁸⁵, Maria Tambouratzi⁸⁵, Despoina Maritsi⁸⁵, Antonios
 1493 Marmarinos⁸⁵, Marietta Xagorari⁸⁵, Lourida Panagiota⁸⁶, Pefanis Aggelos⁸⁶, Akinosoglou
 1494 Karolina⁸⁷, Gogos Charalambos⁸⁷, Maragos Markos⁸⁷, Voulgarelis Michalis⁸⁸, Stergiou
 1495 Ioanna⁸⁸, Marieke Emonts^{89,90,91}, Emma Lim^{90,91,92}, John Isaacs⁸⁹, Kathryn Bell⁹³, Stephen
 1496 Crulley⁹³, Daniel Fabian⁹³, Evelyn Thomson⁹³, Caroline Miller⁹³, Ashley Bell⁹³, Fabian J.S.
 1497 van der Velden^{89,90}, Geoff Shenton⁹⁴, Ashley Price^{95,96}, Owen Treloar^{89,90}, Daisy Thomas^{89,90},
 1498 Pablo Rojo^{97,98}, Cristina Epalza^{97,99}, Serena Villaverde⁹⁷, Sonia Márquez⁹⁹, Manuel Gijón⁹⁹,
 1499 Fátima Machín⁹⁹, Laura Cabello⁹⁹, Irene Hernández⁹⁹, Lourdes Gutiérrez⁹⁹, Ángela
 1500 Manzanares⁹⁷, Taco Kuijpers^{100,101}, Martijn van de Kuip¹⁰⁰, Marceline van Furth¹⁰⁰, Merlijn
 1501 van den Berg¹⁰⁰, Giske Biesbroek¹⁰⁰, Floris Verkuil¹⁰⁰, Carlijn van der Zee¹⁰⁰, Dasja Pajkrt¹⁰⁰,
 1502 Michael Boele van Hensbroek¹⁰⁰, Dieneke Schonenberg¹⁰⁰, Mariken Gruppen¹⁰⁰, Sietse
 1503 Nagelkerke^{100,101}, Machiel H. Jansen¹⁰⁰, Ines Goetschalckx¹⁰¹, Lorenza Romani¹⁰², Maia De
 1504 Luca¹⁰², Sara Chiurchiù¹⁰², Martina Di Giuseppe¹⁰², Clementien L. Vermont¹⁰³, Henriëtte A.

1505 Moll¹⁰⁴, Dorine M. Borensztajn¹⁰⁴, Nienke N. Hagedoorn¹⁰⁴, Chantal Tan¹⁰⁴, Joany
1506 Zachariasse¹⁰⁴, Medical students¹⁰⁴, W. Dik¹⁰⁵, Ching-Fen Shen^{106,2}, Dace Zavadzka^{107,108},
1507 Sniedze Laivacuma^{107,108}, Aleksandra Rudzate^{107,108}, Diana Stoldere^{107,108}, Arta
1508 Barzdina^{107,108}, Elza Barzdina^{107,108}, Sniedze Laivacuma^{107,109}, Monta Madelane^{107,109}, Dagne
1509 Gravele¹⁰⁸, Dace Svile¹⁰⁸, Romain Basmaci^{110,111}, Noémie Lachaume¹¹⁰, Pauline Bories¹¹⁰,
1510 Raja Ben Tkhatat¹¹⁰, Laura Chériaux¹¹⁰, Juraté Davoust¹¹⁰, Kim-Thanh Ong¹¹⁰, Marie
1511 Cotillon¹¹⁰, Thibault de Groc¹¹⁰, Sébastien Le¹¹⁰, Nathalie Vergnault¹¹⁰, Hélène Sée¹¹⁰, Laure
1512 Cohen¹¹⁰, Alice de Tugny¹¹⁰, Nevena Danekova¹¹⁰, Marine Mommert-Tripon¹¹², Karen
1513 Brengel-Pesce^{112,113,114}, Marko Pokorn^{115,116,117}, Mojca Kolnik^{115,116}, Tadej Avcin^{116,117}, Tanja
1514 Avramoska^{115,116}, Natalija Bahovec¹¹⁵, Petra Bogovic¹¹⁵, Lidija Kitanovski^{116,117}, Mirijam
1515 Nahtigal¹¹⁵, Lea Papst¹¹⁵, Tina Plankar Srovin¹¹⁵, Franc Strle^{115,116}, Anja Srpceic¹¹⁶, Katarina
1516 Vincek¹¹⁵, Michiel van der Flier^{118,119}, Wim J.E. Tissing¹¹⁹, Roelie M. Wösten-van
1517 Asperen¹²⁰, Sebastiaan J. Vastert¹²¹, Daniel C. Vijlbrief¹²², Louis J. Bont^{118,119}, Tom F.W.
1518 Wolfs^{118,119}, Coco R. Beudeker^{118,119}, Philipp Agyeman¹²³, Luregn Schlapbach^{124,125},
1519 Christoph Aebi¹²³, Mariama Usman¹²³, Stefanie Schlüchter¹²³, Verena Wyss¹²³, Nina
1520 Schöbi¹²³, Elisa Zimmermann¹²⁴, Kathrin Weber¹²⁴, Eric Giannoni^{126,127}, Martin Stocker¹²⁸,
1521 Klara M. Posfay-Barbe¹²⁹, Ulrich Heininger¹³⁰, Sara Bernhard-Stirnemann¹³¹, Anita Niederer-
1522 Loher¹³², Christian Kahlert¹³², Giancarlo Natalucci¹³³, Christa Relly¹³⁴, Thomas Riedel¹³⁵,
1523 Christoph Berger¹³⁴, Marie Voice¹⁸, Michael Steele¹⁸, Colin Fink¹⁸, Jennifer Holden¹⁸, Leo
1524 Calvo-Bado¹⁸, Benjamin Evans¹⁸, Jake Stevens¹⁸, Peter Matthews¹⁸, Kyle Billing¹⁸, Werner
1525 Zenz¹³⁶, Alexander Binder¹³⁶, Benno Kohlmaier¹³⁶, Daniela S. Kohlfürst¹³⁶, Nina A.
1526 Schweintzger¹³⁶, Christoph Zurl¹³⁶, Susanne Hösele¹³⁶, Manuel Leitner¹³⁶, Lena Pölz¹³⁶,
1527 Alexandra Rusu¹³⁶, Glorija Rajic¹³⁶, Bianca Stoiser¹³⁶, Martina Strempl¹³⁶, Manfred G.
1528 Sagmeister¹³⁶, Sebastian Bauchinger¹³⁶, Martin Benesch^{137,136}, Astrid Ceolotto¹³⁶, Ernst
1529 Eber¹³⁸, Siegfried Gallistl¹³⁶, Harald Haidl¹³⁶, Almuthe Hauer¹³⁶, Christa Hude¹³⁶, Andreas
1530 Kapper¹³⁹, Markus Keldorfer¹⁴⁰, Sabine Löffler¹⁴⁰, Tobias Niedrist¹⁴¹, Heidemarie Pilch¹⁴⁰,
1531 Andreas Pflieger¹³⁸, Klaus Pfurtscheller^{142,137}, Siegfried Rödl^{142,137}, Andrea Skrabl-
1532 Baumgartner¹³⁶, Volker Strenger¹³⁷, Elmar Wallner¹³⁹, Dennie Tempel¹⁴³, Danielle van
1533 Keulen¹⁴³, Annelieke M. Strijbosch¹⁴³, Maike K. Tauchert¹⁴⁴, Ulrich von Both^{145,146}, Laura
1534 Kolberg¹⁴⁵, Patricia Schmied¹⁴⁵, Irene Alba-Alejandre¹⁴⁷, Katharina Danhauser¹⁴⁸, Nikolaus
1535 Haas¹⁴⁹, Florian Hoffmann¹⁵⁰, Matthias Griese¹⁵¹, Tobias Feuchtinger¹⁵², Sabrina Juranek¹⁵³,
1536 Matthias Kappler¹⁵¹, Eberhard Lurz¹⁵⁴, Esther Maier¹⁵³, Karl Reiter¹⁵⁰, Carola Schoen¹⁵⁰,
1537 Sebastian Schroepf¹⁵⁵, Shunmay Yeung^{156,157,158}, Manuel Dewez¹⁵⁶, David Bath¹⁵⁸, Elizabeth
1538 Fitchett¹⁵⁶, Fiona Cresswell¹⁵⁶

1539

1540 **PERFORM Consortium**

1541

1542 Michael Levin², Aubrey Cunnington², Tisham De², Jethro Herberg², Mysini Kaforou²,
1543 Victoria Wright², Lucas Baumard², Evangelos Bellos², Giselle D'Souza², Rachel Galassini²,
1544 Dominic Habgood-Coote², Shea Hamilton², Clive Hoggart², Sara Hourmat², Heather
1545 Jackson², Ian Maconochie², Stephanie Menikou², Naomi Lin², Samuel Nichols², Ruud
1546 Nijman², Ivonne Pena Paz², Oliver Powell², Priyen Shah², Clare Wilson², Amina Abdulla⁴¹,
1547 Ladan Ali⁴¹, Sarah Darnell⁴¹, Rikke Jorgensen⁴¹, Sobia Mustafa⁴¹, Salina Persand⁴¹, Molly
1548 Stevens⁴², Eunjung Kim⁴², Benjamin Pierce⁴², Katy Fidler⁴⁸, Julia Dudley⁴⁸, Vivien
1549 Richmond^{48,50}, Emma Tavliavini^{48,50}, Ching-Fen Shen^{106,2}, Ching-Chuan Liu¹⁵⁹, Shih-Min
1550 Wang¹⁵⁹, Federico Martín-Torres^{77,78}, Antonio Salas^{77,78,79,80}, Fernando Álvarez
1551 González^{77,78,79,80}, Cristina Balo Farto^{77,78}, Ruth Barral-Arca^{77,78,79,80}, Maria Barreiro
1552 Castro^{77,78}, Xabier Bello^{77,78,79,80}, Mirian Ben García^{77,78}, Sandra Carnota^{77,78}, Miriam Cebey-
1553 López^{77,78}, María José Curras-Tuala^{77,78,79,80}, Carlos Durán Suárez^{77,78}, Luisa García
1554 Vicente^{77,78}, Alberto Gómez-Carballa^{77,78,79,80}, Jose Gómez Rial^{77,78}, Pilar Leboráns

1555 Iglesias^{77,78}, Federico Martinón-Torres^{77,78}, Nazareth Martinón-Torres^{77,78}, José María
 1556 Martinón Sánchez^{77,78}, Belén Mosquera Pérez^{77,78}, Jacobo Pardo-Seco^{77,78,79,80}, Lidia Piñeiro
 1557 Rodríguez^{77,78}, Sara Pischedda^{77,78,79,80}, Sara Rey Vázquez^{77,78}, Irene Rivero Calle^{77,78},
 1558 Carmen Rodríguez-Tenreiro^{77,78}, Lorenzo Redondo-Collazo^{77,78}, Miguel Sadiki Ora^{77,78},
 1559 Sonia Serén Fernández^{77,78}, Cristina Serén Trasorras^{77,78}, Marisol Vilas Iglesias^{77,78}, Dace
 1560 Zavadska^{107,108}, Anda Balode^{107,108}, Arta Barzdina^{107,108}, D?rta Deksne^{107,108}, Dagne
 1561 Gravele¹⁰⁸, Ilze Grope^{107,108}, Anija Meiere^{107,108}, Ieva Nokalna^{107,108}, Jana Pavare^{107,108}, Zanda
 1562 Pucuka^{107,108}, Katrina Selecka^{107,108}, Aleksandra Sidorova^{107,108}, Dace Svile¹⁰⁸, Urzula Nora
 1563 Urbane^{107,108}, Effua Usuf¹⁶⁰, Kalifa Bojang¹⁶⁰, Syed M.A. Zaman¹⁶⁰, Fatou Secka¹⁶⁰, Suzanne
 1564 Anderson¹⁶⁰, Anna RocaIsatou Sarr¹⁶⁰, Momodou Saidykhan¹⁶⁰, Saffiatou Darboe¹⁶⁰, Samba
 1565 Ceesay¹⁶⁰, Umberto D'alessandro¹⁶⁰, Henriëtte A. Moll¹⁰⁴, Dorine M. Borensztajn¹⁰⁴, Nienke
 1566 N. Hagedoorn¹⁰⁴, Chantal Tan¹⁰⁴, Clementien L. Vermont¹⁰³, Joany Zachariasse¹⁰⁴, W. Dik¹⁰⁵,
 1567 Philipp Agyeman¹²³, Luregn J Schlapbach^{161,125,162}, Christoph Aebi¹²³, Verena Wyss¹²³,
 1568 Mariama Usman¹²³, Eric Giannoni^{126,127}, Martin Stocker¹²⁸, Klara M. Posfay-Barbe¹²⁹, Ulrich
 1569 Heininger¹³⁰, Sara Bernhard-Stirнемann¹³¹, Anita Niederer-Loher¹³², Christian Kahlert¹³²,
 1570 Giancarlo Natalucci¹³³, Christa Relly¹³⁴, Thomas Riedel¹³⁵, Christoph Berger¹³⁴, Enitan D.
 1571 Carrol^{81,82,83}, Stéphane Paulus⁸¹, Elizabeth Cocklin⁸¹, Rebecca Jennings⁸⁴, Joanne Johnston⁸⁴,
 1572 Simon Leigh⁸¹, Karen Newall⁸⁴, Sam Romaine⁸¹, Maria Tsolia⁸⁵, Irini Eleftheriou⁸⁵, Maria
 1573 Tambouratzi⁸⁵, Antonis Marmarinos⁸⁵, Marietta Xagorari⁸⁵, Kelly Syggelou⁸⁵, Colin Fink¹⁸,
 1574 Marie Voice¹⁸, Leo Calvo-Bado¹⁸, Werner Zenz¹³⁶, Benno Kohlmaier¹³⁶, Nina A.
 1575 Schweintzger¹³⁶, Manfred G. Sagmeister¹³⁶, Daniela S. Kohlfürst¹³⁶, Christoph Zurl¹³⁶,
 1576 Alexander Binder¹³⁶, Susanne Hösele¹³⁶, Manuel Leitner¹³⁶, Lena Pölz¹³⁶, Glorija Rajic¹³⁶,
 1577 Sebastian Bauchinger¹³⁶, Hinrich Baumgart¹⁴², Martin Benesch^{137,136}, Astrid Ceolotto¹³⁶,
 1578 Ernst Eber¹³⁸, Siegfried Gallistl¹³⁶, Gunther Gores¹⁴⁰, Harald Haidl¹³⁶, Almuthe Hauer¹³⁶,
 1579 Christa Hude¹³⁶, Markus Keldorfer¹⁴⁰, Larissa Krenn¹³⁷, Heidemarie Pilch¹⁴⁰, Andreas
 1580 Pflieger¹³⁸, Klaus Pfurtscheller^{142,137}, Gudrun Nordberg¹⁴⁰, Tobias Niedrist¹⁴¹, Siegfried
 1581 Rödl^{142,137}, Andrea Skrabl-Baumgartner¹³⁶, Matthias Sperl¹⁶³, Laura Stampfer¹⁴⁰, Volker
 1582 Strenger¹³⁷, Holger Till¹⁶⁴, Andreas Trobisch¹⁴⁰, Sabine Löffler¹⁴⁰, Shunmay Yeung^{156,157,158},
 1583 Juan Emmanuel Dewez¹⁵⁶, Martin Hibberd¹⁵⁶, David Bath¹⁵⁸, Alec Miners¹⁵⁸, Ruud
 1584 Nijman¹⁵⁷, Catherine Wedderburn¹⁵⁶, Anne Meierford¹⁵⁶, Baptiste Laurent¹⁶⁵, Ronald de
 1585 Groot¹⁶⁶, Michiel van der Flier^{166,167,168}, Marien I. de Jonge¹⁶⁸, Koen van Aerde^{166,167},
 1586 Wynand Alkema¹⁶⁶, Bryan van den Broek¹⁶⁶, Jolein Gloerich¹⁶⁶, Alain J. van Gool¹⁶⁶,
 1587 Stefanie Henriët^{166,167}, Martijn Huijnen¹⁶⁶, Ria Philipsen¹⁶⁶, Esther Willems¹⁶⁶, G.P.J.M.
 1588 Gerrits¹⁶⁹, M. van Leur¹⁶⁹, J. Heidema¹⁷⁰, L. de Haan^{166,167}, C.J. Miedema¹⁷¹, C. Neeleman¹⁶⁶,
 1589 C.C. Obihara¹⁷², G.A. Tramper-Stranders^{172,173}, Andrew J. Pollard^{72,73,74,75}, Rama
 1590 Kandasamy^{74,75}, Stéphane Paulus^{74,75}, Michael J. Carter^{74,75}, Daniel O'Connor^{74,75}, Sagida
 1591 Bibi^{74,75}, Dominic F. Kelly^{74,75}, Meeru Gurung⁷⁶, Stephen Thorson⁷⁶, Imran Ansari⁷⁶, David
 1592 R. Murdoch¹⁷⁴, Shrijana Shrestha⁷⁶, Marieke Emonts^{89,90,91}, Emma Lim^{90,91,92}, Lucille
 1593 Valentine¹⁷⁵, Karen Allen⁹³, Kathryn Bell⁹³, Adora Chan⁹³, Stephen Crulley⁹³, Kirsty
 1594 Devine⁹³, Daniel Fabian⁹³, Sharon King⁹³, Paul McAlinden⁹³, Sam McDonald⁹³, Anne
 1595 McDonnell^{90,93}, Ailsa Pickering^{90,93}, Evelyn Thomson⁹³, Amanda Wood⁹³, Diane Wallia⁹³,
 1596 Phil Woodsford⁹³, Frances Baxter⁹³, Ashley Bell⁹³, Mathew Rhodes⁹³, Rachel Agbeko¹⁷⁶,
 1597 Christine Mackerness¹⁷⁶, Bryan Baas⁹⁰, Lieke Kloosterhuis⁹⁰, Wilma Oosthoek⁹⁰, Tasnim
 1598 Arief⁹⁴, Joshua Bennet⁹⁰, Calvin Collings⁹⁰, Iona van der Giessen⁹⁰, Alex Martin⁹⁰, Aqeela
 1599 Rashid⁹⁴, Emily Rowlands⁹⁰, Gabriella de Vries⁹⁰, Fabian van der Velden⁹⁰, Mike Martin¹⁷⁷,
 1600 Ravi Mistry⁹⁰, Ulrich von Both^{145,146}, Laura Kolberg¹⁴⁵, Manuela Zwerenz¹⁴⁵, Judith
 1601 Buschbeck¹⁴⁵, Christoph Bidlingmaier¹⁵³, Vera Binder¹⁵², Katharina Danhauser¹⁴⁸, Nikolaus
 1602 Haas¹⁴⁹, Matthias Griese¹⁵¹, Tobias Feuchtinger¹⁵², Julia Keil¹⁵⁰, Matthias Kappler¹⁵¹,
 1603 Eberhard Lurz¹⁵⁴, Georg Muench¹⁵⁵, Karl Reiter¹⁵⁰, Carola Schoen¹⁵⁰, François
 1604 Mallet^{112,113,114}, Karen Brengel-Pesce^{112,113,114}, Alexandre Pachot¹¹², Marine Mommert^{112,113},

1605 Marko Pokorn^{115,116,178}, Mojca Kolnik^{115,116}, Katarina Vincek¹¹⁵, Tina Plankar Srovin¹¹⁵,
1606 Natalija Bahovec¹¹⁵, Petra Prunk¹¹⁵, Veronika Osterman¹¹⁵, Tanja Avramoska^{115,116}, Taco
1607 Kuijpers^{100,179}, Ilse Jongerius¹⁷⁹, J.M. van den Berg¹⁰⁰, D. Schonenberg¹⁰⁰, A.M.
1608 Barendregt¹⁰⁰, D. Pajkrt¹⁰⁰, M. van der Kuip^{100,180}, A.M. van Furth^{100,180}, Evelien
1609 Sprenkeler¹⁷⁹, Judith Zandstra¹⁷⁹, G. van Mierlo¹⁷⁹, J. Geissler¹⁷⁹
1610

1611 **ISARIC Consortium**

1612
1613 Kenneth Baillie²⁵, Malcolm Gracie Semple^{29,30}, Gail Carson¹⁸¹, Peter J.M. Openshaw^{182,183},
1614 Jake Dunning^{184,182}, Laura Merson¹⁸¹, Clark D. Russell¹⁸⁵, David Dorward¹⁸⁶, Maria
1615 Zambon²⁶, Meera Chand²⁶, Richard S. Tedder^{187,188,189}, Say Khoo¹⁹⁰, Lance C.W. Turtle^{191,192},
1616 Tom Solomon^{191,193}, Samreen Ijaz¹⁹⁴, Tom Fletcher¹⁹⁵, Massimo Palmarini⁴⁰, Antonia Y.W.
1617 Ho⁴⁰, Emma Thomson⁴⁰, Nicholas Price^{196,197}, Judith Breuer^{1,3}, Thushan de Silva¹⁹⁸, Chloe
1618 Donohue¹⁹⁹, Hayley Hardwick¹⁹¹, Wilna Oosthuyzen²⁶, Miranda Odam²⁵, Primrose
1619 Chikowore²⁵, Lauren Obosi²⁶, Sara Clohisey²⁶, Andrew Law²⁶, Lucy Norris²⁰⁰, Sarah Tait¹⁶,
1620 Murray Wham²⁰¹, Richard Clark²⁰², Audrey Coutts²⁰², Lorna Donnelly²⁰², Angie Fawkes²⁰²,
1621 Tammy Gilchrist²⁰², Katarzyna Hafezi²⁰², Louise MacGillivray²⁰², Alan Maclean²⁰², Sarah
1622 McCafferty²⁰², Kirstie Morrice²⁰², Lee Murphy²⁰², Nicola Wrobel²⁰², Sarah E.
1623 McDonald^{139,203}, Victoria Shaw²⁰⁴, Jane A. Armstrong²⁰⁵, Lauren Lett²⁰⁶, Paul Henderson²⁰⁷,
1624 Louisa Pollock²⁰⁸, Shyla Kishore²⁰⁹, Helen Brotherton^{210,211}, Lawrence Armstrong^{212,213},
1625 Andrew Mita²¹⁴, Anna Dall²¹⁵, Kristyna Bohmova²¹⁶, Sheena Logan²¹⁶, Louise Gannon²¹⁷,
1626 Ken Agwuh²¹⁸, Srikanth Chukkambotla²¹⁹, Ingrid DuRand²²⁰, Duncan Fullerton²²¹, Sanjeev
1627 Garg²²², Clive Graham²²³, Tassos Grammatikopoulos³³, Stuart Hartshorn⁷¹, Luke Hodgson²²⁴,
1628 Paul Jennings²²⁵, George Koshy²²⁶, Tamas Leiner²²⁶, James Limb²²⁷, Jeff Little²²⁸, Elijah
1629 Matovu²²¹, Fiona McGill²²⁹, Craig Morris²³⁰, John Morrice^{210,211}, David Price²³¹, Henrik
1630 Reschreiter²³², Tim Reynolds²³⁰, Paul Whittaker²³³, Rachel Tayler²³⁴, Clare Irving²³⁵, Maxine
1631 Ramsay²⁰⁷, Margaret Millar²⁰⁷, Barry Milligan²³⁶, Naomi Hickey²³⁶, Maggie Connon²⁰⁹,
1632 Catriona Ward²⁰⁹, Laura Beveridge²¹⁰, Susan MacFarlane²³⁷, Karen Leitch²³⁸, Claire Bell²¹²,
1633 Lauren Finlayson²¹⁵, Joy Dawson²¹⁵, Janie Candlish²¹⁴, Laura McGenily²¹⁶, Tara Roome⁷¹,
1634 Cynthia Diaba²³⁹, Jasmine Player²⁴⁰, Natassia Powell³³, Ruth Howman⁷¹, Sara Burling⁷¹,
1635 Sharon Floyd²²⁴, Sarah Farmer²¹⁸, Susie Ferguson²⁴¹, Susan Hope²⁴², Lucy Rubick²³², Rachel
1636 Swingle²⁴³, Emma Collins²⁴⁴, Collette Spencer²²⁹, Amaryl Jones²²¹, Barbara Wilson²⁴⁵,
1637 Diane Armstrong²⁴⁶, Mark Birt²⁴⁷, Holly Dickinson²³⁰, Rosemary Harper²⁴⁶, Darran
1638 Martin²⁴⁸, Amy Roff²³², Sarah Mills²³²
1639

- 1640 41. Children's Clinical Research Unit, St. Mary's Hospital, London, UK
1641 42. Department of Electrical and Electronic Engineering, Imperial College London,
1642 London, UK
1643 43. Section of Adult Infectious Disease, Department of Infectious Disease, Imperial
1644 College London, London, UK
1645 44. Evelina London Children's Hospital, Guy's and St. Thomas' NHS Foundation Trust,
1646 London, UK
1647 45. Department of Women and Children's Health, School of Life Course Sciences, King's
1648 College London, London, UK
1649 46. Department of Infectious Diseases, School of Immunology and Microbial Sciences,
1650 King's College London, London, UK
1651 47. Department of Intensive Care Medicine, Guy's and St. Thomas' NHS Foundation
1652 Trust, London, UK
1653 48. Royal Alexandra Children's Hospital, University Hospitals Sussex, Brighton, UK
1654 49. Department of Infectious Diseases, University Hospitals Sussex, Brighton, UK
1655 50. Research Nurse Team, University Hospitals Sussex, Brighton, UK
1656 51. National Institute for Health Research Southampton Clinical Research Facility,
1657 University Hospital Southampton NHS Foundation Trust, Southampton, UK,
1658 52. University of Southampton, Southampton, UK
1659 53. Department of Research and Development, University Hospital Southampton NHS
1660 Foundation Trust, Southampton, UK
1661 54. Royal London Hospital, London, UK
1662 55. Newham University Hospital, London, UK
1663 56. Whipps Cross University Hospital, London, UK
1664 57. Barts Health NHS Trust, London, UK
1665 58. Great Ormond Street Hospital NHS Foundation Trust, London, UK
1666 59. Great Ormond Street Institute of Child Health, University College London, London,
1667 UK
1668 60. Addenbrooke's Hospital, Cambridge, UK
1669 61. Department of Paediatrics, University of Cambridge, Cambridge, UK
1670 62. University College London Hospital, London, UK
1671 63. St George's Hospital, London, UK
1672 64. University Hospital Lewisham, London, UK
1673 65. Queen Elizabeth Hospital Greenwich, London, UK
1674 66. Aintree University Hospital, Liverpool, UK
1675 67. Royal Liverpool Hospital, Liverpool, UK
1676 68. Leeds Children's Hospital, Leeds, UK
1677 69. Sheffield Children's Hospital, Sheffield, UK
1678 70. Leicester General Hospital, Leicester, UK
1679 71. Birmingham Women's and Children's NHS Foundation Trust, Birmingham, UK,
1680 72. John Radcliffe Hospital, Oxford University Hospitals NHS Foundation Trust, Oxford,
1681 UK
1682 73. Department of Paediatrics, University of Oxford, Oxford, UK
1683 74. Oxford Vaccine Group, Department of Paediatrics, University of Oxford, Oxford, UK
1684 75. National Institute for Health Research Oxford Biomedical Research Centre, Oxford,
1685 UK
1686 76. Paediatric Research Unit, Patan Academy of Health Sciences, Kathmandu, Nepal
1687 77. Translational Paediatrics and Infectious Diseases, Paediatrics Department, Hospital
1688 Clínico Universitario de Santiago, Santiago de Compostela, Spain

- 1689 78. GENVIP Research Group, Instituto de Investigación Sanitaria de Santiago,
1690 Universidad de Santiago de Compostela, Galicia, Spain
- 1691 79. Unidade de Xenética, Departamento de Anatomía Patolóxica e Ciencias Forenses,
1692 Instituto de Ciencias Forenses, Facultade de Medicina, Universidade de Santiago de
1693 Compostela, Galicia, Spain
- 1694 80. GenPop Research Group, Instituto de Investigaciones Sanitarias (IDIS), Hospital
1695 Clínico Universitario de Santiago, Galicia, Spain
- 1696 81. Department of Clinical Infection, Microbiology and Immunology, University of
1697 Liverpool Institute of Infection and Global Health, Veterinary and Ecological
1698 Sciences, Liverpool, UK
- 1699 82. Department of Infectious Diseases, Alder Hey Children's Hospital, Liverpool, UK
- 1700 83. Liverpool Health Partners, Liverpool Science Park, Liverpool, UK
- 1701 84. Clinical Research Business Unit, Alder Hey Children's Hospital, Liverpool, UK,
- 1702 85. Department of Paediatrics, National and Kapodistrian University of Athens (NKUA),
1703 P, and A. Kyriakou Children's Hospital, Athens, Greece
- 1704 86. Department of Infectious Diseases, Sotiria General Hospital, Athens, Greece
- 1705 87. Pathology Department, University of Patras, Panagia i Voithia General Hospital,
1706 Patras, Greece
- 1707 88. Pathophysiology Department, Medical Faculty, National and Kapodistrian University
1708 of Athens (NKUA), Laiko General Hospital, Athens, Greece
- 1709 89. Translational and Clinical Research Institute, Newcastle University, Newcastle upon
1710 Tyne, UK
- 1711 90. Paediatric Immunology, Infectious Diseases and Allergy, Great North Children's
1712 Hospital, Newcastle upon Tyne Hospitals NHS Foundation Trust, Newcastle upon
1713 Tyne, UK
- 1714 91. National Institute for Health Research Newcastle Biomedical Research Centre,
1715 Newcastle upon Tyne Hospitals NHS Foundation Trust and Newcastle University,
1716 Newcastle upon Tyne, UK
- 1717 92. Population Health Sciences Institute, Newcastle University, Newcastle upon Tyne,
1718 UK
- 1719 93. Research Unit, Great North Children's Hospital, Newcastle upon Tyne Hospitals NHS
1720 Foundation Trust, Newcastle upon Tyne, UK
- 1721 94. Paediatric Oncology, Great North Children's Hospital, Newcastle upon Tyne
1722 Hospitals NHS Foundation Trust, Newcastle upon Tyne, UK
- 1723 95. Department of Infection and Tropical Medicine, Newcastle upon Tyne Hospitals NHS
1724 Foundation Trust, Newcastle upon Tyne, UK
- 1725 96. National Institute for Health Research Newcastle In Vitro Diagnostics Co-operative
1726 (Newcastle MIC), Newcastle upon Tyne, UK
- 1727 97. Servicio Madrileño de Salud (SERMAS), Paediatric Infectious Diseases Unit,
1728 Department of Paediatrics, Hospital Universitario 12 de Octubre, Madrid, Spain
- 1729 98. Universidad Complutense de Madrid, Faculty of Medicine, Department of Paediatrics,
1730 Madrid, Spain
- 1731 99. Fundación Biomédica del Hospital Universitario 12 de Octubre (FIB-H12O), Unidad
1732 Pediátrica de Investigación y Ensayos Clínicos (UPIC), Hospital Universitario 12 de
1733 Octubre, Instituto de Investigación Sanitaria Hospital 12 de Octubre (i+12), Madrid,
1734 Spain
- 1735 100. Department of Paediatric Immunology, Rheumatology and Infectious Disease,
1736 Amsterdam University Medical Centre, University of Amsterdam, Amsterdam, The
1737 Netherlands

- 1738 101.Sanquin Research Institute and Department of Molecular Hematology, University
1739 Medical Centre, Amsterdam, The Netherlands
- 1740 102.Infectious Disease Unit, Academic Department of Paediatrics, Bambino Gesù
1741 Children's Hospital IRCCS, Rome, Italy
- 1742 103.Department of Paediatric Infectious Diseases and Immunology, Erasmus Medical
1743 Centre-Sophia Children's Hospital, Rotterdam, The Netherlands
- 1744 104.Department of General Paediatrics, Erasmus Medical Centre-Sophia Children's
1745 Hospital, Rotterdam, The Netherlands
- 1746 105.Department of Immunology, Erasmus Medical Centre, Rotterdam, The Netherlands
- 1747 106.Division of Infectious Disease, Department of Paediatrics, National Cheng Kung
1748 University, Tainan, Taiwan
- 1749 107.Riga Stradins University, Riga, Latvia
- 1750 108.Children's Clinical University Hospital, Riga, Latvia
- 1751 109.Riga East Clinical University Hospital, Riga, Latvia
- 1752 110.Service de Pédiatrie-Urgences, AP-HP, Hôpital Louis-Mourier, Colombes, France
- 1753 111.Université Paris Cité, Inserm, Paris, France
- 1754 112.Open Innovation and Partnerships, bioMérieux, Lyon, France
- 1755 113.Joint research unit Hospice Civils de Lyon □ bioMérieux, Centre Hospitalier Lyon
1756 Sud, Lyon, France
- 1757 114.Pathophysiology of Injury-induced Immunosuppression, University of Lyon, Lyon,
1758 France
- 1759 115.Department of Infectious Diseases, University Medical Centre Ljubljana, Ljubljana,
1760 Slovenia
- 1761 116.University Children's Hospital, University Medical Centre Ljubljana, Ljubljana,
1762 Slovenia
- 1763 117.Faculty of Medicine, University of Ljubljana, Ljubljana, Slovenia
- 1764 118.Paediatric Infectious Diseases and Immunology, Wilhelmina Children's Hospital,
1765 University Medical Centre Utrecht, Utrecht, The Netherlands
- 1766 119.Princess Maxima Centre for Paediatric Oncology, Utrecht, The Netherlands
- 1767 120.Paediatric Intensive Care Unit, Wilhelmina Children's Hospital, University Medical
1768 Centre Utrecht, Utrecht, The Netherlands
- 1769 121.Paediatric Rheumatology, Wilhelmina Children's Hospital, University Medical Centre
1770 Utrecht, Utrecht, The Netherlands
- 1771 122.Paediatric Neonatal Intensive Care, Wilhelmina Children's Hospital, University
1772 Medical Centre Utrecht, Utrecht, The Netherlands
- 1773 123.Department of Paediatrics, Inselspital, Bern University Hospital, University of Bern,
1774 Bern, Switzerland
- 1775 124.Department of Intensive Care and Neonatology and Children`s Research Centre,
1776 University Children`s Hospital Zurich, Zurich, Switzerland
- 1777 125.Child Health Research Centre, University of Queensland, Brisbane, Australia
- 1778 126.Clinic of Neonatology, Department Mother-Woman-Child, Lausanne University
1779 Hospital and University of Lausanne, Lausanne, Switzerland
- 1780 127.Infectious Diseases Service, Department of Medicine, Lausanne University Hospital
1781 and University of Lausanne, Lausanne, Switzerland
- 1782 128.Department of Paediatrics, Children's Hospital Lucerne, Lucerne, Switzerland
- 1783 129.Paediatric Infectious Diseases Unit, Children's Hospital of Geneva, University
1784 Hospitals of Geneva, Geneva, Switzerland
- 1785 130.Infectious Diseases and Vaccinology, University of Basel Children's Hospital, Basel,
1786 Switzerland
- 1787 131.Children's Hospital Aarau, Aarau, Switzerland

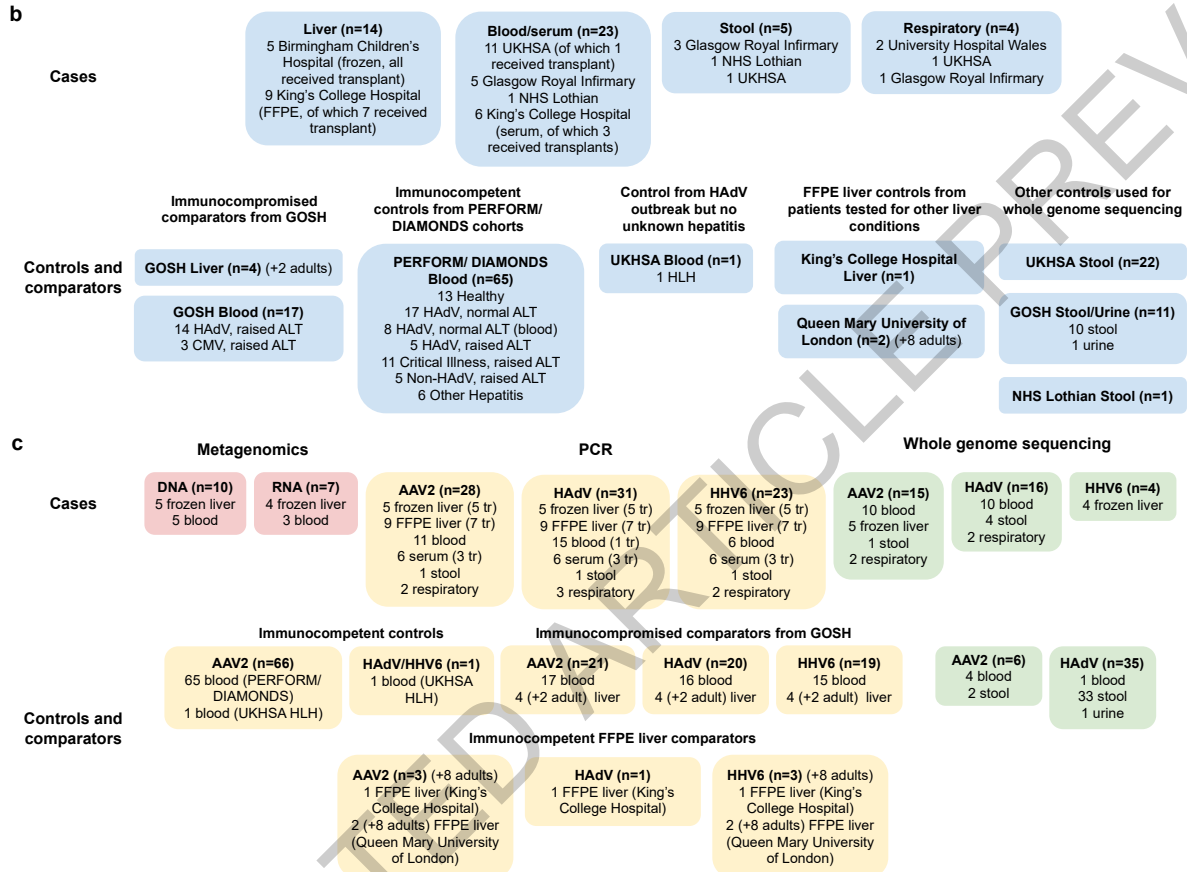
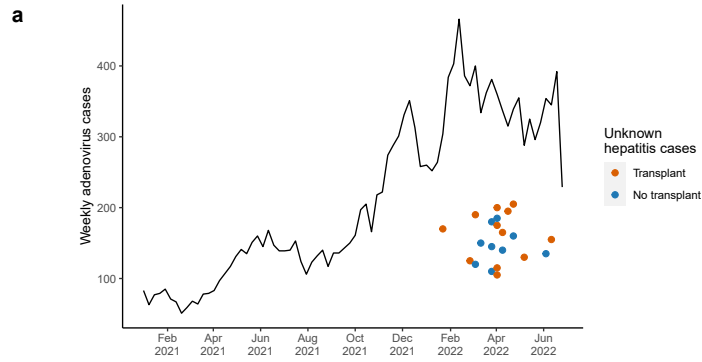
- 1788 132.Division of Infectious Diseases and Hospital Epidemiology, Children's Hospital of
1789 Eastern Switzerland St. Gallen, St. Gallen, Switzerland
1790 133.Department of Neonatology, University Hospital Zurich, Zurich, Switzerland
1791 134.Division of Infectious Diseases and Hospital Epidemiology and Children's Research
1792 Centre, University Children's Hospital Zurich, Zurich, Switzerland
1793 135.Children's Hospital Chur, Chur, Switzerland
1794 136.Department of Paediatrics and Adolescent Medicine, Division of General Paediatrics,
1795 Medical University of Graz, Graz, Austria
1796 137.Department of Paediatric Hematooncology, Medical University of Graz, Graz, Austria
1797 138.Department of Paediatric Pulmonology, Medical University of Graz, Graz, Austria
1798 139.Department of Internal Medicine, State Hospital Graz II, Graz, Austria
1799 140.University Clinic of Paediatrics and Adolescent Medicine Graz, Medical University
1800 of Graz, Graz, Austria
1801 141.Clinical Institute of Medical and Chemical Laboratory Diagnostics, Medical
1802 University of Graz, Graz, Austria
1803 142.Paediatric Intensive Care Unit, Medical University of Graz, Graz, Austria
1804 143.SkylineDx, Rotterdam, The Netherlands
1805 144.Biobanking and BioMolecular Resources Research Infrastructure – European
1806 Research Infrastructure Consortium (BBMRI-ERIC), Graz, Austria
1807 145.Division of Paediatric Infectious Diseases, Hauner Children's Hospital, University
1808 Hospital, Ludwig Maximilian University Munich, Munich, Germany
1809 146.German Centre for Infection Research (DZIF), Partner Site Munich, Munich,
1810 Germany
1811 147.Department of Gynecology and Obstetrics, University Hospital, Ludwig Maximilian
1812 University Munich, Munich, Germany
1813 148.Division of Paediatric Rheumatology, Hauner Children's Hospital, University
1814 Hospital, Ludwig Maximilian University Munich, Munich, Germany
1815 149.Department of Paediatric Cardiology and Paediatric Intensive Care, Hauner Children's
1816 Hospital, University Hospital, Ludwig Maximilian University Munich, Munich,
1817 Germany
1818 150.Paediatric Intensive Care Unit, Hauner Children's Hospital, University Hospital,
1819 Ludwig Maximilian University Munich, Munich, Germany
1820 151.Division of Paediatric Pulmonology, Hauner Children's Hospital, University Hospital,
1821 Ludwig Maximilian University Munich, Munich, Germany
1822 152.Division of Paediatric Haematology and Oncology, Hauner Children's Hospital,
1823 University Hospital, Ludwig Maximilian University Munich, Munich, Germany
1824 153.Division of General Paediatrics, Hauner Children's Hospital, University Hospital,
1825 Ludwig Maximilian University Munich, Munich, Germany
1826 154.Division of Paediatric Gastroenterology, Hauner Children's Hospital, University
1827 Hospital, Ludwig Maximilian University Munich, Munich, Germany
1828 155.Neonatal Intensive Care Unit, Hauner Children's Hospital, University Hospital,
1829 Ludwig Maximilian University Munich, Munich, Germany
1830 156.Faculty of Infectious and Tropical Disease, London School of Hygiene and Tropical
1831 Medicine, London, UK
1832 157.Department of Paediatrics, St. Mary's Hospital, London, UK
1833 158.Faculty of Public Health and Policy, London School of Hygiene and Tropical
1834 Medicine, London, UK
1835 159.Centre of Clinical Medicine Research, National Cheng Kung University, Tainan,
1836 Taiwan

- 1837 160. Medical Research Council Unit The Gambia at the London School for Hygiene and
1838 Tropical Medicine, Fajara, The Gambia
- 1839 161. Neonatal and Paediatric Intensive Care Unit, Children's Research Centre, University
1840 Children's Hospital Zurich, University of Zurich, Zurich, Switzerland
- 1841 162. Queensland Children's Hospital, Brisbane, Australia
- 1842 163. Department of Paediatric Orthopedics, Medical University of Graz, Graz, Austria
- 1843 164. Department of Paediatric and Adolescence Surgery, Medical University of Graz,
1844 Graz, Austria
- 1845 165. Faculty of Epidemiology and Population Health, London School of Hygiene and
1846 Tropical Medicine, London, UK
- 1847 166. Radboud University Medical Centre, Nijmegen, The Netherlands
- 1848 167. Amalia Children's Hospital, Nijmegen, The Netherlands
- 1849 168. Wilhelmina Children's Hospital, University Medical Centre Utrecht, Utrecht, The
1850 Netherlands
- 1851 169. Canisius Wilhelmina Hospital, Nijmegen, The Netherlands
- 1852 170. St. Antonius Hospital, Nieuwegein, The Netherlands
- 1853 171. Catharina Hospital, Eindhoven, The Netherlands
- 1854 172. ETZ Elisabeth, Tilburg, The Netherlands
- 1855 173. Franciscus Gasthuis, Rotterdam, The Netherlands
- 1856 174. Department of Pathology, University of Otago, Christchurch, New Zealand
- 1857 175. Newcastle University Business School, Centre for Knowledge, Innovation,
1858 Technology and Enterprise (KITE), Newcastle upon Tyne, UK
- 1859 176. Paediatric Intensive Care Unit, Great North Children's Hospital, Newcastle upon Tyne
1860 Hospitals NHS Foundation Trust, Newcastle upon Tyne, UK
- 1861 177. Northumbria University, Newcastle upon Tyne, UK
- 1862 178. Department of Infectious Diseases and Epidemiology, Faculty of Medicine,
1863 University of Ljubljana, Ljubljana, Slovenia
- 1864 179. Sanquin Research Institute and Landsteiner Laboratory at the AMC, University of
1865 Amsterdam, Amsterdam, The Netherlands
- 1866 180. Department of Paediatric Infectious Diseases and Immunology, Amsterdam
1867 University Medical Centre, Free University (VU) Amsterdam, Amsterdam, The
1868 Netherlands (former affiliation)
- 1869 181. ISARIC Global Support Centre, Centre for Tropical Medicine and Global Health,
1870 Nuffield Department of Medicine, University of Oxford, Oxford, UK
- 1871 182. National Heart and Lung Institute, Imperial College London, London, UK
- 1872 183. Imperial College Healthcare NHS Foundation Trust, London, UK
- 1873 184. National Infection Service, Public Health England, London, UK
- 1874 185. Centre for Inflammation Research, The Queen's Medical Research Institute,
1875 University of Edinburgh, Edinburgh, UK
- 1876 186. Edinburgh Pathology, University of Edinburgh, Edinburgh, UK
- 1877 187. Blood Borne Virus Unit, Virus Reference Department, National Infection Service,
1878 Public Health England, London, UK
- 1879 188. Transfusion Microbiology, National Health Service Blood and Transplant, London,
1880 UK
- 1881 189. Department of Medicine, Imperial College London, London, UK
- 1882 190. Department of Pharmacology, University of Liverpool, Liverpool, UK
- 1883 191. National Institute for Health Research Health Protection Research Unit, Institute of
1884 Infection, Veterinary and Ecological Sciences, Faculty of Health and Life Sciences,
1885 University of Liverpool, Liverpool, UK

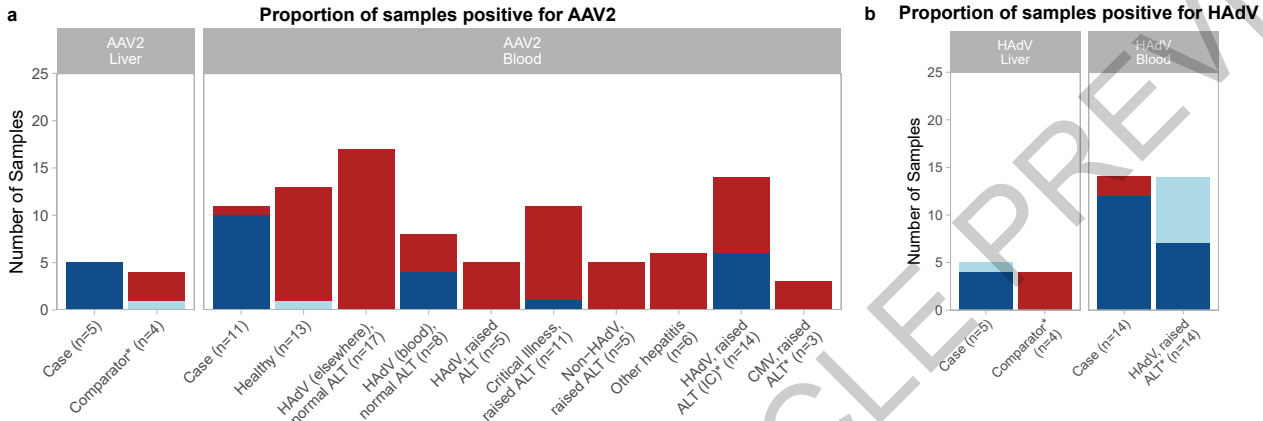
- 1886 192. Tropical and Infectious Disease Unit, Royal Liverpool University Hospital, Liverpool,
1887 UK
1888 193. Walton Centre NHS Foundation Trust, Liverpool, UK
1889 194. Virology Reference Department, National Infection Service, Public Health England,
1890 London, UK
1891 195. Liverpool School of Tropical Medicine, Liverpool, UK
1892 196. Centre for Clinical Infection and Diagnostics Research, Department of Infectious
1893 Diseases, School of Immunology and Microbial Sciences, King's College London,
1894 London, UK
1895 197. Department of Infectious Diseases, Guy's and St. Thomas' NHS Foundation Trust,
1896 London, UK
1897 198. The Florey Institute for Host-Pathogen Interactions, Department of Infection,
1898 Immunity and Cardiovascular Disease, University of Sheffield, Sheffield, UK
1899 199. Liverpool Clinical Trials Centre, University of Liverpool, Liverpool, UK
1900 200. Edinburgh Parallel Computing Centre (EPCC), University of Edinburgh, Edinburgh,
1901 UK
1902 201. Medical Research Council Human Genetics Unit, Medical Research Council Institute
1903 of Genetics and Molecular Medicine, University of Edinburgh, Edinburgh, UK
1904 202. Edinburgh Clinical Research Facility, University of Edinburgh, Edinburgh, UK
1905 203. Department of Histopathology, Great Ormond Street Hospital for Children NHS
1906 Foundation Trust, London, UK
1907 204. Institute of Translational Medicine, University of Liverpool, Liverpool, UK
1908 205. Sheffield Teaching Hospitals NHS Foundation Trust, Sheffield, UK
1909 206. University of Liverpool, Liverpool, UK
1910 207. Royal Hospital For Children and Young People, Edinburgh, UK
1911 208. Department of Paediatric Infectious Diseases and Immunology, Royal Hospital for
1912 Children Glasgow, Glasgow, UK
1913 209. Royal Aberdeen Children's Hospital, Aberdeen, UK
1914 210. Queen Margaret Hospital, Dumfermline, Fife, UK
1915 211. Victoria Hospital, Kirkcaldy, Fife, UK
1916 212. University Hospital Crosshouse, Crosshouse, UK
1917 213. University Hospital Ayr, Ayr, UK
1918 214. Dumfries and Galloway Royal Infirmary, Dumfries, UK
1919 215. Borders General Hospital, Melrose, UK
1920 216. Forth Valley Hospital, Larbert, UK
1921 217. Tayside Children's Hospital and Ninewells Hospital, NHS Tayside, Dundee, UK
1922 218. Doncaster and Bassetlaw NHS Foundation Trust, Doncaster, UK
1923 219. Burnley General Hospital, Burnley, UK
1924 220. Hereford County Hospital, Hereford, UK
1925 221. Leighton Hospital, Leighton, UK
1926 222. Walsall Healthcare NHS Foundation Trust, Walsall, UK
1927 223. Cumberland Infirmary, Cumberland, UK
1928 224. St. Richard's Hospital, Chichester, UK
1929 225. Airedale Hospital, Keighley, UK
1930 226. Hinchingsbrooke Hospital, Huntingdon, UK
1931 227. Darlington Memorial Hospital, Darlington, UK
1932 228. Warrington Hospital, Warrington, UK
1933 229. Leeds Teaching Hospitals NHS Trust, Leeds, UK
1934 230. Queen's Hospital Burton, Burton, UK
1935 231. Royal Victoria Infirmary, Newcastle upon Tyne, UK

- 1936 232. University Hospitals Dorset NHS Foundation Trust, Dorset, UK
1937 233. Bradford Royal Infirmary, Bradford, UK
1938 234. Department of Paediatric Gastroenterology, Hepatology and Nutrition, Royal Hospital
1939 for Children Glasgow, Glasgow, UK
1940 235. Avon and Wiltshire Mental Health Partnership NHS Foundation Trust, Bath, UK
1941 236. Queen Elizabeth University Hospital, Glasgow, UK
1942 237. Tayside Children's Hospital, Dundee, UK
1943 238. University Hospital Wishaw, Wishaw, UK
1944 239. Royal Free Hospital, London, UK
1945 240. Diana Princess of Wales Hospital, Grimsby, UK
1946 241. Weston General Hospital, Weston-super-Mare, UK
1947 242. Barnsley Hospital, Barnsley, UK
1948 243. Bradford Teaching Hospitals NHS Foundation Trust, Bradford, UK
1949 244. Wye Valley NHS Foundation Trust, Hereford, UK
1950 245. Newcastle Upon Tyne Hospitals, Newcastle upon Tyne, UK
1951 246. West Cumberland Hospital, Whitehaven, UK
1952 247. University of North Durham, Durham, UK
1953 248. Worthing Hospital, Worthing, UK
1954

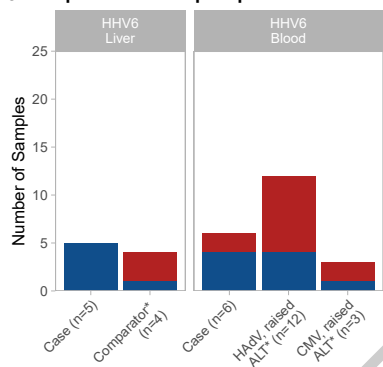
ACCELERATED ARTICLE PREVIEW



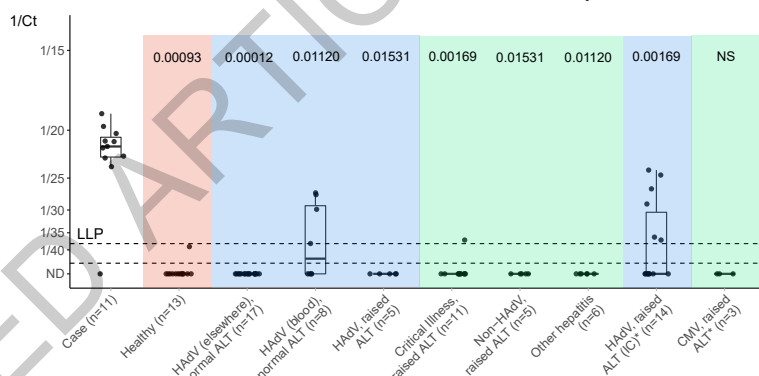
PCR result Positive Low-level positive Negative



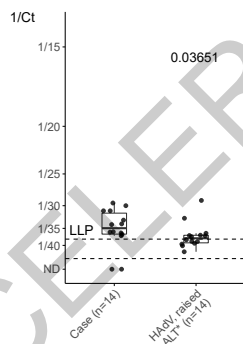
c Proportion of samples positive for HHV6



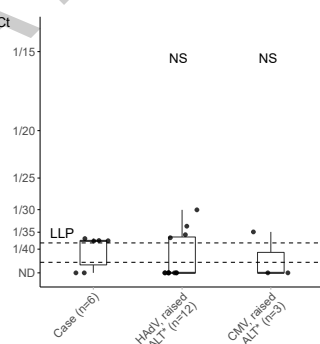
d AAV2 in whole blood from cases and controls/comparators



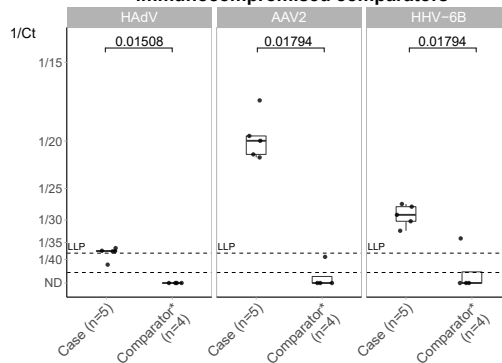
e HAAdV in whole blood from cases and controls/comparators

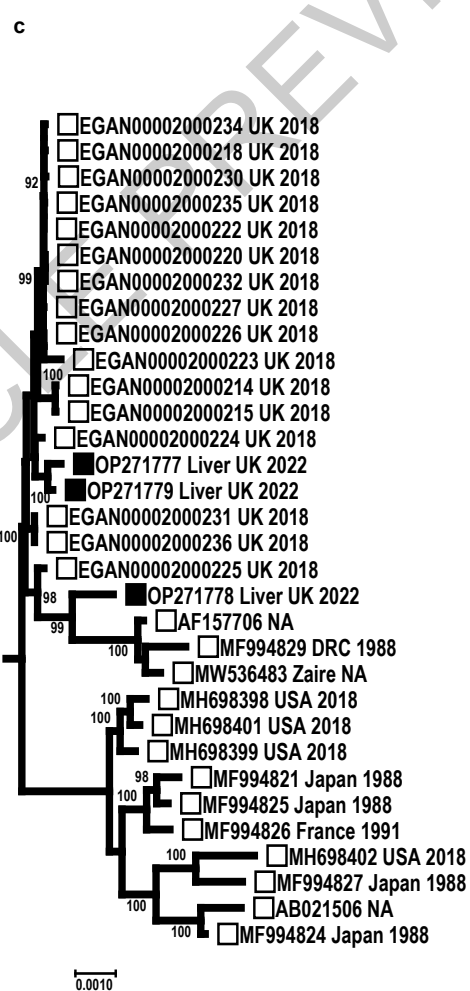
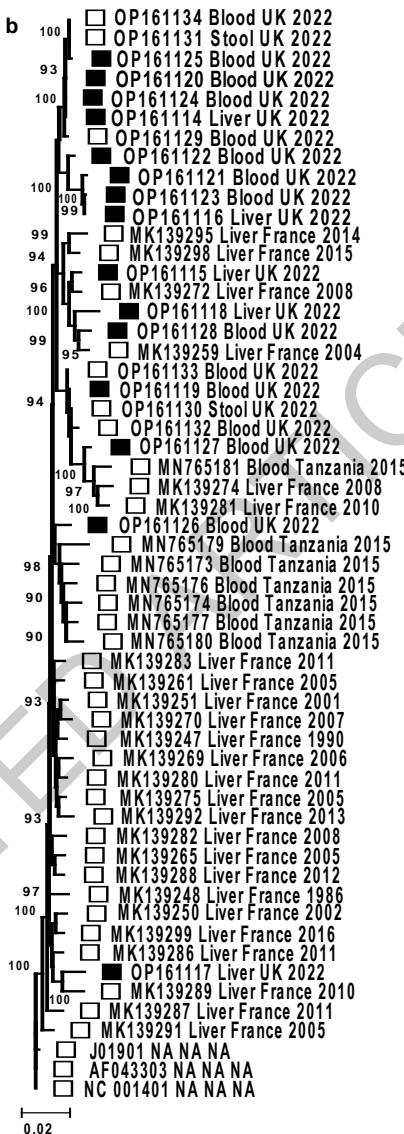
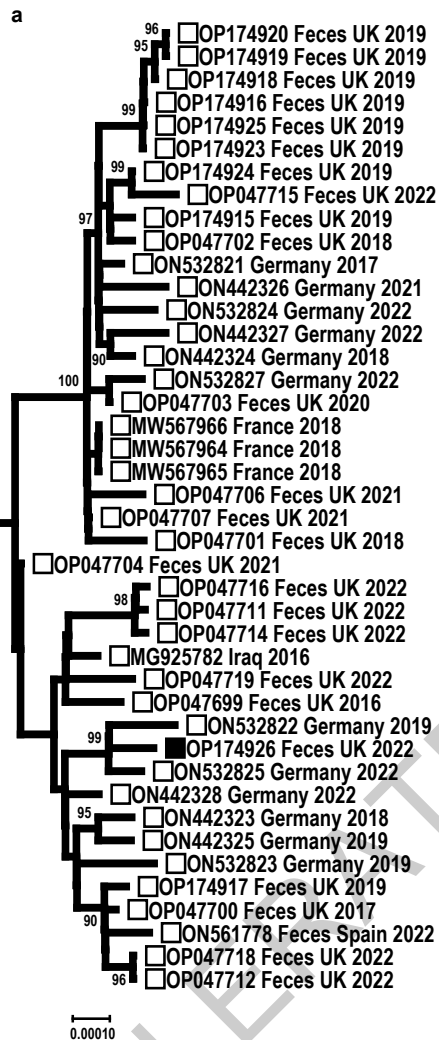


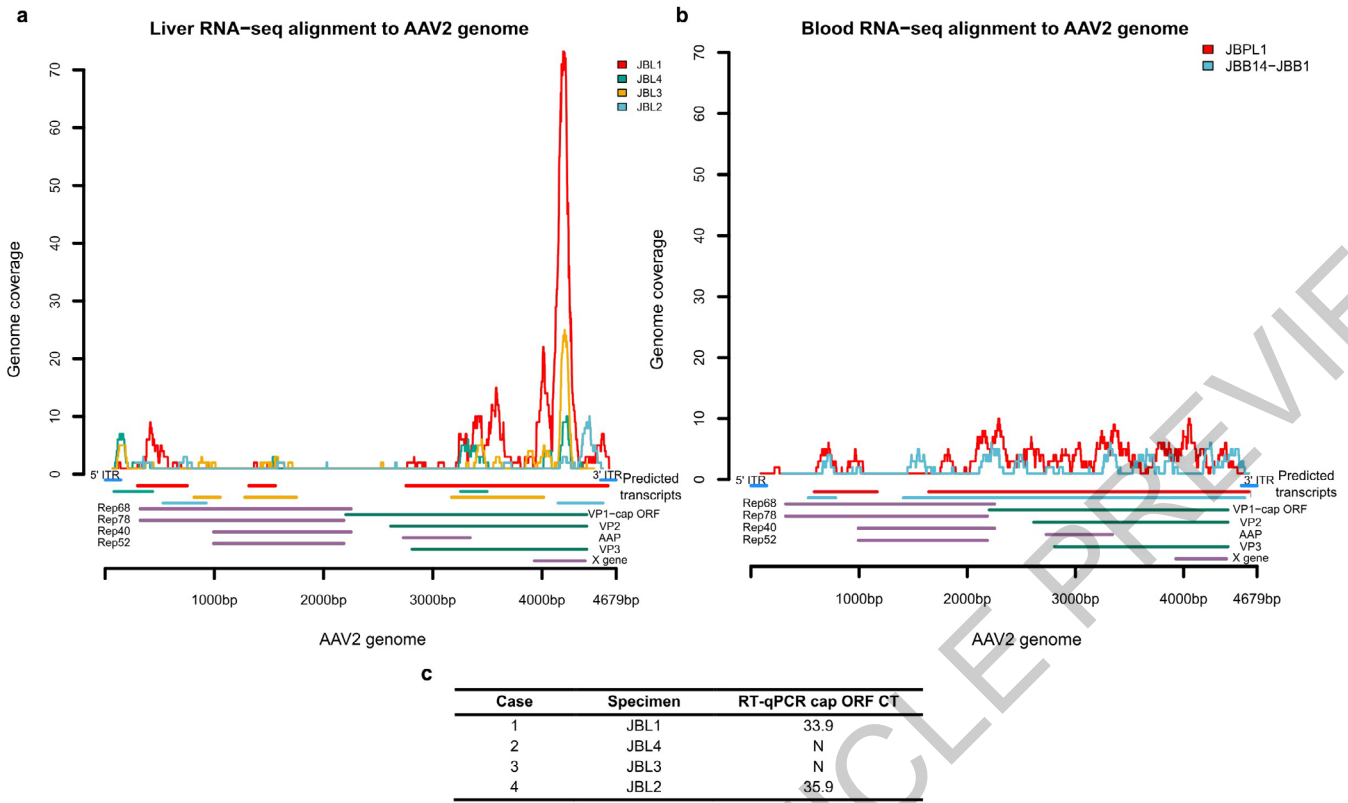
f HHV6 in whole blood from cases and controls/comparators



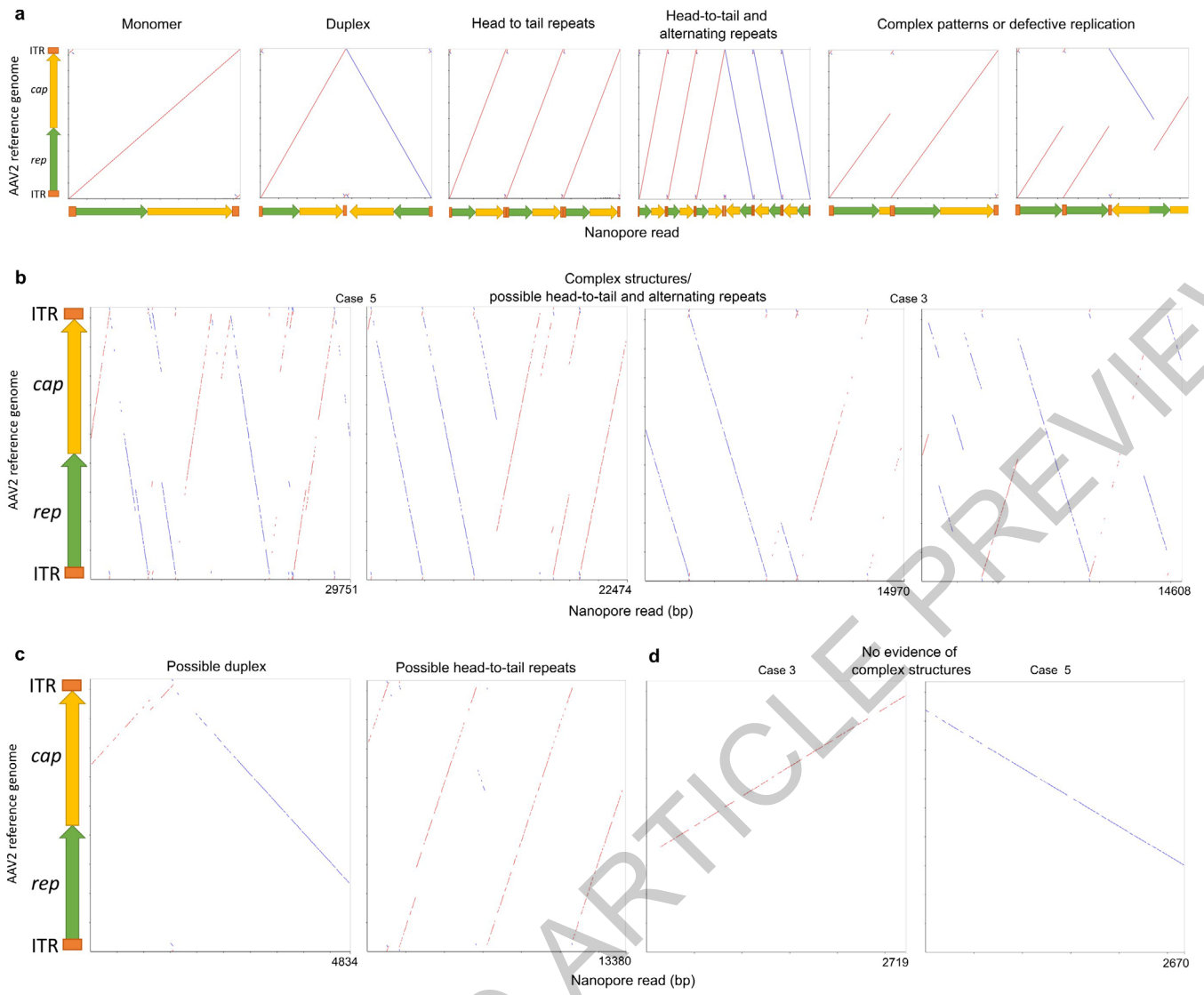
g Liver biopsies from cases and immunocompromised comparators





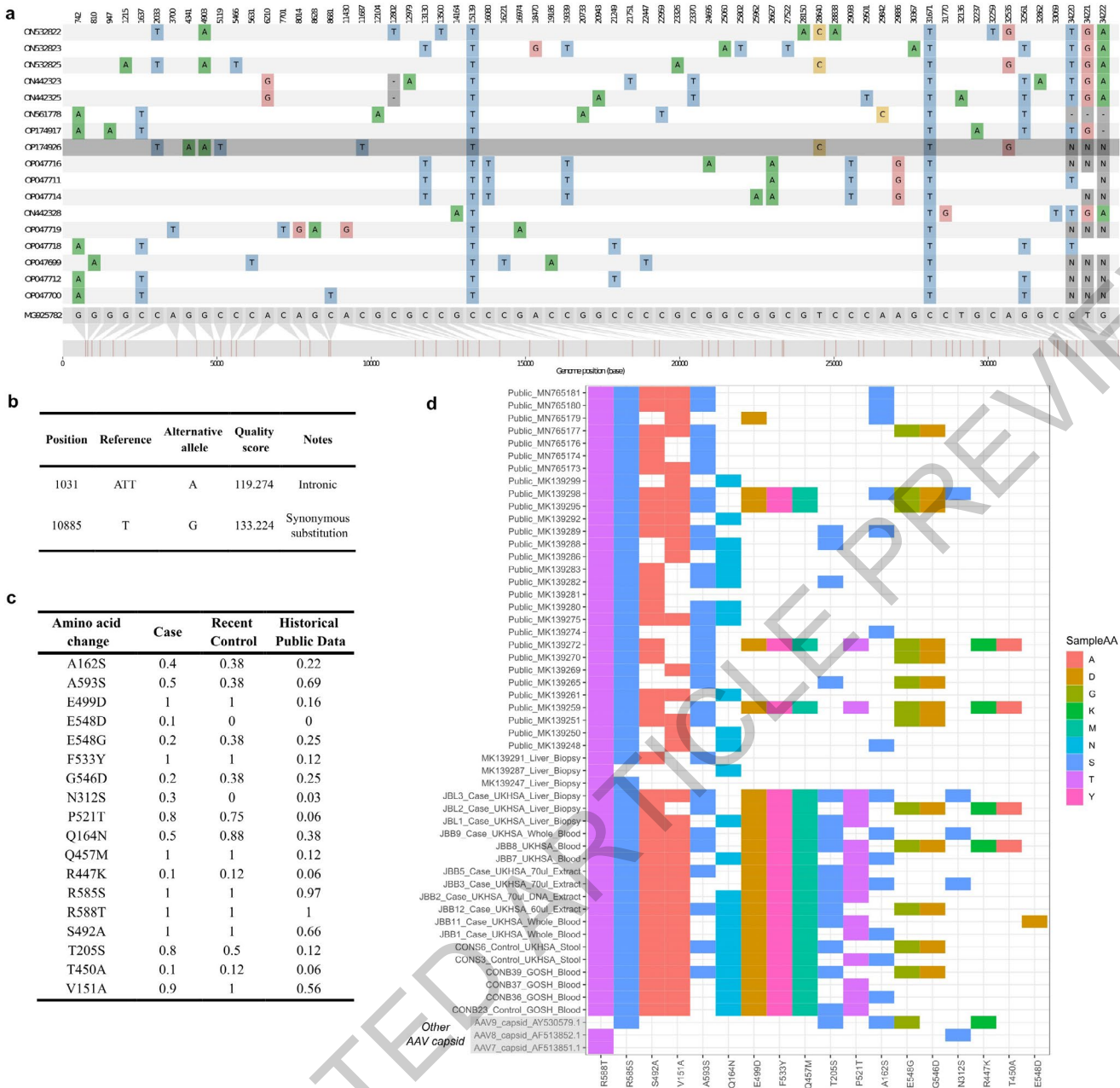


Extended Data Fig. 1



Extended Data Fig. 2

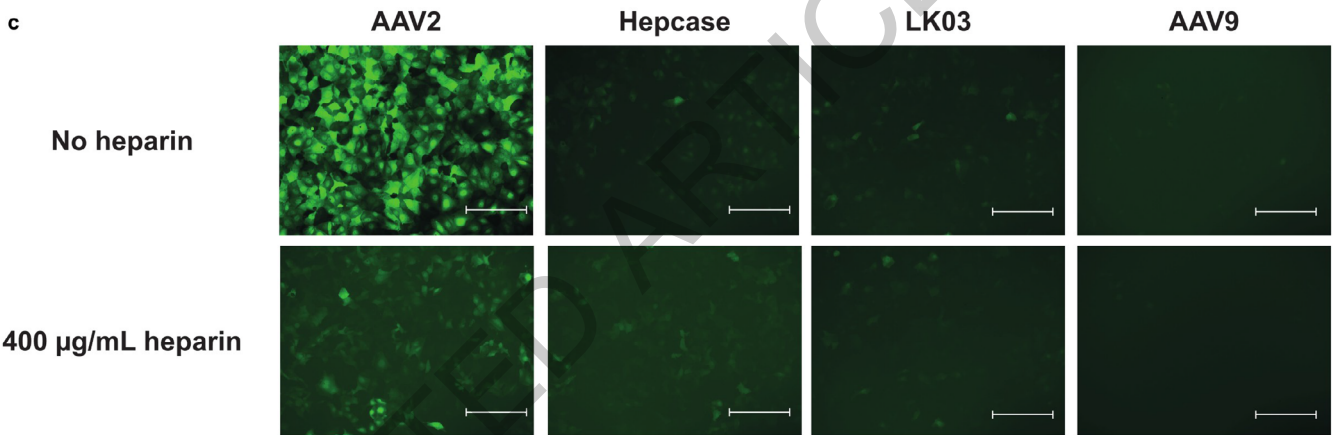
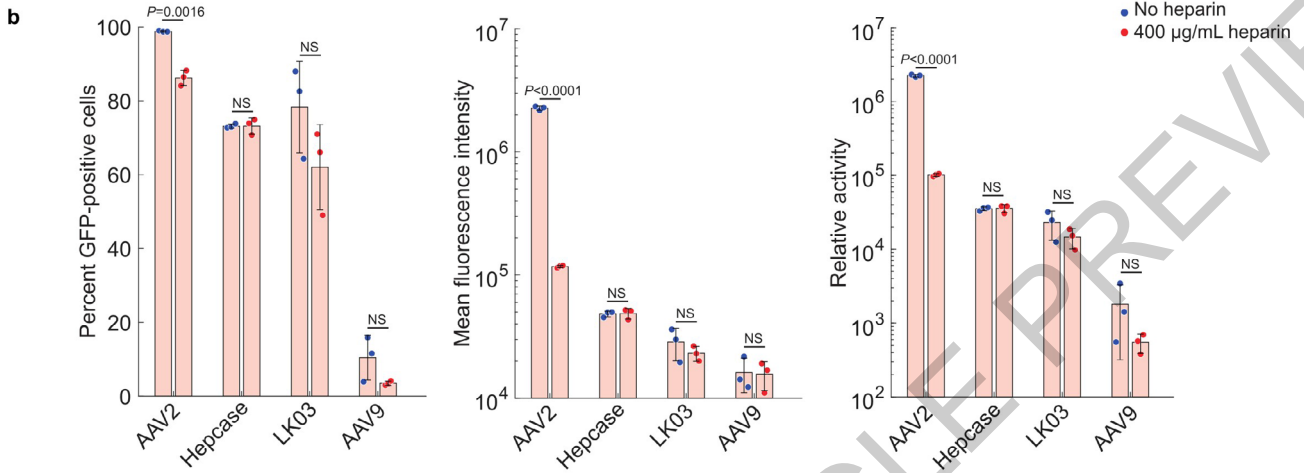
ACCELERATED ARTICLE PREVIEW



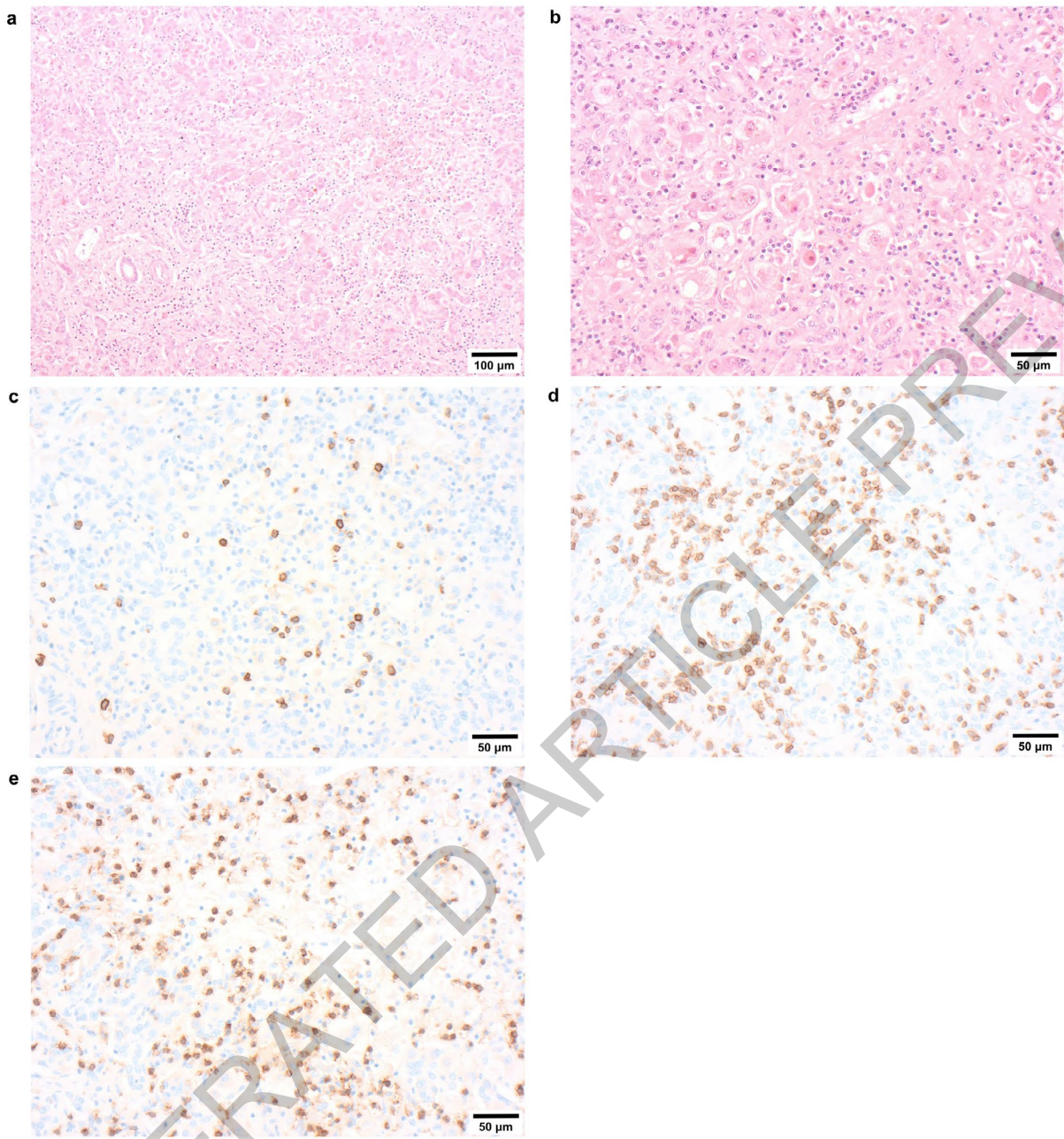
Extended Data Fig. 3

a

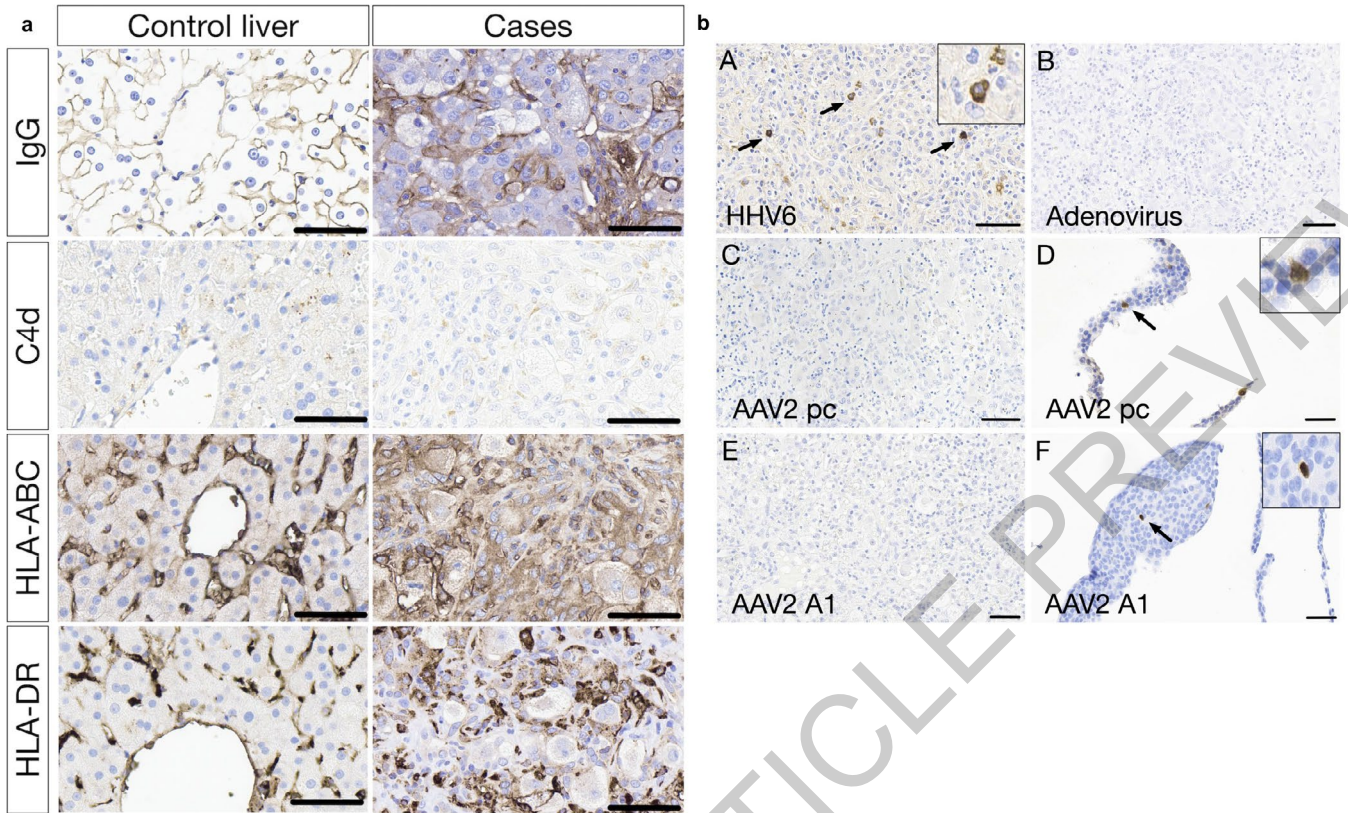
AAVhepCase	1	MAADGYLPDWLEDTLSEGI	RQWKLKPGPPPKPAERHKDDSRGLVLPYKYLGPFNGLDKGEPVNEADAAL	EHDKAYDRQLDSGDNPYLKYNHDAEFQERLKEEDTSFGGNLGRAVFQ
AAV2gp.05	1
AAVhepCase	121	AKKRVLEPLGLVEEPVKTAPGKKRVEHSPAE	PDSSSTGKAGNQFARKRLNFGQTGDADSVDP	PLGQPPAAPSGLGTNTMASGSGAPMAINNEGADGV
AAV2gp.05	121
AAVhepCase	241	TTSTRTALPTYNHLYKQISSQSGASNDNHY	FGYSTPWGYFDNRFHCFSPRDWQRLINNNWGF	RPKRLNFKLENIQVKEVTQNDGTTIANNLSTVQV
AAV2gp.05	241
AAVhepCase	361	CLPFPFADVFMVQYGYLTLNNGSQAVGRSS	FYCYLEYPFSQMLRTGNFTFSYTFEDVFPFHSS	YAHQSQSLDRIMNPLIDQYLYLSRTNTPSGTT
AAV2gp.05	361
AAVhepCase	481	PCYRQQRVSKTAADNNNSDYSWTGATKYHL	NGRDSLVPNGTAMASHKDDREKYFPQSGVLIF	GGKQSEKTNVDIEKVMITDEEEIRTTNPVATE
AAV2gp.05	481
AAVhepCase	601	LPGMVWQDRDVLQGP	IWAKIPHITDGHFHPSPLMGGFGLKHP	PPQILIKNTVPVNPSTTFSAAKFASFTQYST
AAV2gp.05	601
AAVhepCase	721	SEPRPICTRYLTRNL*
AAV2gp.05	721



Extended Data Fig. 4



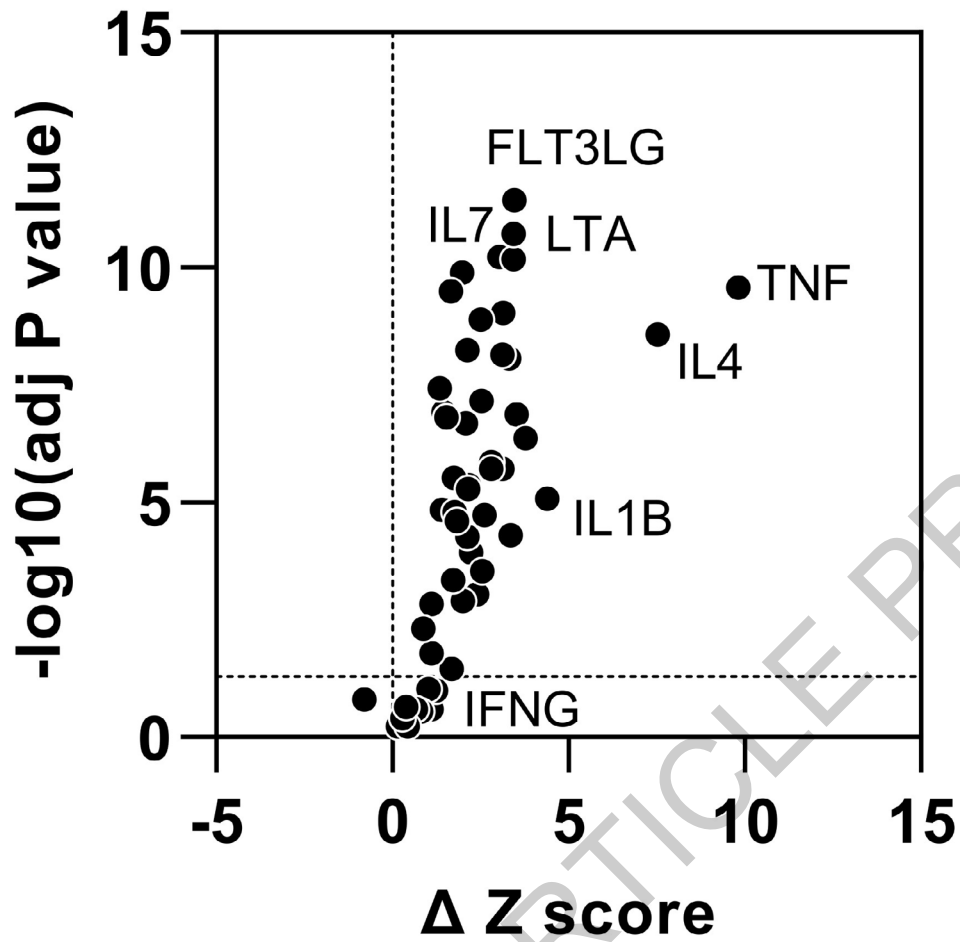
Extended Data Fig. 5



Extended Data Fig. 6

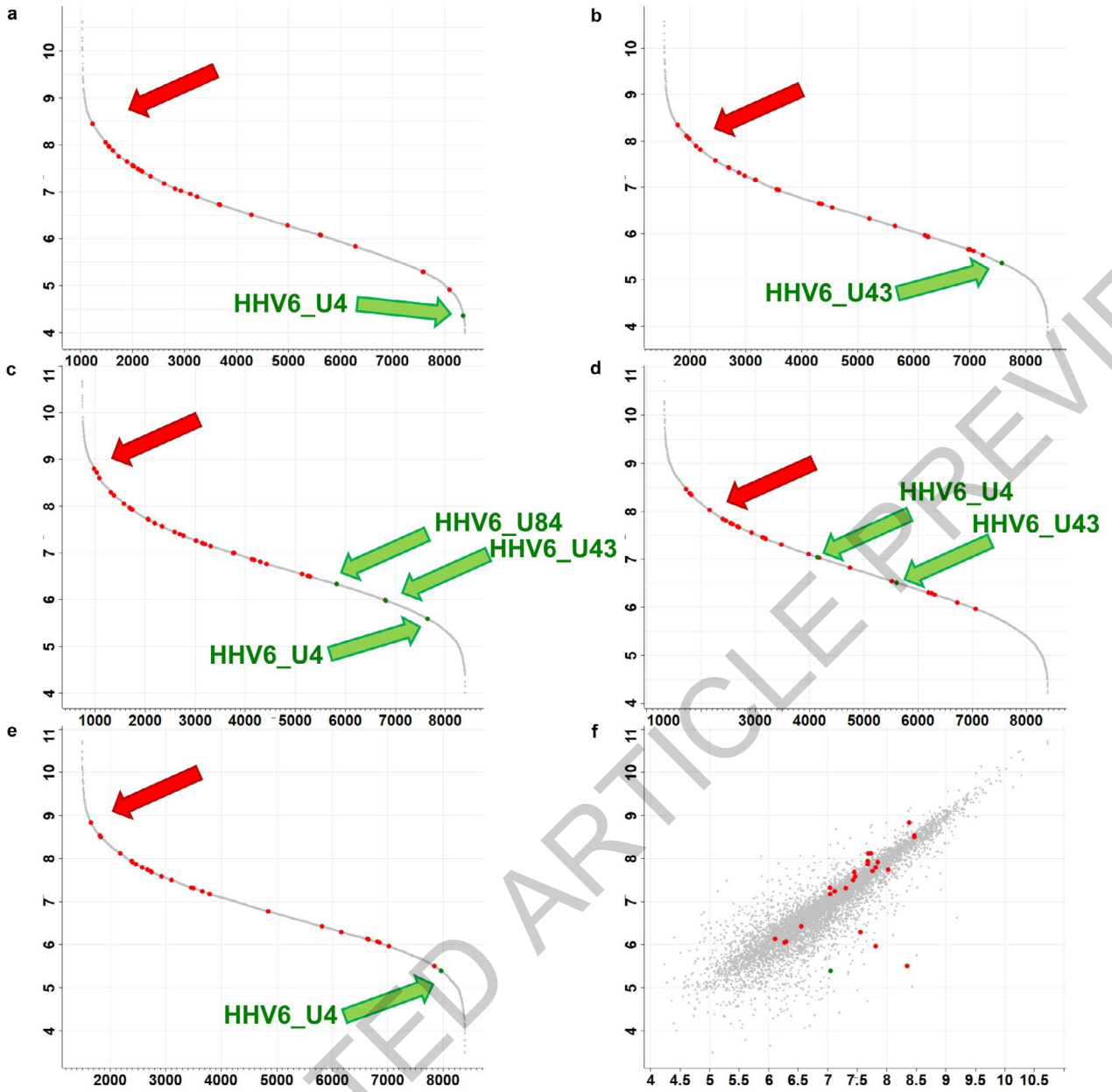
ACCELERATED ARTICLE PREVIEW

AAV2 v HBV hepatitis



**Higher in AAV2
associated hepatitis**

Extended Data Fig. 7



Extended Data Fig. 8

Case	Sample	PCR CT values			Viral WGS Coverage		
		AAV2	HAdV	HHV-6B	AAV2 (10X)	HAdV (1X)	HAdV (30X)
Blood							
6	JBB9	20	36	37	94	35.52	-
7	JBB11	21	36	37	94	29.35	-
8	JBB13	22	P/N	-/N	94	-	-
11	JBB2	20	31	37	94	7.25	0.22
12	JBB12	21	37	N/N	94	-	-
13	JBB7	21	31	-	95	-	-
14	JBB8	20	30	-	95	-	-
15	JBB3	21	29	-	94	68.47	0.32
15	JBB4	22	30	-	94	76.42	0.39
16	JBB5	23	33	-	94	17.51	0.31
18	JBB19	-	34	N/-	-	15.7	-
19	JBB20	-	36	-	-	4.1	-
19	JBB23	-	37	P	-	1.8	-
20	JBB21	-	36	-	-	13.2	-
25	JBB31	-	P/-	-	-	96.09	0.28
27	JBB24	-	34	-	-	20.8	-
Respiratory							
2	JBN1	25	P/N	-/N	88	-	-
17	JBB18	30	39	45	85	-	-
21	JBB26	-	36	-	-	21.6	-
23	JBB28	-	P/-	-	-	100	99.88
Stool							
17	JBB17	30	-/N	-/N	79	-	-
22	JBB27	-	P/-	-	-	99.99	99.13
23	JBB30	-	P/-	-	-	100	99.51
24	JBB29	-	P/-	-	-	33.54	0.12
26	JBB32	-	P/-	-	-	99.05/91.29	0.5/0.79
Liver (FFPE)							
28 (tr)	JBL6	25	-/N	32	-	-	-
29 (tr)	JBL7	24	-/N	30	-	-	-
29 (tr)	JBL8	25	40	30	-	-	-
30	JBL9	36	-/N	-/N	-	-	-
31 (tr)	JBL10	24	-/N	30	-	-	-
32 (tr)	JBL11	25	-/N	-/N	-	-	-
33 (tr)	JBL12	24	41	31	-	-	-
34 (tr)	JBL13	23	44	37	-	-	-
35	JBL14	34	-/N	-/N	-	-	-
36 (tr)	JBL15	25	41	31	-	-	-
Serum							
32 (tr)	JBB34	28	P/N	N/N	-	-	-
34 (tr)	JBB36	28	P/N	P/N	-	-	-
35	JBB35	29	P/N	P/N	-	-	-
36 (tr)	JBB37	27	42	-/N	-	-	-
37	JBB38	27	39	P/N	-	-	-
38	JBB39	32	P/N	-/N	-	-	-

Extended Data Table 1

a

Control Group	PERFORM	DIAMONDS	Total
Healthy control	13	0	13
Adenovirus, normal ALT	10	7	17
Adenovirus, normal ALT (blood)	8	0	8
Adenovirus, raised ALT	4	1	5
Critical Illness, raised ALT	6	5	11
Non-adenovirus, raised ALT	4	1	5
Other hepatitis	5	1	6
Total	50	15	65

b

Control group	ALT (U/L)	Sample type	Number of controls
Adenovirus, raised ALT	>500	Blood	14
CMV, raised ALT	>500	Blood	3
Liver biopsy	198–3528	Tissue	4

c

Age (years)	GOSH	DIAMONDS	PERFORM
0-1	12	9	15
2-3	3	1	9
4-5	2	3	17
6-7	0	2	9
Total	17	15	50

Extended Data Table 2

Reporting Summary

Nature Portfolio wishes to improve the reproducibility of the work that we publish. This form provides structure for consistency and transparency in reporting. For further information on Nature Portfolio policies, see our [Editorial Policies](#) and the [Editorial Policy Checklist](#).

Statistics

For all statistical analyses, confirm that the following items are present in the figure legend, table legend, main text, or Methods section.

n/a Confirmed

- The exact sample size (n) for each experimental group/condition, given as a discrete number and unit of measurement
- A statement on whether measurements were taken from distinct samples or whether the same sample was measured repeatedly
- The statistical test(s) used AND whether they are one- or two-sided
Only common tests should be described solely by name; describe more complex techniques in the Methods section.
- A description of all covariates tested
- A description of any assumptions or corrections, such as tests of normality and adjustment for multiple comparisons
- A full description of the statistical parameters including central tendency (e.g. means) or other basic estimates (e.g. regression coefficient) AND variation (e.g. standard deviation) or associated estimates of uncertainty (e.g. confidence intervals)
- For null hypothesis testing, the test statistic (e.g. F , t , r) with confidence intervals, effect sizes, degrees of freedom and P value noted
Give P values as exact values whenever suitable.
- For Bayesian analysis, information on the choice of priors and Markov chain Monte Carlo settings
- For hierarchical and complex designs, identification of the appropriate level for tests and full reporting of outcomes
- Estimates of effect sizes (e.g. Cohen's d , Pearson's r), indicating how they were calculated

Our web collection on [statistics for biologists](#) contains articles on many of the points above.

Software and code

Policy information about [availability of computer code](#)

Data collection

Provide a description of all commercial, open source and custom code used to collect the data in this study, specifying the version used OR state that no software was used.

Data analysis

Bowtie2, version 2.2.9 (metagenomics), version 2.4.1 (AAV2 assembly)
 Trimgalore, version 0.3.7 (metagenomics), version 0.6.7 (WGS)
 Prinseq-lite, version 0.20.3
 BLAST, version 2.9.0
 DIAMOND, version 0.9.30
 metaMix, version 0.4
 Samtools, version 1.9
 Picard, version 2.26.9
 SPADES, version 3.15.5
 Primalscheme, online version accessed July 2022
 Viral recon pipeline, version 2.4.1
 MAFFT, version 7.271 (AAV2), G-INS-I v7.481(AdV/HHV6)
 BWA-mem, version 0.7.17
 AYUKA doi 10.5281/zenodo.6521576 <https://github.com/afonsoguerra/AYUKA>
 BBSplit, version 38.68
 BCFtools, version 1.15.1
 IQTree2, version 2.2.0
 R, version 4.2.0

Tidyverse, version 1.3.1
 Perseus, version 2.05
 Origin Pro version 2022b
 EPI2ME Fast SV caller for Human pipeline, v2021.11.26
 minimap2, version 2.17
 EPI2ME WIMP, v2021.11.26
 Vseq-Toolkit
 DEP R package version 1.18.0
 Kraken2 version 2.0.8-beta
 Redotable, version 1.1
 FASTQC, v0.11.9
 MaxQuant v2.1
 EMBOSS Sixpack

The metagenomics and PCR analysis code can be found at:
<https://github.com/sarah-buddle/unknown-hepatitis>

The transcriptomics analysis code can be found at:
https://github.com/innate2adaptive/Bulk-RNAseq-analysis/tree/main/Zscore_gene_expression_module_analysis

The proteomics differential expression analysis code can be found at:
https://github.com/MahdiMoradiMarjaneh/proteomics_and_transcriptomics_of_hepatitis

For manuscripts utilizing custom algorithms or software that are central to the research but not yet described in published literature, software must be made available to editors and reviewers. We strongly encourage code deposition in a community repository (e.g. GitHub). See the Nature Portfolio [guidelines for submitting code & software](#) for further information.

Data

Policy information about [availability of data](#)

All manuscripts must include a [data availability statement](#). This statement should provide the following information, where applicable:

- Accession codes, unique identifiers, or web links for publicly available datasets
- A description of any restrictions on data availability
- For clinical datasets or third party data, please ensure that the statement adheres to our [policy](#)

All consensus genomes from sequencing data have been deposited to Genbank. Accession codes are in the manuscript.

Human research participants

Policy information about [studies involving human research participants and Sex and Gender in Research](#).

Reporting on sex and gender

Of 22 cases where the gender was known, 12 were female and 10 were male

Population characteristics

We had ISARIC ethics for 5 transplant cases and we could study their human transcriptomic/proteomic data. We subsequently obtained consent for a further 7 cases from UKHSA and 10 cases from King's College Hospital, and obtained some clinical data from these patients. For the remaining cases that we had ethics permitting us to only perform diagnostic tests on their clinical specimens. The ISARIC codes can be found in the Ethics section at the start of the Methods.

Of cases where age was known, median age 3 years, with range 1.5-9.
 Where known, all cases were of white ethnicity other than 2.

Recruitment

Describe how participants were recruited. Outline any potential self-selection bias or other biases that may be present and how these are likely to impact results.

Ethics oversight

ISARIC

Note that full information on the approval of the study protocol must also be provided in the manuscript.

Field-specific reporting

Please select the one below that is the best fit for your research. If you are not sure, read the appropriate sections before making your selection.

Life sciences Behavioural & social sciences Ecological, evolutionary & environmental sciences

For a reference copy of the document with all sections, see [nature.com/documents/nr-reporting-summary-flat.pdf](https://www.nature.com/documents/nr-reporting-summary-flat.pdf)

Life sciences study design

All studies must disclose on these points even when the disclosure is negative.

Sample size	NA - case series
Data exclusions	We have excluded controls to age-match the cases (<8 years old) or controls that were in disease categories that had less than 3 subjects, addressing one of referees comments.
Replication	<i>Describe the measures taken to verify the reproducibility of the experimental findings. If all attempts at replication were successful, confirm this OR if there are any findings that were not replicated or cannot be reproduced, note this and describe why.</i>
Randomization	NA
Blinding	NA

Reporting for specific materials, systems and methods

We require information from authors about some types of materials, experimental systems and methods used in many studies. Here, indicate whether each material, system or method listed is relevant to your study. If you are not sure if a list item applies to your research, read the appropriate section before selecting a response.

Materials & experimental systems

Methods

n/a	Involved in the study
<input type="checkbox"/>	<input checked="" type="checkbox"/> Antibodies
<input type="checkbox"/>	<input type="checkbox"/> Eukaryotic cell lines
<input type="checkbox"/>	<input type="checkbox"/> Palaeontology and archaeology
<input type="checkbox"/>	<input type="checkbox"/> Animals and other organisms
<input type="checkbox"/>	<input checked="" type="checkbox"/> Clinical data
<input type="checkbox"/>	<input type="checkbox"/> Dual use research of concern

n/a	Involved in the study
<input type="checkbox"/>	<input type="checkbox"/> ChIP-seq
<input type="checkbox"/>	<input type="checkbox"/> Flow cytometry
<input type="checkbox"/>	<input type="checkbox"/> MRI-based neuroimaging

Antibodies

Antibodies used

Adenovirus immunohistochemistry was carried out using the Ventana Benchmark ULTRA, Optiview Detection Kit, PIER with Protease 1 for 4min, Ab incubation 32min (Adenovirus clone 2/6 & 20/11, Roche, 760-4870, pre-diluted).

AAV2 immunohistochemistry was carried out with three commercial kits

Leica Bond-III, Bond Polymer Refine Detection Kit with DAB Enhancer, HIER with Bond Epitope Retrieval Solution 1 (citrate based pH 6) for 30min, Ab incubation 30min (Anti-AAV VP1/VP2/VP3 clone B1, PROGEN, 690058S, 1:100).

Leica Bond-III, Bond Polymer Refine Detection Kit with DAB Enhancer, HIER with Bond Epitope Retrieval Solution 1 (citrate based pH 6) for 40min, Ab incubation 30min (Anti-AAV VP1/VP2/VP3 rabbit polyclonal, OriGene, BP5024, 1:100)

HHV-6 immunohistochemistry staining was carried out with:

Leica Bond-III, Bond Polymer Refine Detection Kit with DAB Enhancer, PIER with Bond Enzyme 1 Kit 10min, Ab incubation 30min (Mouse monoclonal [C3108-103] to HHV-6, ABCAM, ab128404, 1:100).

Validation

Describe the validation of each primary antibody for the species and application, noting any validation statements on the manufacturer's website, relevant citations, antibody profiles in online databases, or data provided in the manuscript.

Eukaryotic cell lines

Policy information about [cell lines and Sex and Gender in Research](#)

Cell line source(s)

State the source of each cell line used and the sex of all primary cell lines and cells derived from human participants or vertebrate models.

Authentication

Describe the authentication procedures for each cell line used OR declare that none of the cell lines used were authenticated.

Mycoplasma contamination

Confirm that all cell lines tested negative for mycoplasma contamination OR describe the results of the testing for mycoplasma contamination OR declare that the cell lines were not tested for mycoplasma contamination.

Commonly misidentified lines
(See [ICLAC](#) register)

Name any commonly misidentified cell lines used in the study and provide a rationale for their use.

Palaeontology and Archaeology

Specimen provenance

Provide provenance information for specimens and describe permits that were obtained for the work (including the name of the issuing authority, the date of issue, and any identifying information). Permits should encompass collection and, where applicable, export.

Specimen deposition

Indicate where the specimens have been deposited to permit free access by other researchers.

Dating methods

If new dates are provided, describe how they were obtained (e.g. collection, storage, sample pretreatment and measurement), where they were obtained (i.e. lab name), the calibration program and the protocol for quality assurance OR state that no new dates are provided.

Tick this box to confirm that the raw and calibrated dates are available in the paper or in Supplementary Information.

Ethics oversight

Identify the organization(s) that approved or provided guidance on the study protocol, OR state that no ethical approval or guidance was required and explain why not.

Note that full information on the approval of the study protocol must also be provided in the manuscript.

Animals and other research organisms

Policy information about [studies involving animals](#); [ARRIVE guidelines](#) recommended for reporting animal research, and [Sex and Gender in Research](#)

Laboratory animals

For laboratory animals, report species, strain and age OR state that the study did not involve laboratory animals.

Wild animals

Provide details on animals observed in or captured in the field; report species and age where possible. Describe how animals were caught and transported and what happened to captive animals after the study (if killed, explain why and describe method; if released, say where and when) OR state that the study did not involve wild animals.

Reporting on sex

Indicate if findings apply to only one sex; describe whether sex was considered in study design, methods used for assigning sex. Provide data disaggregated for sex where this information has been collected in the source data as appropriate; provide overall numbers in this Reporting Summary. Please state if this information has not been collected. Report sex-based analyses where performed, justify reasons for lack of sex-based analysis.

Field-collected samples

For laboratory work with field-collected samples, describe all relevant parameters such as housing, maintenance, temperature, photoperiod and end-of-experiment protocol OR state that the study did not involve samples collected from the field.

Ethics oversight

Identify the organization(s) that approved or provided guidance on the study protocol, OR state that no ethical approval or guidance was required and explain why not.

Note that full information on the approval of the study protocol must also be provided in the manuscript.

Clinical data

Policy information about [clinical studies](#)

All manuscripts should comply with the ICMJE [guidelines for publication of clinical research](#) and a completed [CONSORT checklist](#) must be included with all submissions.

Clinical trial registration

NA

Study protocol

NA

Data collection

public health agencies,

Outcomes

NA

Dual use research of concern

Policy information about [dual use research of concern](#)

Hazards

Could the accidental, deliberate or reckless misuse of agents or technologies generated in the work, or the application of information presented in the manuscript, pose a threat to:

- | | | |
|-------------------------------------|--------------------------|----------------------------|
| No | Yes | |
| <input checked="" type="checkbox"/> | <input type="checkbox"/> | Public health |
| <input checked="" type="checkbox"/> | <input type="checkbox"/> | National security |
| <input checked="" type="checkbox"/> | <input type="checkbox"/> | Crops and/or livestock |
| <input checked="" type="checkbox"/> | <input type="checkbox"/> | Ecosystems |
| <input checked="" type="checkbox"/> | <input type="checkbox"/> | Any other significant area |

Experiments of concern

Does the work involve any of these experiments of concern:

- | | | |
|-------------------------------------|--------------------------|---|
| No | Yes | |
| <input checked="" type="checkbox"/> | <input type="checkbox"/> | Demonstrate how to render a vaccine ineffective |
| <input checked="" type="checkbox"/> | <input type="checkbox"/> | Confer resistance to therapeutically useful antibiotics or antiviral agents |
| <input checked="" type="checkbox"/> | <input type="checkbox"/> | Enhance the virulence of a pathogen or render a nonpathogen virulent |
| <input checked="" type="checkbox"/> | <input type="checkbox"/> | Increase transmissibility of a pathogen |
| <input checked="" type="checkbox"/> | <input type="checkbox"/> | Alter the host range of a pathogen |
| <input checked="" type="checkbox"/> | <input type="checkbox"/> | Enable evasion of diagnostic/detection modalities |
| <input checked="" type="checkbox"/> | <input type="checkbox"/> | Enable the weaponization of a biological agent or toxin |
| <input checked="" type="checkbox"/> | <input type="checkbox"/> | Any other potentially harmful combination of experiments and agents |

ChIP-seq

Data deposition

- Confirm that both raw and final processed data have been deposited in a public database such as [GEO](#).
- Confirm that you have deposited or provided access to graph files (e.g. BED files) for the called peaks.

Data access links

May remain private before publication.

For "Initial submission" or "Revised version" documents, provide reviewer access links. For your "Final submission" document, provide a link to the deposited data.

Files in database submission

Provide a list of all files available in the database submission.

Genome browser session

(e.g. [UCSC](#))

Provide a link to an anonymized genome browser session for "Initial submission" and "Revised version" documents only, to enable peer review. Write "no longer applicable" for "Final submission" documents.

Methodology

Replicates

Describe the experimental replicates, specifying number, type and replicate agreement.

Sequencing depth

Describe the sequencing depth for each experiment, providing the total number of reads, uniquely mapped reads, length of reads and whether they were paired- or single-end.

Antibodies

Describe the antibodies used for the ChIP-seq experiments; as applicable, provide supplier name, catalog number, clone name, and lot number.

Peak calling parameters

Specify the command line program and parameters used for read mapping and peak calling, including the ChIP, control and index files used.

Data quality

Describe the methods used to ensure data quality in full detail, including how many peaks are at FDR 5% and above 5-fold enrichment.

Software

Describe the software used to collect and analyze the ChIP-seq data. For custom code that has been deposited into a community repository, provide accession details.

Flow Cytometry

Plots

Confirm that:

- The axis labels state the marker and fluorochrome used (e.g. CD4-FITC).
- The axis scales are clearly visible. Include numbers along axes only for bottom left plot of group (a 'group' is an analysis of identical markers).
- All plots are contour plots with outliers or pseudocolor plots.
- A numerical value for number of cells or percentage (with statistics) is provided.

Methodology

Sample preparation

Describe the sample preparation, detailing the biological source of the cells and any tissue processing steps used.

Instrument

Identify the instrument used for data collection, specifying make and model number.

Software

Describe the software used to collect and analyze the flow cytometry data. For custom code that has been deposited into a community repository, provide accession details.

Cell population abundance

Describe the abundance of the relevant cell populations within post-sort fractions, providing details on the purity of the samples and how it was determined.

Gating strategy

Describe the gating strategy used for all relevant experiments, specifying the preliminary FSC/SSC gates of the starting cell population, indicating where boundaries between "positive" and "negative" staining cell populations are defined.

- Tick this box to confirm that a figure exemplifying the gating strategy is provided in the Supplementary Information.

Magnetic resonance imaging

Experimental design

Design type

Indicate task or resting state; event-related or block design.

Design specifications

Specify the number of blocks, trials or experimental units per session and/or subject, and specify the length of each trial or block (if trials are blocked) and interval between trials.

Behavioral performance measures

State number and/or type of variables recorded (e.g. correct button press, response time) and what statistics were used to establish that the subjects were performing the task as expected (e.g. mean, range, and/or standard deviation across subjects).

Acquisition

Imaging type(s)

Specify: functional, structural, diffusion, perfusion.

Field strength

Specify in Tesla

Sequence & imaging parameters

Specify the pulse sequence type (gradient echo, spin echo, etc.), imaging type (EPI, spiral, etc.), field of view, matrix size, slice thickness, orientation and TE/TR/flip angle.

Area of acquisition

State whether a whole brain scan was used OR define the area of acquisition, describing how the region was determined.

Diffusion MRI

Used

Not used

Preprocessing

Preprocessing software

Provide detail on software version and revision number and on specific parameters (model/functions, brain extraction, segmentation, smoothing kernel size, etc.).

Normalization

If data were normalized/standardized, describe the approach(es): specify linear or non-linear and define image types used for transformation OR indicate that data were not normalized and explain rationale for lack of normalization.

Normalization template

Describe the template used for normalization/transformation, specifying subject space or group standardized space (e.g. original Talairach, MNI305, ICBM152) OR indicate that the data were not normalized.

Noise and artifact removal

Describe your procedure(s) for artifact and structured noise removal, specifying motion parameters, tissue signals and physiological signals (heart rate, respiration).

Volume censoring

*Define your software and/or method and criteria for volume censoring, and state the extent of such censoring.***Statistical modeling & inference**

Model type and settings

Specify type (mass univariate, multivariate, RSA, predictive, etc.) and describe essential details of the model at the first and second levels (e.g. fixed, random or mixed effects; drift or auto-correlation).

Effect(s) tested

*Define precise effect in terms of the task or stimulus conditions instead of psychological concepts and indicate whether ANOVA or factorial designs were used.*Specify type of analysis: Whole brain ROI-based BothStatistic type for inference
(See [Eklund et al. 2016](#))*Specify voxel-wise or cluster-wise and report all relevant parameters for cluster-wise methods.*

Correction

*Describe the type of correction and how it is obtained for multiple comparisons (e.g. FWE, FDR, permutation or Monte Carlo).***Models & analysis**

n/a | Involved in the study

 Functional and/or effective connectivity Graph analysis Multivariate modeling or predictive analysis

Functional and/or effective connectivity

Report the measures of dependence used and the model details (e.g. Pearson correlation, partial correlation, mutual information).

Graph analysis

Report the dependent variable and connectivity measure, specifying weighted graph or binarized graph, subject- or group-level, and the global and/or node summaries used (e.g. clustering coefficient, efficiency, etc.).

Multivariate modeling and predictive analysis

Specify independent variables, features extraction and dimension reduction, model, training and evaluation metrics.